INVESTIGATION ON THERMAL DIFFUSIVITY OF SOME SELECTED MATERIALS USING LASER INDUCED PHOTOACOUSTIC TECHNIQUE

SANKARA RAMAN.S

THE THESIS SUBMITTED TO
THE COCHIN UNIVERSITY OF SCIENCE AND TECHNOLOGY
IN FULFILLMENT OF THE REQUIREMENTS FOR THE AWARD OF
THE DEGREE OF **DOCTOR OF PHILOSOPHY**
IN THE FACULTY OF SCIENCE

INTERNATIONAL SCHOOL OF PHOTONICS

COCHIN UNIVERSITY OF SCIENCE AND TECHNOLOGY

COCHIN, 1999

CERTIFICATE

Certified that the research work presented in this thesis entitled *Investigation on thermal diffusivitty of some selected materials using laser induced photoacoustic technique* is based on the original work carried out by Mr.Sankara raman. S in the International School of Photonics, Cochin University of Science and Technology, under my guidance and supervision and has not been included in any other thesis submitted previously for the award of any degree.

Prof. V.P.N. Nampoori

Cochin-22

2/7/99

PREFACE

In its broadest sense, spectroscopy can be defined as the study of the interaction of radiation with matter as a function of radiation. As such, it is a science encompassing many disciplines and techniques. In the field of high energy Physics, the radiation is energetic enough to perturb or to transform the matter with which it interacts, whereas in optical domain, the energy is too low to perturb or to transform the matter under study. Because of its versatility, range and non-destructive nature, optical spectroscopy is widely used as an important tool for investigating and characterizing the properties of matter.

The conventional optical spectroscopy can be grouped into two categories. The first category involves the study of the optical photons that are transmitted through the material without interaction. The second category involves the study of light that is scattered or reflected from the material, i.e., those photons that have undergone some interaction with the material.

Optical spectroscopy has been a scientific tool for over a century, and has proven invaluable in studies on transparent media. There are several instances where the conventional transmission spectroscopy is inadequate even for transparent media. Such a situation arises when one is attempting to measure a weak absorption, which in turn involves the measurement of the slight change in the intensity of the transmitted signal. Various techniques have been developed to overcome this difficulty. Apart from these weakly absorbing materials, there are several non-homogeneous substances that are not readily amenable to the conventional transmission or reflection modes of optical spectroscopy. Other difficult materials are those that are optically opaque. Several techniques have been developed to permit the study of highly scattering and opaque substances. The most common of these are attenuated total reflection (ATR) and internal reflection spectroscopy and Raman scattering. Though these methods are useful, they are limited only to a small category of materials, only over a small wavelength range and the data obtained are difficult to interpret.

During the past few years two more optical techniques have been developed mainly to study those materials which are unsuitable for conventional methods. These techniques

are called Photoacoustic spectroscopy or PAS and Optical beam deflection or "mirage" technique. These methods differ from the conventional techniques chiefly in that even though the incident energy is in the form of optical photons, the interaction of these photons with the material is studied not through subsequent detection and analysis of transmitted/reflected photons, but through a direct measure of the energy associated with non-radiative de-excitation by atoms/molecules of the medium as a result of interaction with the photon beam.

The present thesis is an attempt to bring out some of the factors influencing the thermal parameters of a material. With the advent of lasers and data acquisition systems, PA technique has now emerged as a non-destructive technique to study the optical and thermal properties of materials. The thesis comprises of seven chapters and two appendices.

In the first chapter a brief review of various photothermal phenomena and their detection technique are given. Advantages of PAS over the conventional methods and applications of the technique to various problems are also briefly described.

In the second chapter, the theory put forwarded by Rosencwaig and Gersho for PA effect in condensed media is described. The extension of the theory for thermal diffusivity measurement is also given.

The general aspects of PA instrumentation are given in the third chapter. It also deals with the design of a PA spectrometer. The methods of modulation and signal processing are also described. Standardisation of the experimental set-up for thermal diffusivity measurements is given towards the end of the chapter.

Alumina is an important material in low temperature Physics, microelectronics and solid state technology as substrate material. A knowledge of its thermal diffusivity and the factors governing it will be helpful for the people using it for variety of technological applications. Chapter 4 is an attempt to bring out one of the factors that influence thermal diffusivity of alumina. The chapter gives a vivid picture of the role of OH groups in the thermal diffusivity of alumina.

The method of preparation of a material has significant role in its physical properties. A material prepared by two different procedures will exhibit slightly

different physical properties. This is exemplified in chapter 5 taking Nd_2O_3, an important material in electronic components and device fabrication, piezo, pyro and electrooptic applications and in industry.

Benzimidazole complexes have recently gained considerable attention of scientists and technologists by virtue of their bio-medical and photonic applications. Chapter 6 and 7 describe the thermal behaviour of the complex on replacement of its metal/halogen part. In chapter 7 the complex is given a polystyrene support and its role along with metal as well as halogen part in the thermal diffusivity of the sample is studied.

Aranmula mirror is a metallic mirror prepared by ethanometallurgical process by a group of families at Aranmula, a village in Kerala. The PA technique has been used to study its optical property viz. the reflection coefficient and is included in the thesis as appendix 1.

Photothermal deflection or Mirage effect is another thermo optical phenomena that can be effectively used for thermal as well as optical characterization being one of the several nondestructive techniques. In appendix 2, use of the technique for thermal diffusivity measurements of

some phthalocyanines, organic semiconductors, is described. A brief theoretical and experimental detail of the technique is also given.

The thesis ends up with an overall conclusion and summary.

PAPERS PUBLISHED / COMMUNICATED IN JOURNALS

[1] *Photoacoustic study of the effect of degassing temperature on thermal diffusivity of hydroxyl loaded alumina.*

S. Sankara raman, V.P.N. Nampoori, C.P.G. Vallabhan, G. Ambadas, and S. Sugunan,
Appl. Phys. Lett., 67, (1995) 2939.

[2] *Measurement of thermal diffusivity of some halogeno benzimidazole complexes of cobalt (II), copper (II) and copper (I) using laser induced photoacoustic effect.*

S. Sankara raman, V.P.N. Nampoori, C.P.G. Vallabhan, N. Saravanan, and K.K. Mohammed Yusuff,
J. Mat. Sci. Lett., 15 (1996) 230.

[3] *Photoacoustic study of the effect of hydroxyl ion on thermal diffusivity of γ-alumina*

S. Sankara raman, V.P.N. Nampoori, C.P.G. Vallabhan, G. Ambadas, and S. Sugunan,
J. Appl. Phys., Vol.85, No.2, (1999) *In press*.

[4] Thermal diffusivity of some polymer supported halogeno benzimidazole complexes of *cobalt(II), copper(II) - A Photoacoustic study.*

S. Sankara raman, V.P.N. Nampoori, C.P.G. Vallabhan, N. Saravanan, and K.K. Mohammed Yusuff,
J. Mat. Sci. Lett. (*In press*)

[5] *Thermal diffusivity of Nd_2O_3 - Photoacoustic study of the effect of method of preparation.*

S. Sankara raman, V.P.N. Nampoori, C.P.G. Vallabhan, G. Ambadas, and S. Sugunan,
J. Phys and Chem. of solids (Communicated)

[6] *Photoacoustic study in Aranmula mirror.*

S. Sankara raman, V.P.N. Nampoori and C.P.G . Vallabhan
J. Opt. (Communicated)

[7] *Interferometric study of variation of refractive index of solution with concentration.*

S. Sankara raman, Priya Varghese and K. Viswambharan
Phys. Edn. July 1994.

PAPERS PRESENTED IN SEMINARS AND SYMPOSIA

[8] *Photoacoustic study of the effect of rare-earth doping on the thermal diffusivity of alumina.*

S. Sankara raman, Annieta Philip, B. Ambadi, V.P.N. Nampoori, C.P.G. Vallabhan, G. Ambadas, and S. Sugunan,
Proceedings of *Seminar on Recent Development in the Sci. & Tech. of Rare Earth*, IRE, Udyogamandal, Aluva, Kerala.

[9] *Preparation route and thermal diffusivity of rare earth oxides - A Photoacoustic study.*

S. Sankara raman, B. Ambadi, V.P.N. Nampoori, C.P.G. Vallabhan, G. Ambadas, and S. Sugunan,
Proceedings of *Seminar on Recent Development in the Sci. & Tech. of Rare Earth,* IRE, Udyogamandal, Aluva, Kerala.

[10] *Laser induced photoacoustic study of the effect of hydroxyl ion on thermal diffusivity of γ- alumina.*

S. Sankara raman, V.P.N. Nampoori and
C.P.G. Vallabhan,
Proceedings of 8th Kerala Science Congress, 1996,p.333.

[11]] Effect of laser irradiation on growth and metabolism in plants.

A.Sabu, Geetha K Varier and **S. Sankara raman**
Proceedings of 8th Kerala Science Congress, 1996,p 448.

CONTENTS

CHAPTER 1

PHOTOACOUSTIC EFFECT -AN OVERVIEW

ABSTRACT

A brief review of various photothermal effects and their detection techniques with special reference to Photoacoustics (PA) is given in this chapter. The various possible methods of direct and indirect PA generation are described briefly. The advantages of PA technique over the conventional spectroscopic and calorimetric technique are also given. Applications of photothermal techniques, with an emphasis to Photoacoustic spectroscopy are briefly explained in the last section.

1.1 INTRODUCTION

Photothermal phenomena have been emerged as a powerful technique in Science and Technology during the last decade. Though the phenomenon was known to man in eighteenth century, he could not tap its potential in its complete sense. With the advent of Lasers in 1960 and sophisticated data acquisition systems, the versatile face of photothermal phenomena gradually began to expose to the world. Now it finds significant place in science and technology mainly, not only as a non-destructive technique but also as a spectroscopic technique where the conventional methods collapse. Modern medical Science, Biology, Bio-Technology, Microelectronics, Solid State Technology, what more, almost in all branches of Science and technology it has proven its potential. Of several branches of photothermal phenomena, Photoacoustics is only one among them.

The Photoacoustic effect was discovered by Alexander Graham Bell [1,2], who found that an acoustic signal was produced when a sample in an enclosed cell was illuminated with light having a periodically varying intensity (i.e. chopped light). This effect provides a means for the study of optical absorption in the sample, such studies being

called Photoacoustic Spectroscopy (PAS). The Photoacoustic spectroscopy has been used in the study of gaseous, solid and liquid samples [3-17].

Photoacoustic (PA) generation is generally due to photothermal heating effect apart from other mechanisms. Some possible mechanisms are shown in figure 1.1, where the PA generation efficiency η (*i*.e. acoustic energy generated/ light energy absorbed) generally increases downwards for the mechanisms listed. For electrostriction and for thermal expansion (or thermo elastic) mechanisms η is small, of the order of 10^{-12} to 10^{-3} while for break down mechanism η can be as large as 30% [18].

The P A generation can be classified as direct or indirect [19,20]. In the direct PA generation, the acoustic wave is produced in the sample whereas in indirect PA generation the acoustic wave is generated in the coupling medium adjacent to the sample usually due to heat leakage and to acoustic transmission from the sample. The PA generation can also be classified according to the two excitation modes: the continuous-wave (cw) modulation mode where by the excitation beam is modulated near 50% duty cycle and pulsed mode, whereby excitation beam is of very low duty cycle but high peak power. In the cw case, the

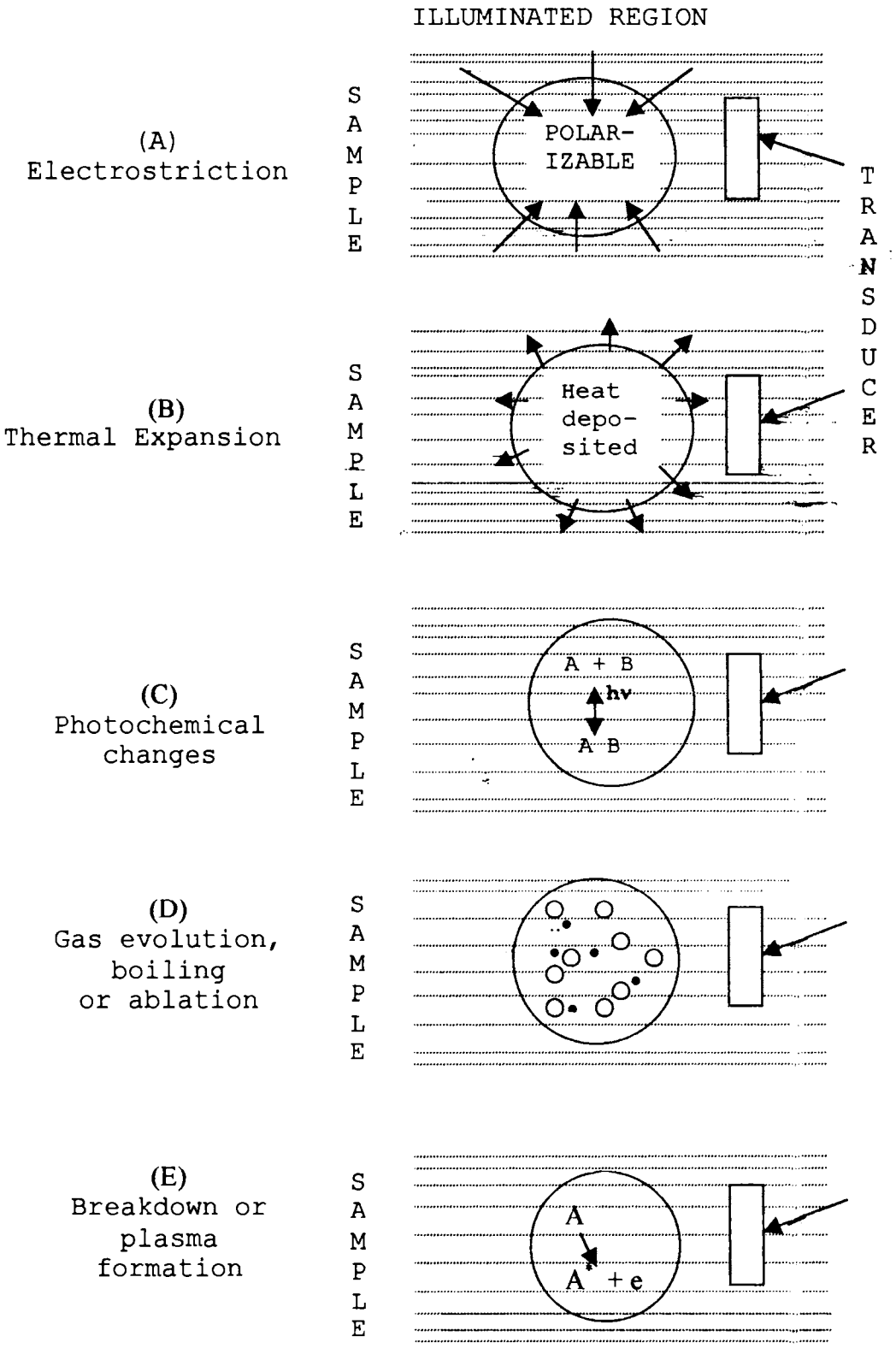

Fig. 1.1 Some of the common direct PA generations mechanisms, listed in the order of efficiency.

signal is analysed in the frequency domain while in the pulsed technique, the signal is acquired and analysed in the time domain. Discussions of these two PA generation techniques are given by Atalar and Tam and Coufal [19,20].

In pulsed PA measurements the excitation pulse is typically short ($<< 10^{-6}$sec) and the acoustic propagation distance during the excitation pulse is typically much smaller than the dimension of the sample so that the PA pulse shape, is independent of the boundary reflections and the sample can be treated as infinite in extent. In cw modulated PA measurements, the modulation frequency is in the 10^3 Hz regime and the acoustic propagation distance during a period is much larger than the sample cell. The PA generation efficiency with cw modulated mode is lower than with the pulsed mode [21].

The indirect PA generation requiring acoustic detection in the coupling media in contact with the sample does not provide as high sensitivity as the direct PA generation for detecting weak absorption. However indirect PA generation is much significant when the optical absorption is high and no light passes through the sample.

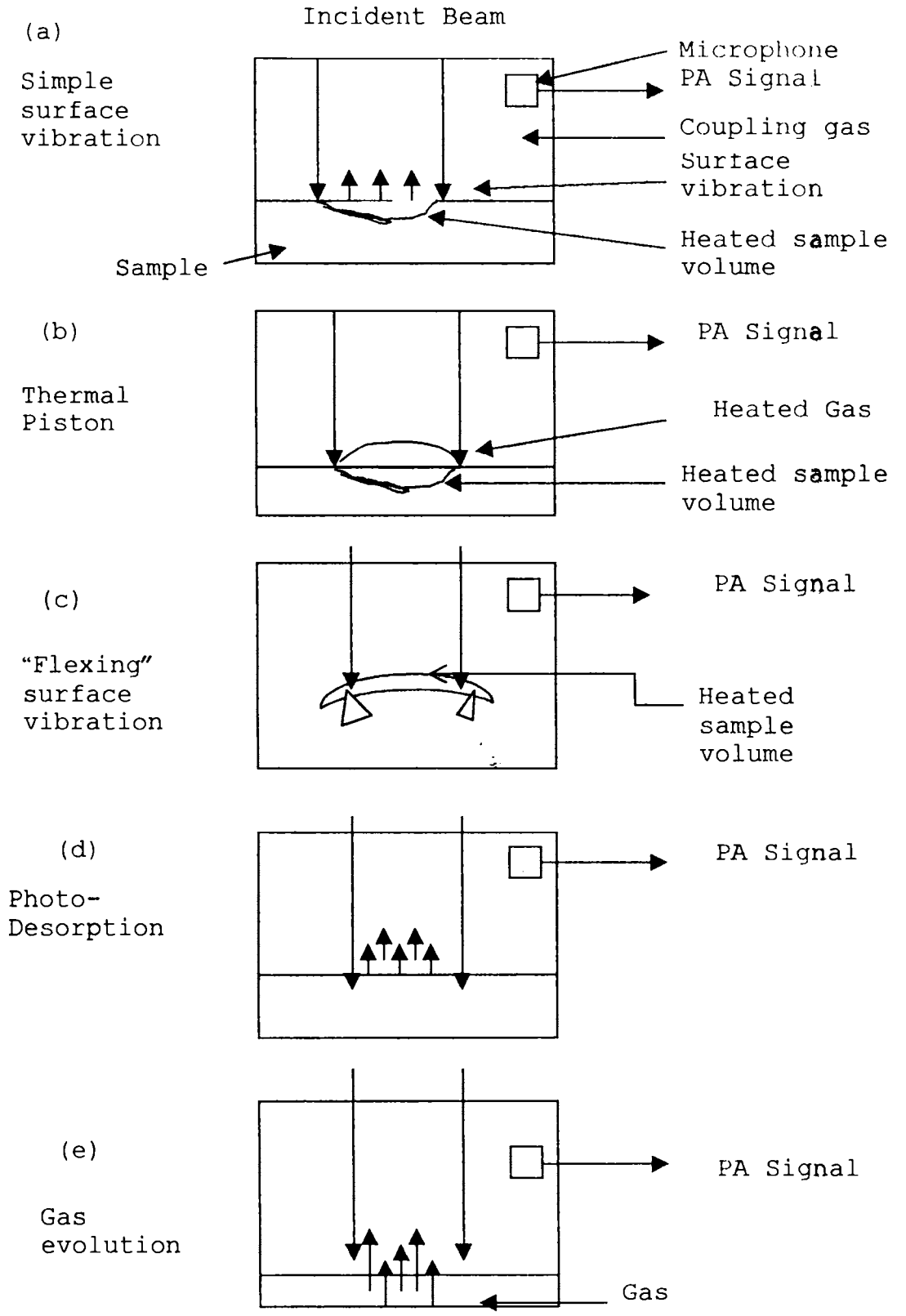

Fig. 1.2: Various possible cases of indirect PA Generation

Various possible causes of indirect PA generation is shown in figure 1.2 [22-24].

Photothermal (PT) heating due to the absorption of an excited beam at a surface can generate surface acoustic wave and affect the propagation of surface acoustic waves. The former effect is some times called PA Rayleigh surface wave generation while the latter can be called as surface wave probing of PT generation [25]. Indirect PA spectroscopy is discussed in this chapter.

In PA spectroscopy, the sample to be studied is often placed in a closed cell or chamber. In the case of gases or liquids the sample generally fills the entire chamber and in the case of solids, the sample fills only a small portion of the chamber and remaining portion is filled with a non-absorbing gas such as air. In order to detect the pressure variations in the chamber, a sensitive microphone is placed inside the chamber. The sample is illuminated with chopped monochromatic light using electromechanical choppers or intensity modulators. On absorbing the incident photons by the sample, the internal energy levels within the sample are excited and on de-excitation of these energy levels, all or part of the absorbed photon energy is converted in to heat energy through non-radiative de-

excitation process. In a gas this heat energy appears as kinetic energy of gas molecules, while in a solid or liquid, it appears as vibrational energy of ions or atoms. Since the incident radiation is intensity modulated, the heat generated with in the sample also will be modulated so as to produce a thermal wave or acoustic wave. The various steps involved in the process of PA signal generations are schematically shown in figure 1.3.

Since PA measures the internal heating of the sample, it clearly is a form of calorimetry as well as a form of optical spectroscopy. The classical calorimetric techniques based on the temperature sensors such as thermistors and thermopiles [26] have several inherent disadvantages for PA spectroscopy in terms of sensitivity, detector rise time and the speed at which measurements can be made. More suitable calorimetric technique measures the heat production through volume and pressure changes produced in the sample or in an appropriate transducing material in contact with the sample,

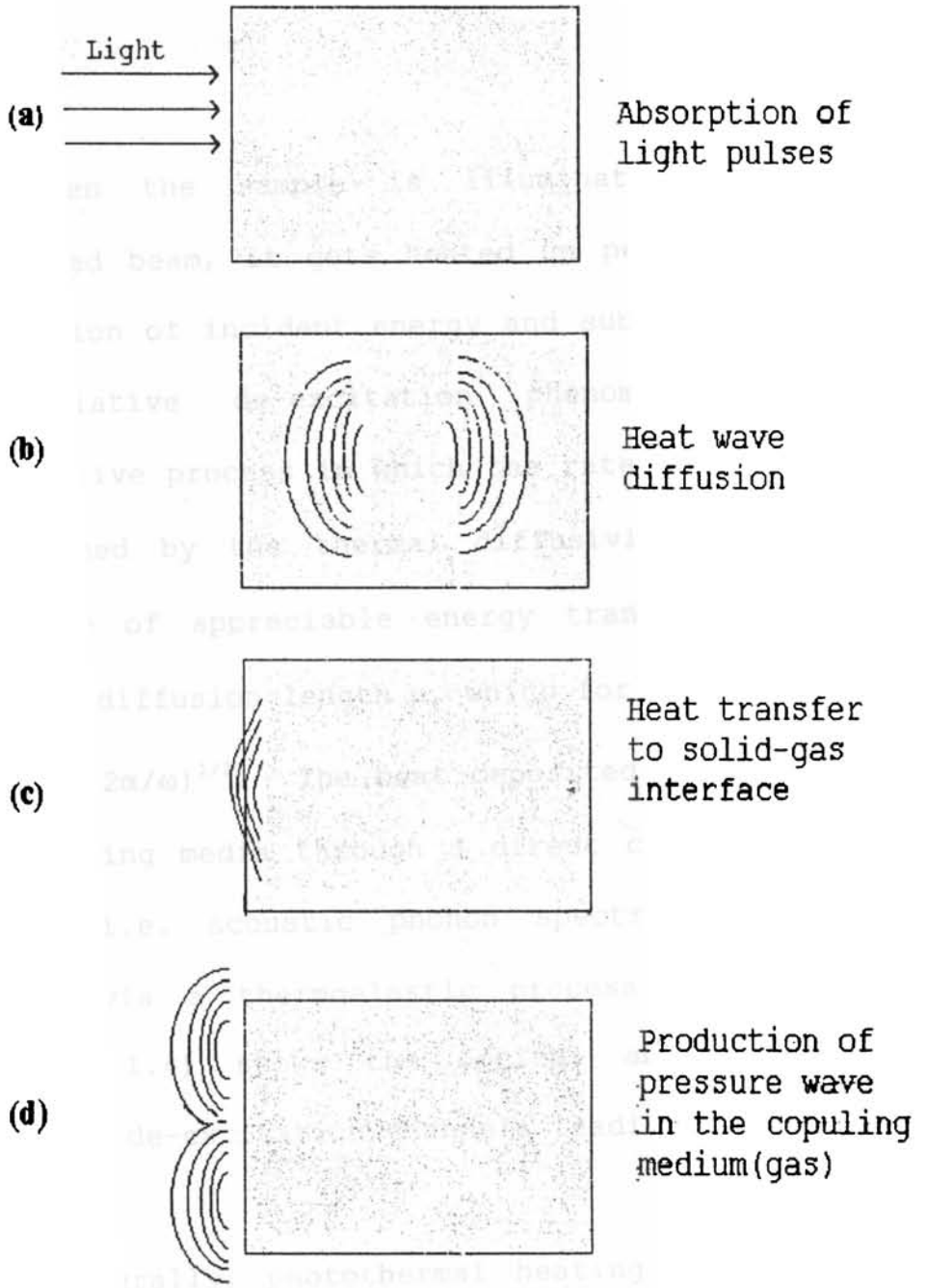

Fig. 1.3: Various steps involved in PA signal generation

1.2 DETECTION TECHNIQUES FOR PHOTOTHERMAL PHENOMENA

When the sample is illuminated by an intensity-modulated beam, it gets heated up periodically due to the absorption of incident energy and subsequent excitation and non-radiative de-excitation phenomena. This is a dissipative process in which the rate of energy transfer is determined by the thermal diffusivity $\alpha = k/\rho c$ and the distance of appreciable energy transfer is given by the thermal diffusion length μ, which for periodically deposited heat $\mu=(2\alpha/\omega)^{1/2}$. The heat deposited can be transferred to surrounding media through a direct coupling to vibrational modes (i.e. acoustic phonon spectrum) of the material, namely via a thermoelastic process. The block diagram (figure 1.4) shows the optical absorption and various possible de-excitation channels leading to PT effects.

Generally, photothermal heating of a sample leads to thermal and stress induced changes in the physical properties either of sample or of its surrounding medium. One can monitor several physical properties of the sample such as the sample surface displacement or the changes in

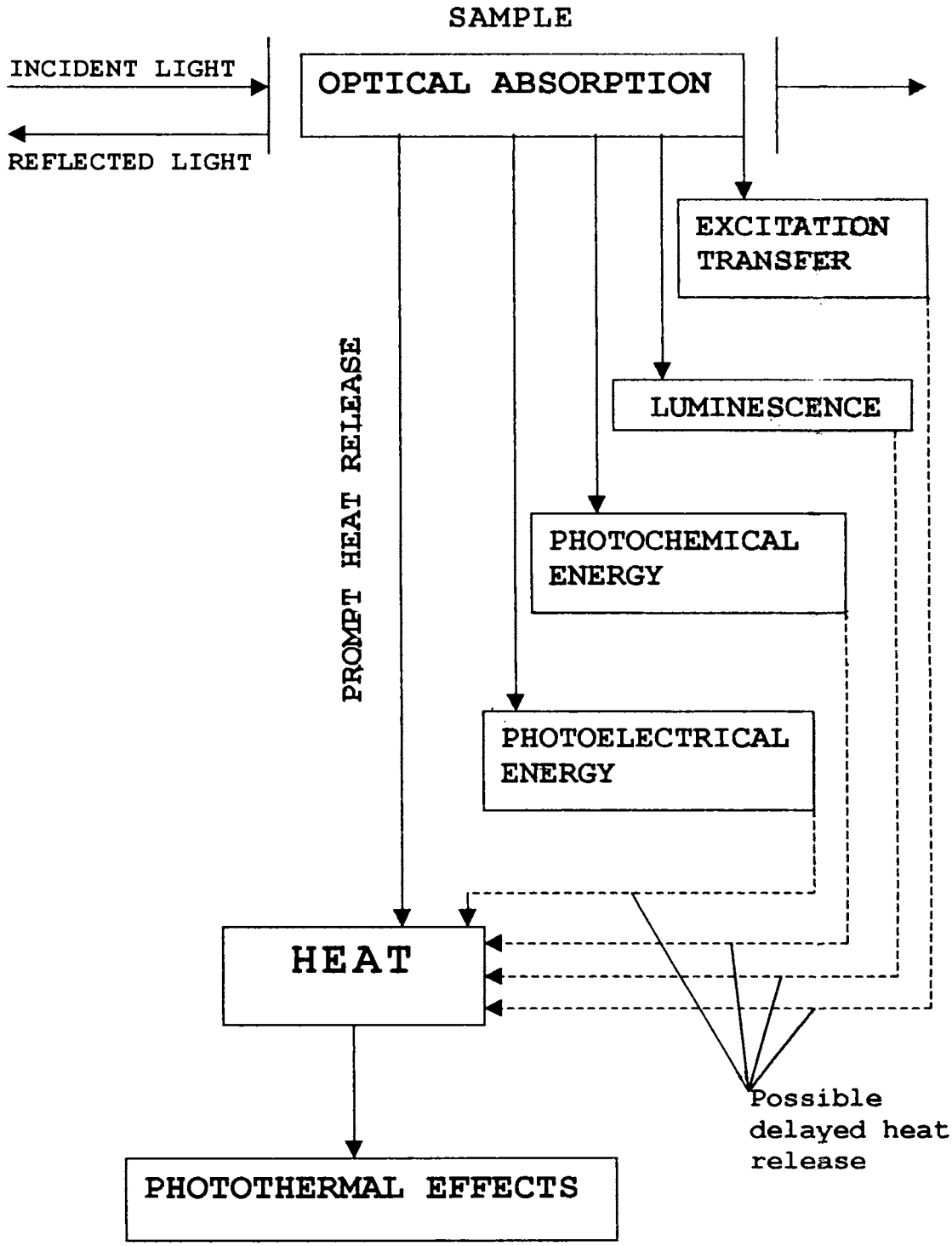

Fig. 1.4: Block diagram showing the optical absorption and various possible de-excitation channels leading to PT effects

the refractive index of both the sample and the surrounding medium to study the deposited heat.

The photothermal (PT) effects occur simultaneously with the cause or with time delays. The choice of a particular photothermal technique for a study and the signal detection methods will depend on the nature of the sample and its environment, the source used and the purpose of measurement. Detection methods can either be applied to the sample directly when it is called direct PT effect or to the coupling medium adjacent to the sample which is the indirect PT effect. The second method lies on the assumption that only the sample absorbs the indirect light but not the coupling medium. Some of the detection techniques are briefly described below.

1.2.1 ELECTRET MICROPHONE AND PIEZOELECTRIC DETECTION

The conventional P A microphone detection technique is a non-contact, remote sensing technique. When the sample is illuminated by intensity modulated beam, the internal heating occurs. In gaseous samples, the volume changes can be quite large as a result of internal heating. In these cases, a displacement sensitive detector such as a

capacitor microphone proves to be an excellent heat detector. With the availability of sensitive microphone and associated electronics, it is possible to detect temperature rise in a gas of 10^{-6} ^{o}C or a thermal in put of the order 10^{-9} cal/cm^{3} -sec. The disadvantage with a detector that responds to volume is that the response time is limited both by the transit time for a sound wave in the gas with in the cell cavity and by the low frequency response of the microphone. These two factors tend to limit the response time of the gas-microphone system to the order of 100 μ sec or longer [27].

In the case of solids or liquids, it is possible to measure the heat produced in the sample by means of a piezoelectric detector (usually, a lead zinconate titanate (PZT) ceramic) placed in intimate contact with the sample. These detectors can detect temperature changes of 10^{-7} ^{o}C to 10^{-6} ^{o}C, which for a particular solids or liquids corresponds to thermal inputs of the order of 10^{-6} cal/cm^{3}-sec. Since the volume expansion of solid or liquids is 10 to 100 times smaller than that of gases, the measurement of heat production with in the sample with a displacement sensitive detector such as microphone would be 10 to 100 times less sensitive than a pressure sensitive device such as a piezoelectric detector.

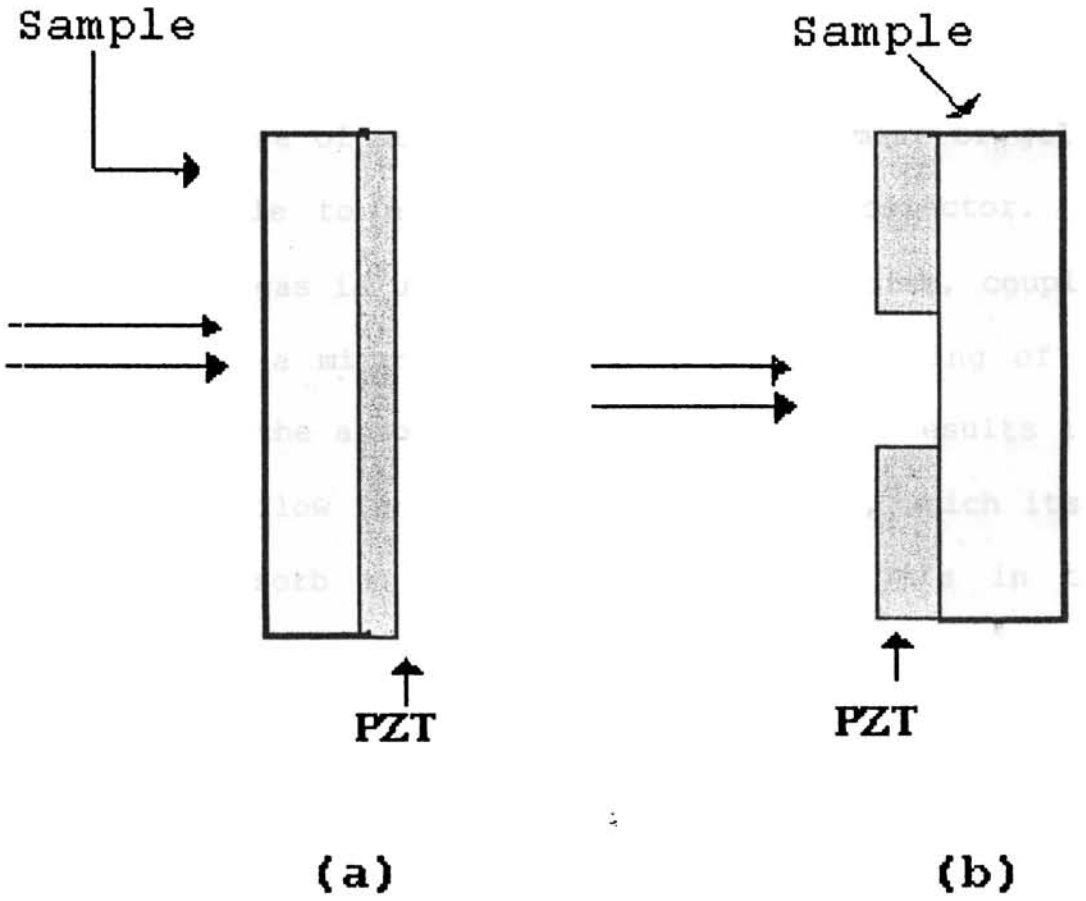

Fig. 1.5: Transducer assembly for PZT detection for solids (a) opaque and (b) transparent.

The transducer can be assembled in different ways depending on the particular experiment. Figure 1.5(a & b) shows two typical transducer assemblies for PZT detection in solid samples. For opaque samples, it is better to attach the PZT to the back surface of the sample (Figure 1.5a). For optically transparent samples transducer, in the form of an annulus, is located on either side of the sample. In the case of liquid samples the PZT transducer

is mounted on one of the walls of the liquid container [28-38].

In the case of powdered samples, or a smear or gel it is not possible to employ a piezoelectric detector. In these cases a gas is used as a transducing medium, coupling the sample to a microphone. The periodic heating of the sample due to the absorption of optical energy results in a periodic heat flow from the sample to the gas, which itself does not absorb the optical radiation. This in turn produces a pressure and volume change in the gas that drives the microphone. This method, though indirect, is quite sensitive for solids with large surface to volume ratios, such as powders, and is capable of detecting temperature rise of 10^{-6} to 10^{-5} ^{0}C in such samples or thermal inputs of about 10^{-6} to 10^{-5} cal/cm^{3}-sec. From the above discussion, it is evident that Photoacoustics is a combination of optical spectroscopy and calorimetry. Hence it will be appropriate to call this technique as photocalorimetry. But we use the term Photoacoustics because this method employs microphone or piezoelectric detectors for the detection of pressure variations in the coupling media.

1.2.2 PHOTOTHERMAL BEAM DEFLECTION (PBD)

This is a non-contact technique originally proposed by Boccara et al [39,40] and Fournier et al [41]. It is based on the concept of beam deflection by thermally induced changes in the refractive index. The absorption of a modulated pumping beam followed by the diffusion of the deposited heat causes a gradient in the refractive index in a thin layer of gas (or liquid) adjacent to the sample surface. A second Beam (say, tangential to the sample surface) can probe this refractive index gradient and its deflection can be related with the sample surface temperature. As the increase of the sample surface temperature depends on the optical absorption coefficient of the sample as well as on its thermal properties, both spectroscopic and thermal characterization studies can be conducted by measuring the deflection of the probe beam [42-44]. Assuming that the probe beam passes through the coupling medium parallel to the sample surface at a distance x from the surface, it will be deflected by an angle ϕ from its original path (Figure 1.6). For small deflections, ϕ is given by [39,42,44]

$$\phi = (L/n_o)\,[\partial n/\partial T]_{T_o}\,[\partial T_g/\partial x]_{x=x_o} \qquad (1.1)$$

where $T_g(x,t) = \theta \exp.(-\sigma_g.x).\ \exp.(j\omega t)$ is the temperature distribution in the coupling medium(gas), n_o is the refractive index of the gas at ambient temperature (T_o) and L is the length of the sample illuminated by the pump beam.

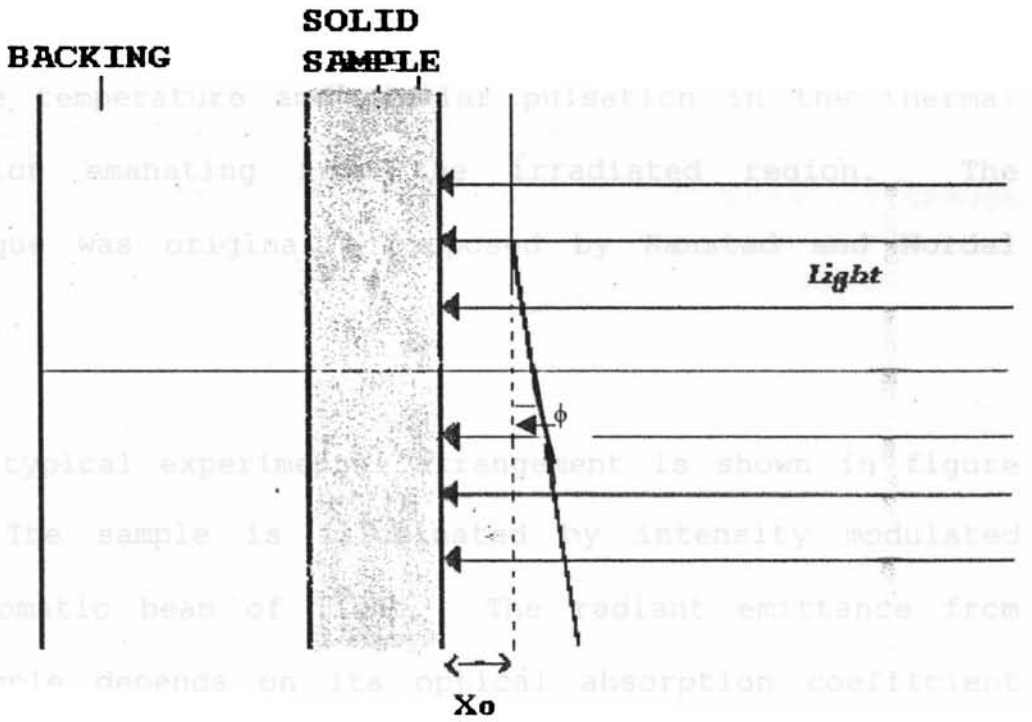

Fig. 1.6: Typical PBD experimental configuration

The PBD technique has been employed in the measurement of optical absorption coefficient of thin films, solids, liquids and gases [39-45] and more recently to a quite diverse class of problems ranging from imaging to scanning microscopy.

1.2.3 PHOTOTHERMAL RADIOMETRY AND OTHER REMOTE SENSING TECHNIQUES

Photothermal radiometry (PTR) is another example of a non-contact technique in which the specimen is irradiated with amplitude modulated light. This results in pulsating surface temperature and similar pulsation in the thermal radiation emanating from the irradiated region. The technique was originally proposed by Kanstad and Nordal [46-49].

A typical experimental arrangement is shown in figure 1.7. The sample is illuminated by intensity modulated monochromatic beam of light. The radiant emittance from the sample depends on its optical absorption coefficient (β). The thermal radiation from the illuminated area is collected by an appropriate optical system and focused on an infrared detector. To prevent the scattered radiation from reaching the detector, an optical filter is employed and the signal is processed by a lock-in- amplifier whose out put is recorded as a function of incident light wavelength. The experiment can also be performed using pulsed laser with boxcar or transient detection.

The theoretical description of PTR signal for both CW and pulsed excitation is given by several authors [50-55]. By Stefan - Boltzmann law, the total radiant energy emitted from a body of emissivity 'e' at temperature T is given by

$$W = e\sigma T^4 \qquad (1.2)$$

where σ is the Stefan's constant. For a temperature change δT due to the absorption of energy E from a radiation of wavelength λ, the change in radiant energy is

$$\delta W = 4\sigma e T^3 \delta T \qquad (1.3)$$

The PTR signal in a broadband detector over the entire thermal radiation spectrum may be written as

$$S = 4\sigma e T^3 \, A \, \mathrm{Sin}^2\theta \, dT \qquad (1.4)$$

where A is the detector area and θ the collecting angle.

The remote sensing and non-contact nature of this technique enables the characterization of materials like nuclear fuels [56]. Pulsed PTR has found profound applications in the thermal analysis of composite [57,58]

and multi-layered materials. It is also well suited for scanning and imaging of the surfaces, with respect to spectral characterization as well as thermal /material properties [59-68]. The thermal wave imaging was originally developed by Bausse and recently reviewed by Reynolds in the context of industrial materials applications.

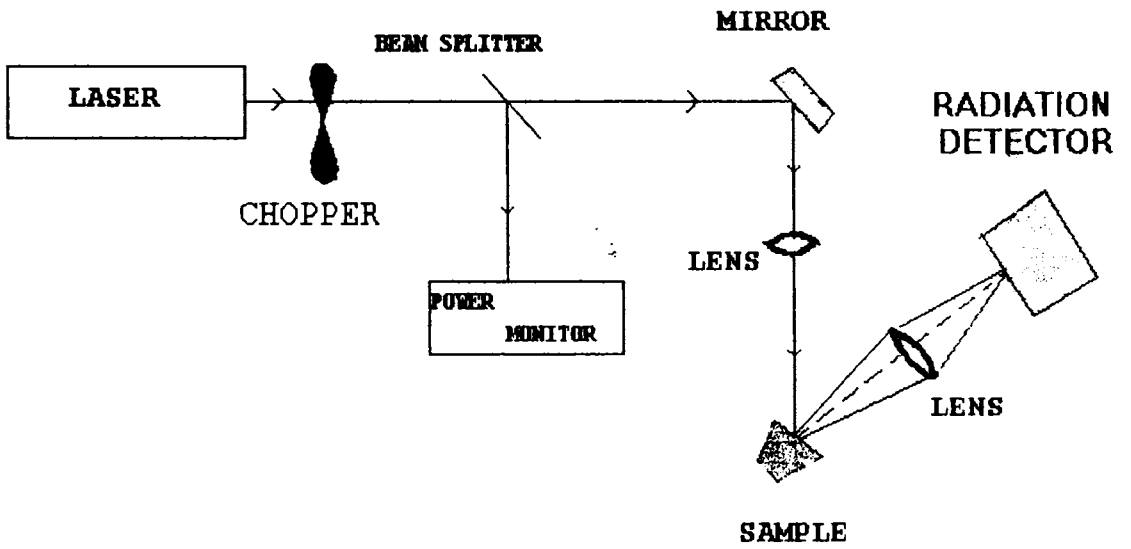

Fig.1.7: Experimental arrangement for PTR measurement

Apart from PTR and PBD techniques some other remote sensing techniques have also been proposed. These include interferometric detection [69-74] of gas displacement of the sample surface due to the modulated heating and thermal lensing detection [75-79].

1.2.3.1 PHOTOTHERMAL DISPLACEMENT SPECTROSCOPY(PDS)

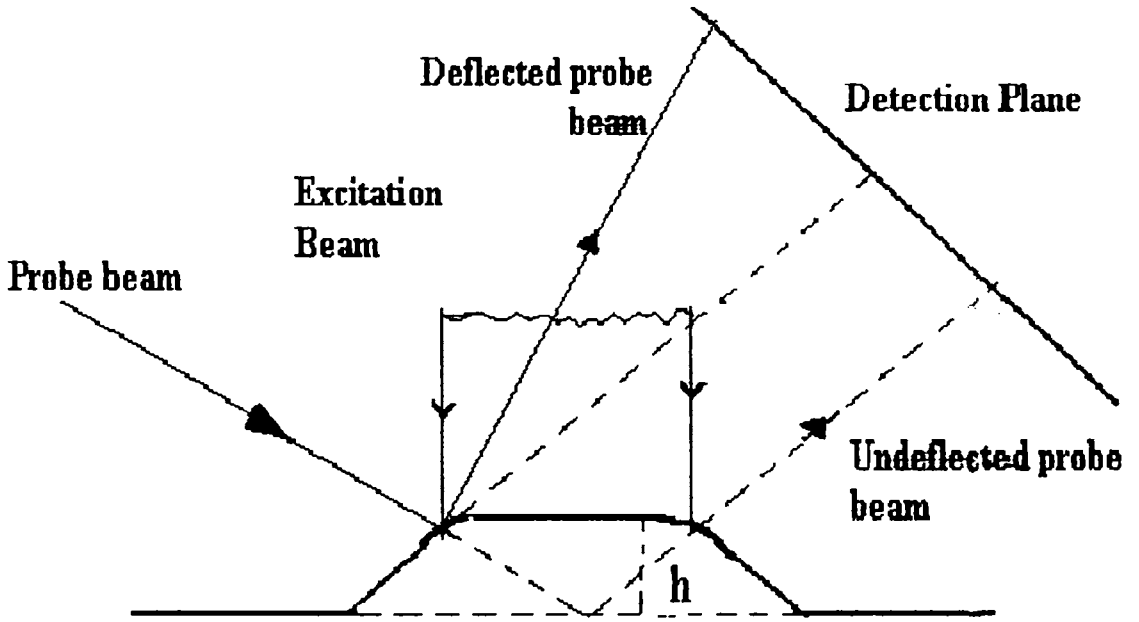

Fig.1.8: The PDS principle

The basic principle involved in PDS is that whenever a sample gets heated due to photothermal effect, the surface expands due to thermal effect thereby getting displaced. The magnitude of displacement is related quantitatively to the optical absorption coefficient [74,75]. A schematic representation of this technique is shown in figure 1.8.

For an absorbing layer of thickness, l, on a transparent substrate, the photothermal surface displacement h is given by

$$h = \alpha_{th}\beta P / 2Afc\rho \qquad (1.5)$$

where α_{th} - thermal expansion coefficient, β - the fraction of the absorbed light, P - incident power, f - modulating frequency, A - area of optically illuminated region, ρ - the mass density and c - specific heat capacity.

1.2.3.2 INTERFEROMETRIC DETECTION

Here the sample is kept in one of the arms of a Michelson interferometer and the position of the mirror in the other arm is modulated to overcome thermally induced drifts and the effect of mechanical vibrations on the interferometers (Figure 1.9). It is reported that the beam reflection approach is easier to implement and serves long term stability requirement [74].

1.2.4 PHOTOPYROELECTRIC DETECTION (PP)

This is another example of contact type photothermal detection technique. It is based on the use of pyroelectric thin films to detect the temperature change in the sample when exposed to modulated heating. In a pyroelectric material a temperature fluctuation induces an

electrical current proportional to the rate of change of its average heat content [81-86].

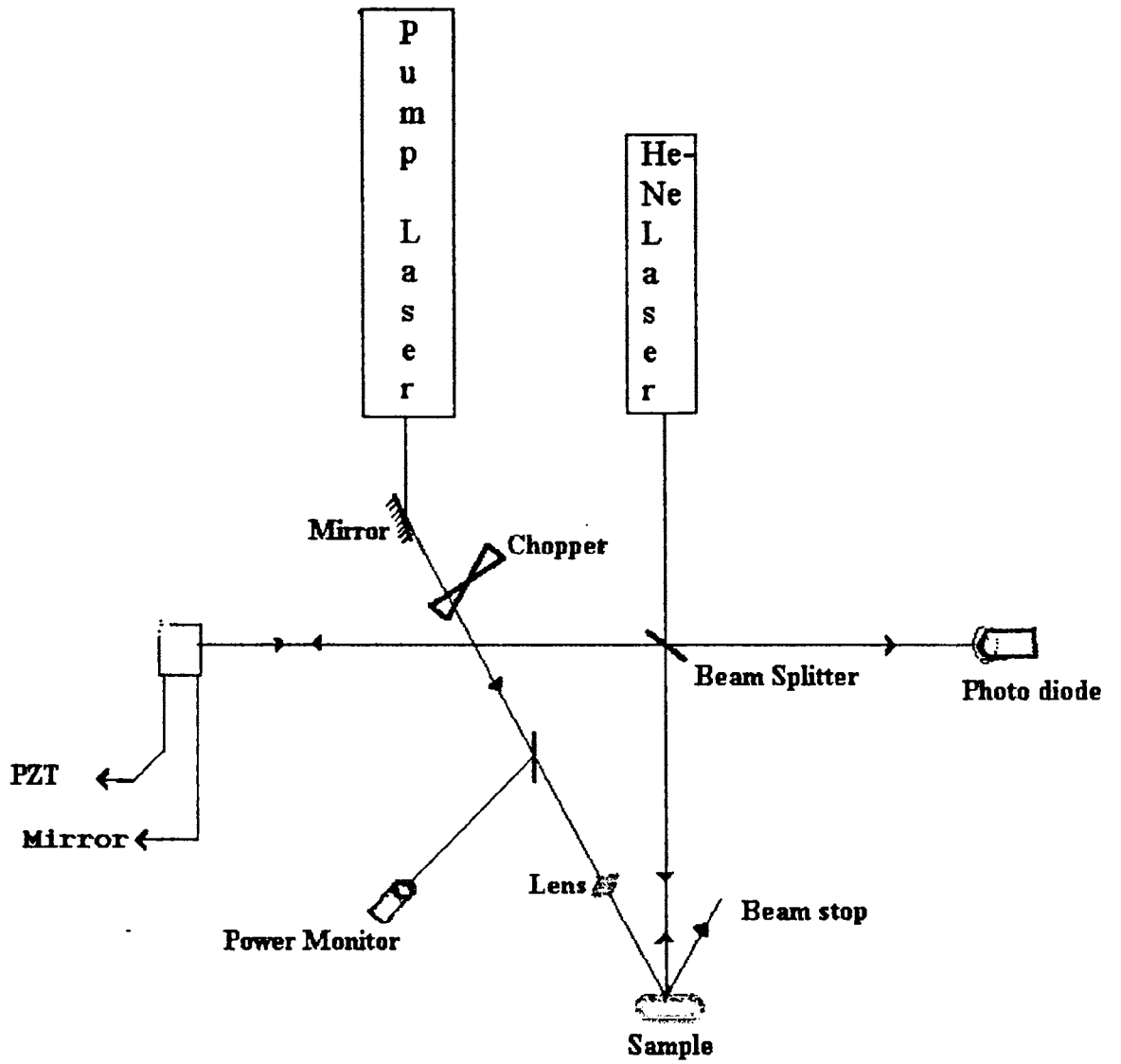

Fig. 1.9: PDS-Interferometric method

A typical experimental arrangement of PP technique is shown in figure 1.10. It consists of thin pyroelectric films (e.g. poyvinyldene difluoride, PVF_2) in intimate contact with the sample on which intensity modulated monochromatic beam is incident. The absorption of light and the subsequent non-radiative de-excitation within the sample results in temperature fluctuation which through heat diffusion reaches the pyroelectric films. As a result of this temperature fluctuations the pyroelectric material changes its polarization and an electric current is induced in the detector [87]. The induced current in the pyroelectric film is

$$i_p = -p\ A\ [d\Delta T/\ dt] \qquad (1.6)$$

where p is the pyroelectric constant of the material, A - the detector area and ΔT - the temperature fluctuation.

PP detection finds applications in spectroscopic studies [81], thermal diffusivity measurements [84,85,88,89], phase transition studies [90], photovoltaic conversion efficiency of solar cells [91] scanning microscopy [92] etc.

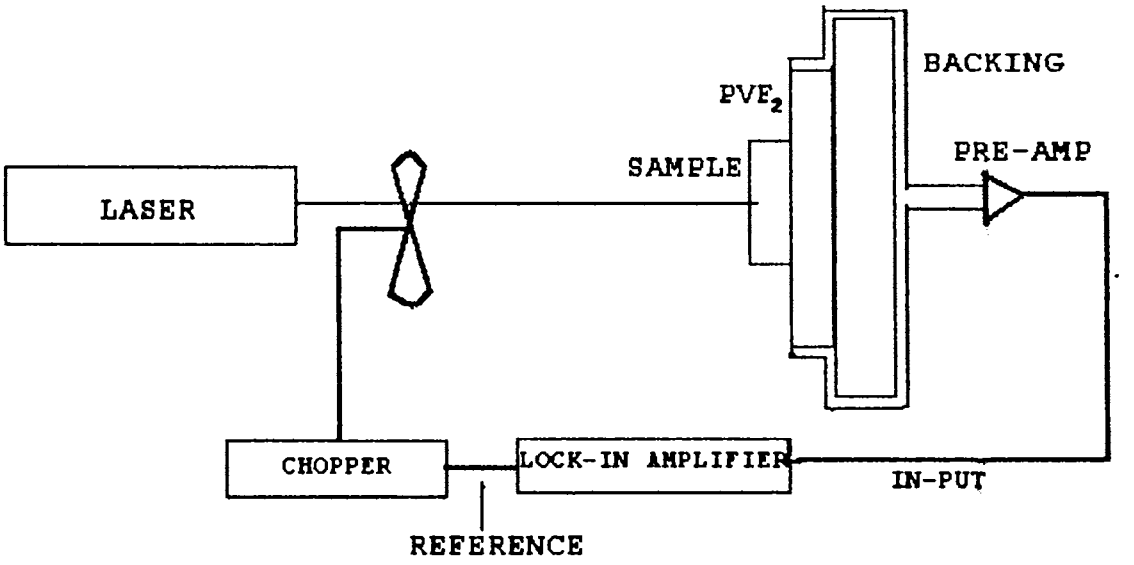

Fig.1.10: Typical experimental set-up for photopyroelectric detection.

1.2.5 THERMAL LENSING SPECTROSCOPY

Photothermal heating of a sample produces refractive index change in the coupling medium. A measure of the change in the refractive index profile in the sample or coupling medium is a convenient technique of material characterisation. The thermal lensing effect was first observed by Gordon in 1964 [93].

When the sample is illuminated by a pump beam, it results in refractive index change. The probe beam passing through this refractive index gradient

gets diverged as if it had passed through a diverging lens. As a result intensity of the probe beam changes. Under certain circumstances the medium acts like a converging lens also. The focal lengths of the astigmatic thermal lens in the x and y direction are given by

$$1/f_x = (\partial n/\partial t)\int(\partial^2 T/\partial x^2)\,ds \qquad (1.7)$$

$$1/f_y = (\partial n/\partial t)\int(\partial^2 T/\partial y^2)\,ds \qquad (1.8)$$

Where T(x,y,t) is the temperature distribution near the heated sample and s the signal.

Since the thermal lensing effect is proportional to the laser intensity, sensitive absorption measurements, as small as 10^{-4} can be carried out [94,95]. The technique is widely used in liquid chromatography [96], energy transfer studies [97-99], bulk thermal properties [100,101] and for the measurement of absolute quantum yield [102]

1.3 ADVANTAGES OF PHOTOACOUSTIC SPECTROSCOPY

Since the photoacoustic signal is generated only after the absorption of optical signal, the light that is transmitted or elastically scattered by the sample does not interfere with the photoacoustic spectroscopic (PAS) measurements. This is of greater importance when one works with essentially transparent media, such as polluted gases that have few absorbing centers. Since the method is insensitive to the scattered radiation it is possible to obtain optical absorption data on highly scattering materials such as powders, amorphous solids, gels and colloids. Another advantage is the capability of obtaining absorption spectra of optically opaque samples, since the method does not depend on the detection of photons. Coupled with this is the capability, unique to photoacoustic spectroscopy, of performing non-destructive depth profile analysis of absorption as a function of depth in to a material. The PA effect results from a radiation-less energy conversion process and is therefore complementary to radiative and photo chemical processes. Thus PAS can be used as a sensitive, though indirect method for studying the phenomena of fluorescence and photosensitivity in matter.

Table 1.1: Comparison of various techniques for weak optical absorption measurement

TECHNIQUES	EXAMPLES	CONDITIONS OR RESTRICTIONS	TYPICAL SENSITIVITY FOR ABSORPTION (cm^{-1})
Gross subtraction (subtract the intensity of the emergent beam from that of incident beam)	Transmission Reflections	Transmitted or Reflected beam available for measurement	10^{-2} to 10^{-4}
Net macroscopic effect (measure macroscopic effects produced by the absorbed energy)	PT Calorimetry Photoacoustics Probe-beam refraction/reflection Photothermal radiometry Photoconductivity Optogalvanic effect	Sample should produce heat or other macroscopic effect of sufficient efficiency. Intermolecular collisions or interactions usually needed.	10^{-5} to 10^{-10}
Net microscopic effect (measure quantum effects after exciting a molecule)	Fluorescence Photoionization Quantum-state chanre	Sample is placed in special environments (e.g. Vacuum) so that the detected quantum effects are not quenched	$< 10^{-10}$

Generally, since all PT effects appear only after the absorption of the incident light, the technique is one of 'zero background' i.e. the signal generated is only from the sample. Hence the technique is superior to the conventional transmission or absorption technique where the intensity of the transmitted or absorbed light is subtracted from the intensity of the incident light to get the absorbed light energy. In other words the conventional method is a 'subtractive' method. However, the technique is less sensitive for the detection of quantum microscopic effects. A comparison of various techniques for weak optical absorption is given in Table 1.1.

1.4 APPLICATIONS OF PHOTOACOUSTIC SPECTROSCOPY

Photoacoustics is much more than spectroscopy. It is a photocalorimetric method that measures how much of the electromagnetic radiation absorbed by the sample is actually converted into heat. As such photoacoustics can be used to measure the absorption or excitation spectrum, the lifetime of excited states, and the energy yield of radiative processes.

1.4.1 DE-EXCITATION PROCESSES

The PA effect is sensitive only to the heat producing de-excitation processes that occur in a sample after absorption of modulated light. If E_o is the energy absorbed by a given system, heat produced is given by

$$Q = E_o \ (1- \sum \gamma_i) \qquad (1.9)$$

where γ_i are the conversion efficiencies of the several non-thermal de-excitation channels. Since the PA signal is proportional to Q, it can be written as

$$S = S_o \ (1- \sum \gamma_i) \qquad (1.10)$$

where S_o represents the PA signal if only the thermal de-excitation channel is active. Equation 1.10 tells that the PA signal is complementary to the other photothermal energy conversion processes.

The PA technique is useful in the study of photovoltaic de-excitation process in semiconductors. In such process the part of the incident radiation is converted in to electrical energy resulting in a

corresponding reduction in the thermal energy produced and hence the PA signal depends upon the energy conversion efficiency of the process [103]. In a phtovoltaic device, the phtovoltaic conversion efficiency $\gamma(R_L)$ is a function of the external electrical load R_L. If the phtovoltaic de-excitation process dominates, equation 1.10 can be written as

$$S(R_L) = S_o\ [1- \sum \gamma(R_L)] \qquad (1.11)$$

where S_o is a constant for fixed cell geometry, optical wavelength and intensity of incident light. Under open circuit conditions (oc), the photovoltaic device has zero energy conversion efficiency. i.e. $\gamma = 0$.

$$\therefore\ S(oc) = S_o \qquad (1.12)$$

Combining eqn. 1.11 and 1.12

$$\gamma(R_L) = 1 - S(R_L)/S(oc) \qquad (1.13)$$

Thus, the photovoltaic conversion efficiency can be readily measured as a function of wavelength (λ) as well as load resistance, using PA effect. The PA techniques are used to determine the photoconductive quantum efficiency of

a thin organic dye film [104] and to determine photocarrier generation quantum efficiency of schottky diode [105].

The technique is also extended to photochemical studies [9], photodissociation of molecule [106] and photo gas generation and consumption [107].

1.4.2 IMAGING AND DEPTH-PROFILE

Attention has also turned to the possibility of using PA effect for imaging applications. By scanning the amplitude-modulated focused light across the surface of the sample and recording the amplitude and phase of the photoacoustic response, it is possible to construct an image that is characteristic of the optical and thermal properties with in a part of the sample. By varying the chopping frequency sub-surface imaging can be done and there by detect the flaws, if any, with in the sample [108-116].

PAS can be used for depth profiling, thickness measurements of thin film samples and for determining the number of layers of different materials in a multi-layered structure [117-121]. The potentialities of PA depth-profile analysis were originally demonstrated by Adams and

Kirkbright [122-123]. This is due to the fact that only the heat generated with in a depth of one thermal diffusion length of the sample contributes to the PA signal. Since the thermal diffusion length is a function of chopping frequency, one can have depth profile analysis of the sample by varying the chopping frequency.

1.4.3 MICROSCOPY

PA microscopy is a rapidly expanding area because of its potential applications in thin-film technologies, medical diagnostics, and non-destructive testing, to name a few examples. In addition to the gas microphone detection, several other detection techniques have been used in photothermal microscopy. These include PZT [124-128], PBD [39,42,129,130] and PTR [63-68] detection as well as photothermal surface displacement [130] measurements.

Photothermal microscopy consists basically of generating a localized heating in a sample due to the absorption of intensity modulated energetic beam and scanning the heating position across the sample. The thermal waves resulting from the absorption of the periodic incident beam propagates from the heated regions and undergo reflections and scattering when they encounter

regions of different thermal and geometrical characteristics. In this way, as the heating beam is scanned across the sample any surface or subsurface change in the characteristics of the sample can be monitored as a change in the thermal wave signal.

1.4.4 MICROWAVE AND INFRARED SPECTROSCOPY

The use of PA detection was shown to be of great advantage in spectroscopic studies. Originally these studies were carried out in the UV -Visible region of the electromagnetic spectrum. Such studies can be carried out at any wavelength provided, the material under study has absorption in the wavelength used. Several authors have used PA detection for microscopic absorption studies over a wide range of materials [131-140]. These include PA detection of ferromagnetic resonance (FMR) of the metallic and nonmetallic sample [132-144], spin wave resonance in thin metallic film [135] and paramagnetic resonance (EPR) in organic and inorganic substances [136-138].

The photon energy and hence the intensity of the PA effect decreases in going from the visible to the IR range, Spectral features in this region can be directly related to molecular structure. The use of PAS in the near IR region

can be carried out using the same instrumentation as for UV-Visible region. The absorption bands observed in the near IR region for solid and liquid samples are attributable to overtones and combinations of the fundamental vibrational modes of particular bands. Most frequently observed bands are those relating to hydrogenic systems e.g.: -CH, -OH, and -NH. The PAS applications in the near IR have been well documented for analytical [141-144] and surface studies [141,145,146].

1.4.5 CHEMICAL STUDIES

PAS is ideally suited to catalytic studies since catalytic substances are by their very nature difficult to investigate by conventional spectroscopic means. These difficulties arise from the fact that in heterogeneous catalysis the catalyst is often in the form of a fine powder

1.4.6 SURFACE STUDIES

PAS can be used in the study of adsorbed and chemisorbed molecular species and compounds on the surface of metals, semiconductors and even insulators. Such studies can be done at any wavelength, provided the

substrate is non-absorbing at that wavelength. The PAS experiment gives optical absorption spectra of the adsorbed or chemisorbed compounds on the surface of the substrate [141-147].

1.4.7 PAS IN BIOLOGY

Many biological materials occur naturally in a soluble state. But some are insoluble and opaque, which can be studied using PA techniques. Thus PAS holds great promise as both a research and diagnostic tool in biology and medicine [148-152]. PA depth profiling has been used by several workers in the study of pigment [121], distribution of lobster shell, β-carotene in skin [153], and the photosynthetic energy storage in hetero system.

One of the most exciting areas of PA studies lies in the field of medicine. One can use PAS to obtain optical data on medical specimens that fails with conventional methods such as in bacterial studies, tissue studies, hydration studies, maturation studies, etc. In the area of Dermatology PAS has been used to study the effects of active drugs in the skin [157] and to determine the drug diffusion rate in human skin. The thermal properties and water content of the skin can also be found out using PA

technique. In the area of food quality control some applications of PAS on the monitoring of food adulterant have also been reported [158,159].

The PA process depends not only on the optical properties of the sample but also on the thermal and geometrical properties as well. We have used the method for the measurement of thermal diffusivity [160-162], the details of which are given in subsequent chapters. PA technique can also be used to study fluorescence, quantum yield, nonlinear optics, phase transition studies etc[163-174]

1.5 CONCLUSION

Various photothermal phenomena and their detection techniques are discussed briefly. Applications of this technique in various fields of science and technology are also given. Advantages of this technique over the conventional technique are also discussed.

REFERENCES

[1] A.G. Bell, Am. J. Sci., 20 (1880) 305.

[2] A.G. Bell, Philoss. Mag., 11 (1881) 510.

[3] A. Rosencwaig and A. Gersho, J. Appl. Phys., 47 (1975) 64.

[4] A. Rosencwaig, Science, 181 (1973) 657.

[5] A. Rosencwaig, Phys. Today, 28 (1975) no. 9,23.

[6] A. Rosencwaig, Anal. Chem., 47(6) (1975) 502A.

[7] A. Rosencwaig, Rev. Sci. Instrum., 48 (1977) 1133 .

[8] A. Rosencwaig, Opt.Commun., 7 (1973) 305.

[9] A. Rosencwaig, Anal.Chem., 47 (1975) 592.

[10] A. Rosencwaig, Advances in Electronics and Electron Physics, Vol.46 (1978, L.Marton Ed.).

[11] G.C. Wetsel. Jr and F.A. Mac Donald, Appl. Phys, Lett., 30 (1977) 252.

[12] A.C. Tam, C.K.N. Patel and R.J. Kerl, Opt. Lett., 4 (1979) 81.

[13] A.C. Tam, Rev.Modern Phys., 56 (1986) 2.

[14] C.L. Cesar, H.Vargas, and L.C.M. Miranda, Appl. Phys. Lett., 32 (1978) 554.

[15] P. Bosquet, Spectroscopy and Its Instrumentation, Crane- Russack, New York (1971).

[16] P.A Wilks, Jr, and T. Hirschfeld, Appl. Spectrosc, Rve.1 (1968) 99.

[17] G.B. Wright, Light scattering of Solids, Springer-Verlag, Berlin and New York (Ed)(1969).

[18] V.S. Teslenko, 1977, Kvant. Elektron (Moscow) 4, 1732 [Sov. J. Quantum Electron,7,981 (1977)]

[19] A. Atalar, Appl. Opt,19 (1980) 3204.

[20] A.C. Tam, and H.Coufal, J.Phy, (Paris) Colloq. C6, 9, 1983b.

[21] A.C. Tam, 1983 in Ultrasensitive Laser Spectroscopy, edited by D. Kliger (Academic, New York), Chapter.1.

[22] F.A. Mc Donald and G.C Wetsel Jr, J. Appl. Phys, 49 (1978) 2313.

[23] J.P. Monchalin, L. Bertrand, G. Rousset and Flepoutre, J. Appl. Phys, 56 (1984) 190.

[24] T. Somasundaram and P Ganguly, J. Phys Paris) coloq. C6 (1983) 239.

[25] R.E. Lee and R.M. White, Appl. Phys. Lett, 12 (1968) 12.

[26] B. Gelernt, A. Findeisen and J.J. Pook, J. Chem. Soc. Faraday TransII, 70 (1974) 939.

[27] J. Shida, H. Takahashi and K.Oikawa, Tantala 41 (1994) 1861.

[28] J. B. Callis, J. Res. Natl. Bur. Stand. A 80 (1976) 413.

[29] A. Hordvik and H. Scholssberg, Appl. Opt. 16 (1977) 101; 16 (1977) 2919.

[30] W. Lahmann, J.J. Ludewig and H. Welling, Chem. Phys. Lett, 45 (1977) 177.

[31] S. Oda, T. Sawada and K. Kamada, Anal. Chem., 50 (1978) 865.

[32] M.M. Farrow, R.K. Burnham, M. Auzaneau, S.L. Olsen, N. Pudie and E.M. Eyring, Appl. Opt, 17 (1978) 1093.

[33] P.Helander, J. Photoacoust 1 (1982) 103.

[34] P.Helander, J. Photoacoust 1 (1982) 203.

[35] P.Helander and I. Lundsrom, J. Appl. Phys.,54 (1983) 5069.

[36] P.Helander, J. Photoacoust 1 (1982) 252.

[37] P.Helander, J. Appl. Phys., 59 (1986) 3339.

[38] D.H. Mc Queen, J. Phys. E., 16 (1983) 738.

[39] A.C. Boccara, D. Fournier and J. Badoz, Appl. Phys. Lett., 36 (1980) 130.

[40] A.C. Boccara, D. Fournier, W. Jackson and N.M. Amer, Opt. Let., 5 (1980) 377.

[41] D. Fournier, A.C. Boccara, N.M. Amer and R. Gelach, Appl. Phys. Lett, 37 (1980) 519.

[42] J.C. Murphy and L.C. Aamodt, J. Appl. Phys., 51 (1980) 4580.

[43] W.D. Jackson, N.M. Amer, A.C. Boccara and D. Fournier, Appl. Opt., 20 (1980) 1331.

[44] A. Mandelis, J. Appl. Phys., 54 (1983) 3404.

[45] B.S.H. Royce, F. Sanchez-Siencio, R. Goldstein, R. Muratore, R. Williams and W.M. Yim, Bull. A. Phys. Soc., 27 (1982) 243.

[46] S.O. Kanstad and P.E. Nordal, Power Technol., 22 (1978) 133.

[47] P.E. Nordal and S.O. Kanstad, Phys. Scr., 20 (1979) 659.

[48] P.E. Nordal and S.O. Kanstad, Appl. Phys. Lett., 38 (1981) 486.

[49] S.O. Kanstad and P.E. Nordal, Appl. Surf. Sci., 6 (1980) 372.

[50] R. Santos and L.C.M. Miranda, J. Appl. Phys., 52 (1981) 4194.

[51] R.D. Tom, E.P. O'Hara and D. Benin, J. Appl. Phys., 53 (1982) 5392.

[52] A.C. Tam and B. Sullivan, Appl. Phys. Lett., 43 (1983) 333.

[53] W.P. Leung and A.C. Tam, Opt. Lett., 9 (1984) 893.

[54] A.C. Tam, Infrared Phys., 25 (1985) 305.

[55] S.O. Kanstad and P.E. Nordal, Can. J. Phys., 64 (1986) 1155.

[56] H.W. Deen and W.D. Wood, Rev. Sci. Instrum., 33 (1962) 1107.

[57] D.L. Balageas, A.A. Deom and D. Boscher, Mat. Eval., 45 (1987) 348.

[58] D.L. Balageas, J.C. Krapez and P. Cielo, J. Appl. Phys., 59 (1986) 348.

[59] A. Lehto, J. Jaarinen, T.Tiusanen, M. Jokinen and M. Luukkala, Electron Lett., 17 (1981) 364.

[60] D.P. Almond, P.M Patel and H. Reiter, J. Physique coll. C6, 44 (1983) 491.

[61] P. Cielo, J. Appl. Phys., 56 (1984) 230.

[62] H. Ernert, F.H. Dacol, R.L. Melcher and T. Baumann, Appl. Phys. Lett., 44 (1984) 1136.

[63] G. Bausse, Infrared Phys., 20 (1980) 419.

[64] G. Bausse, in :Scanned Image Microscopy ed E. Ash (Academic Press, New Yorc, 1980).

[65] M. Luukkala, in :Scanned Image Microscopy ed E. Ash (Academic Press, New Yorc, 1980).

[66] G. Bausse, Appl. Opt., 31 (1982) 107.

[67] G. Bausse and K.F. Renk, Appl. Phys. Lett., 42 (1983) 336.

[68] G. Bausse and P. Eyerer, Appl. Phys. Lett., 34 (1983) 355.

[69] J. Stone, Appl. Opt., 12 (1973) 1828.

[70] A. Hordvik, Appl. Opt., 16n (1977) 2827.

[71] Y. Othsuka and K. Itoh, Appl. Opt., 18 (1979) 219.

[72] S. Ameri, E.A. Ash, V. Neuman and C.R. Petts, Electron Lett., 17 (1981) 357.

[73] L.C.M. Miranda, Appl. Opt., 22 (1983) 2882.

[74] M.A. Olmstead, N.M. Amer, S. Kohn, D. Fournier, and A.C. Boccara, Appl. Phys. A, 32 (1983) 141.

[75] R.C.C. Leite, R.S. Moore and J.R. Whinnery, Appl. Phys. Lett., 5 (1964) 141.

[76] J.R. Whinnery, Acc. Chem. Res., 7 (1974) 225.

[77] R.L. Swofford and J.A. Morrel, J. Appl. Phys., 49 (1978) 3667.

[78] S.J. Sheldon, L.V. Knightand J.M. Thorpe, Appl. Opt., 21 (1982) 1663.

[79] L.C.M. Miranda, Appl. Phys., 32 (1983) 87.

[80] M.A. Olmstead, N.M. Amer, S. Kohn, Bull. Am. Phys. Soc., 27 (1982) 227.

[81] H. Coufal, Appl. Phys. Lett., 44 (1984) 59.

[82] A. Mandelis, Chem. Phys. Lett., 108 (1984) 388.

[83] A. Mandelis and M. Zver, J. Appl. Phys., 57 (1985) 4421.

[84] C.C. Ghizoni and L.C.M. Miranda, Phys. Rev, B, 32 (1985) 8392.

[85] H. Coufal and P. Hefferle, Appl. Phys. A, 38 (1985) 213.

[86] H. Coufal, J. Vac. Sci. Technol. A, 5 (1987) 2875.

[87] S.B. Lang, Source book of Pyroelectricity (Gordon and Breach, London, 1974).

[88] P.K. John, L.C.M. Miranda and A.C. Rastogi, Phys. Rev. B. 34 (1986) 4342.

[89] H. Coufal and P. Hefferle, Can. J. Phys., 64 (1986) 1200.

[90] A. Mandelis, F. Care, K.K. Chan. and L.C.M. Miranda, Appl. Phys. A 38 (1985) 177.

[91] I.F. Faria Jr., C.C. Ghizoni, L.C.M. Miranda and H. Vargas, J. Appl. Phys., 59 (1986) 3294.

[92] I.F. Faria Jr, C.C. Ghizoni, and L.C.M. Miranda, Appl. Phys. Lett., 47 (1985) 1154.

[93] J.P. Gordon, R.C.C. Liete, R.S. Moore, S.P.S. Porto and J.R. Whinnery, J. Appl. Phys., 36 (1965) 3.

[94] R.C.C. Liete, R.S. Moore, and J.R. Whinnery, Appl. Phys. Lett., 5 (1964) 141.

[95] D. solimini, J. Appl. Phys., 37 (1966) 3314.

[96] Y. Tang, T. Viet Ho, Appl. Spectrosc., 41 (1987) 583.

[97] R.T. Bailey, F.R. Cruickshank, D. Pugh and W. Johnstone "Lasers in Chemistry", M West (Ed), Elsevier, London, p 257, (1977).

[98] R.T. Bailey, F.R. Cruickshank, D. Pugh R. Guthrie and I.J.M. Wier, Mol. Phys., 48 (1983) 81.

[99] R.T. Bailey, F.R. Cruickshank, D. Pugh, R. Guthrie and I.J.M. Wier, "Time resolved vibrational spectroscopy", Academic Press, London p 12, (1983).

[100] Calmettes and Laj, J. Physica. (Paris), C1 (1972) 125.

[101] M.C. Gupta, S.D. Hong, A. Gupta and J. Moacanin, Appl. Pjys. Lett., 37 (1980) 505.

[102] N.J. Dovinchi and J.M. Harris, Anal. Chem., 51 (1979) 728.

[103] D. Cahen, Appl. Phys. Lett, 33 (1978) 810.

[104] A.C. Tam. Appl. Phys. Lett, 37, 978(1980).

[105] Thielemann & H Neuman, Phys. Stat. Solidi,(a) 61, K 123, (1980).

[106] G.J. Diebold, J Phys. Chem, 84 (1980) 2213.

[107] R.C. Gray and A.J. Bard, Anal. Chem,50 (1978) 1262.

[108] Y.H. Wong, R.L. Thomas and G.F. Hawkins, Appl. Phys. Lett., 32 (1987) 326.

[109] M. Luukkala and A Penttinem, Electron. Lett., 15 (1979) 326.

[110] G. Busse, Appl. Phys. Lett., 35 (1979) 759.

[111] A. Rosencwaig, Electron. Lett., 16 (1980) 928.

[112] R.L. Thomas, Y.H. Wong, L.D. Favro, P. K. Kuo and A. Rosencwaig, J. Appl. Phys., 51 (1980) 1152.

[113] P. K. Kuo, L.D. Favro, L.J. Inglehart, R.L. Thomas and M. Srinivasan, J. Appl. Phys., 53 (1982) 1258.

[114] K.R. Grice, P. K. Kuo, L.D. Favro, L.J. Inglehart and R.L. Thomas, J. Appl. Phys., 54 (1983) 6245.

[115] Shu-Yi Zhang and L.I. Chen, Can. J. Phys., 46 (1986) 1316.

[116] R. A. MacFarlane and L. D. Hess. Appl. Phys. Lett, 36 (1981) 147.

[117] D. Betteridge, T.C. Lilley and P.J. Meyler, Frezenius, Z. Anal. Chem. 296 (1979) 28.

[118] P. Helander and I.lundstrom, J. Appl. Phys., 52 (1981) 1146.

[119] M. Morita, Jpn. J. Appl. Phys., 20 (1981) 835.

[120] S.D. Campbell, S.S. Yee and M.A. Afromowitz, IEEE Trans. Biomed. Eng. BME 26 (1979) 220.

[121] M.L. McKenthum, R.D. Tom and T.A. Moore, Nature 279 (1979) 215.

[122] M.J. Adams and G.F. Kirkbright, Analyst 102 (1977) 678.

[123] M.J. Adams and G.F. Kirkbright, Spectrosc. Lett. 9 (1976) 255.

[124] A. Rosencwaig, and G. Busse, Appl. Phys. Lett., 36 (1980) 725.

[125] A. Rosencwaig, J. Appl. Phys., 51 (1980) 2210.

[126] E. Brandis and A. Rosencwaig, Appl. Phys. Lett., 37 (1980) 98.

[127] A. Rosencwaig and R. L. White, Appl. Phys. Lett., 38 (1981) 165.

[128] G.C. Wetsel. Jr and F.A. Mac Donald, Appl. Phys. Lett., 41 (1982) 926.

[129] L.J. Inglehart, K.R. Grice, P.K. Kuo, L.D. Favro, and R.L. Thomas, Appl. Phys. Lett., 43 (1983) 446.

[130] Y. Martin, H.K. Wwickramasinghe and E.A. Ash in: Proc. 1982 IEEE Ultrasonics Symposium, ed B.R. McAvoy.

[131] G. Diebold and D.L. McFadden, Appl. Phys. Lett., 29 (1976) 447.

[132] C. Evora, R. Landers and H. Vargas, Appl. Phys. Lett., 36 (1980) 864.

[133] O.A. Cleves Nunes, A.A.M. Monteiro and K. Skeff Neto, Appl. Phys. Lett., 35 (1979) 656.

[134] W. Wetttling, W. Jantz and L. Engelhardt, Appl. Phys. A, 26 (1981) 19.

[135] M. Davis and M. Heath, J. Magn. Mater, 31 (1983) 661.

[136] R. Melcher, Appl. Phys. Lett., 37 (1980) 895.

[137] U. Netzelmann, E.V. Goldammer, J. Pelzl and H. Vargas, Appl. Opt., 21 (1982) 1.

[138] A. Vasson and A.M. Vasson, J. Phys. D 14 (1981) L39.

[139] H. Coufal, Solid State Commun., 39 (1981) 467.

[140] H. Vargas, in Photoacoustic Effect: Principles and Applications, eds E. Luscher, P. Korpium, H. Coufal and R. Tilgner (Vieweg, Braunschweig, 1982).

[141] M.J. Adams, B.C. Beadle and G.F. Kirkbright, Anal. Chem., 50 (1978) 1371.

[142] S.L. Castleden, G.F. Kirkbright and K.R. Menon, Analyst 105 (1980) 1076.

[143] Q. Jin, G.F. Kirkbright and D.E.M. Spillane, Appl. Spectrosc., 36 (1982) 120.

[144] C.M. Ashworth, Kirkbright and D.E.M. Spillane, Analyst 108 (1983) 1481.

[145] C.H. Lochmuller and D.R. Wilder, Anal. Chim. Acta 11 (1980) 101.

[146] M. Natale and L.N.Lewis, Appl. Spectrosc. 36 (1982) 410.

[147] L.J. Fina, Appl. Spectro. Rev. 29 (1994) 309.

[148] T.A. Moore, Photochem. Photobiol. Rev. 7 (1983) 187.

[149] D. Balasubramanian, Biosci. Rep., 3 (1983) 981.

[150] D. Cahen, G. Bults, H. Garty and S. Malkin, J. Biochem. Biophys. Methods, 3 (1980) 293.

[151] D. Balasubramanian and Ch.M. Rao, Can. J. Phys. 64 (1986) 1132.

[152] A. Rosencwaig, Annu. Rev. Biophys. Biophys. Bioeng. 9 (1980) 31.

[153] D.M. Anjo, T.A. Moore, Photochem. Photobiol. 39 (1984) 635.

[154] D. Cahen,S. Malkin and E.I. Lerner, FEBS Lett. 91 (1978) 339.

[155] R. Carpentier, B. Larue and R.M. Leblanc, Arch. Biochem. Biophys. 222 (1983) 403.

[156] R. Carpentier, B. Larue and R.M. Leblanc, Arch. Biochem. Biophys. 222 (1983) 403.

[157] S.D. Campbell, S.S. Sinclair and M.A. Afromowitz, IEEE Trans. Biomed. Eng. BME 26 (1979) 220.

[158] P.S. Benton and S.S. Tanner, Analyst 108 (1984) 591.

[159] C.L. Cesser, C.A.S. Lima, H. Vargas, and L.C.M. Miranda, J. Agric. Food. Chem., 32 (1984) 1355,

[160] S. Sankara raman, V.P.N. Nampoori, C.P. G. Vallabhan, G. Ambadas, and S. Sugunan,
(a) Appl. Phys. Lett., 67 (1995) 2939.
(b) J. Appl. Phys.,85(1999) *In Press.*

[161] S. Sankara raman, V.P.N. Nampoori, C.P.G. Vallabhan, N. Saravanan, and K.K. Mohammed Yusuff, J. Mat. Sci. Lett., 15 (1996) 230.

[162] P.K. Wong, P.C.W. Fung, H.L. Tam and J. Gao, Physical Rev. B, 51 (1995) 523.

[163] Riju C Issac, S.S Hrilal, Geetha K Varier, C.V. Bindu, V.P.N. Nampoori, and C.P.G. Vallabhan, Opt. Engg., 36 (1997)332.

[164] Riju C Issac, S.S Hrilal, Geetha K Varier, C.V. Bindu, V.P.N. Nampoori, and C.P.G. Vallabhan, Mod. Phys. Letts.B 10 (1996) 61.

[165] C.V. Bindu, Riju C Issac, S.S Hrilal, Geetha K Varier, V.P.N. Nampoori, and C.P.G. Vallabhan, Mod. Phys. Letts.B 10 (1996) 1103.

[166] C.V. Bindu, Riju C Issac, S.S Hrilal, Geetha K Varier, V.P.N. Nampoori, and C.P.G. Vallabhan, J. Phys. D: Appl. Phys. 29 (1996) 1074.

[167] K. Rajasree, V. Vidyalal, P. Radhakrishnan, V.P.N. Nampoori, and C.P.G. Vallabhan, J. Liquid Crystals 18 (1995) 167.

[168] S.S Hrilal, Riju C Issac, Geetha K Varier, C.V, Bindu, V.P.N. Nampoori, and C.P.G. Vallabhan, Mod. Phys. Letts.9 (1995) 871.

[169] C.V. Bindu S.S Hrilal, Riju C Issac, Geetha K Varier, V.P.N. Nampoori, and C.P.G. Vallabhan, Pramana- J. Phys. 44 (1995) 225.

[170] K. Rajasree, V. Vidyalal, P. Radhakrishnan, V.P.N. Nampoori, and C.P.G. Vallabhan, Meas. Sci. Technol. 4 (1993) 435.

[171] P. Sathy, Reji Philip, V.P.N. Nampoori, and C.P.G. Vallabhan, Pramana - J. Phys., 34 (1990) 585.

[172] P. Sathy, Reji Philip, V.P.N. Nampoori, Jacob Philip and C.P.G. Vallabhan J. Pure Ultrason., 13 (1991)24.

[173] Reji Philip, P. Sathy, V.P.N. Nampoori, and C.P.G. Vallabhan J. Acoust. Soc. Ind. 18 (1990) 11.

[174] P. Sathy, Reji Philip, V.P.N. Nampoori, and C.P.G. Vallabhan, Opt. Comm. 74 (1990) 313.

★ ★ ★ ★ ★

CHAPTER 2

PHOTOACOUSTIC EFFECT IN CONDENSED MEDIA -THEORY

ABSTRACT

This chapter acknowledges some of the prominent scientists who have made significant contribution to Photoacoustic spectroscopy (PAS). The well-known Rosencwaig-Gersho theory is briefly presented. Application of the theory to thermally thick, thermally thin, optically transparent and optically opaque samples also is given. RG theory for thermal diffusivity measurement also is discussed towards the end of the chapter.

2.1. INTRODUCTION

Even though Alexander Graham Bell [1] discovered PA effect more than a century ago, the potentiality of the technique remained unexplored until recently. With the availability of sensitive microphone -during thirties and forties- people studied PA effect with gaseous samples to determine concentration of gaseous species in gas mixtures and to study the de-excitation and energy transfer processes [1-5]. Though the principle behind PA effect was known at that time, there were no appropriate theoretical explanations. Bell explained that PA effect is due to the internal heating of the sample by the absorbed radiant energy. He hypothesized that acoustic signals are generated as a result of periodic expulsion of gases from air spaces or pores with in the solid sample due to the alternate expansion and contraction of the sample caused by the periodic heating by the incident radiation. In the case of thin membrane or disc type sample, Bell supported the theory proposed by Rayleigh [6], who concluded that the primary source of PA signal was the thermally induced mechanical vibration of the disc. But according to Mecardier [7] the alternate heating and cooling produced by the intermittent radiation in the gaseous layer adhering to the solid surface results in the acoustic signal. A more or less similar explanation was given by Preece [8].

Experiments performed during the last few years indicate that the primary source of the PA signal from condensed sample as measured by the gas-microphone method arises from the periodic heat flow from the sample to the surrounding gas with the subsequent change in the gas pressure with in the cell.

The first attempt to develop a quantitative theory was made in 1973 by Parker [9] who while performing photoacoustic experiments with gases noticed a small but measurable PA signal clearly emanating from his cell windows. But this theory could explain PA effect in highly absorbing materials. Later on a more general theory for the PA effect in condensed media was formulated by Rosencwaig and Gersho (1975-1976) [10,11] and further developed by Mac Donald [12-14] and by Aamodt, Murphy and Parker [15,16]. These models have been found to be reasonably in good agreement with experimental results (for both solid and liquid samples) and thus, the basic mechanisms responsible for the photoacoustic (PA) effect seem to be well explained.

The main goal of theoretical models of PA effect is to allow interpretation of PA signal in terms of optical and thermal properties of sample. In the works of Rosencwaig-

Gersho and Aamodt, Murphy and Parker, the effect of physical and thermal properties of the system on PA signal has been studied so as to show the relation of PA spectra to normal absorption spectra. Mac Donald have shown [14] that absolute absorption coefficient may be determined at any optical wavelength by measuring the PA signal as a function of chopping frequency. Adams and Kirkbright [17] used the phase of the PA signal to determine the thermal properties of transparent materials. All of these applications require a proper theoretical basis to interpret the experimental data.

The Rosencwaig-Gersho theory - commonly known as RG theory - shows that in a gas microphone measurement of PAS signal, the signal depends both on the generation of an acoustic pressure disturbance at the sample-gas interface and on the transport of this disturbance through the gas to the microphone. The pressure variation at the sample-gas interface results from the periodic heat flow from the sample, which is, governed by the thermal diffusion equations. Rosencwaig and Gersho solved the thermal diffusion equations for the sample, the backing material on which the sample is mounted and the coupling gas in the cell so as to obtain exact expressions for the periodic temperature at the sample-gas interface. Though the

thermal part of the theory has been treated exactly, the acoustic part is treated in an approximated heuristic manner, which is, however, valid for the most experimental conditions. Since RG theory is extensively used in interpreting the results of the present work, we feel it would be appropriate to present the salient features of the theory in this chapter so that the thesis will be self-contained.

2.2. ROSENCWAIG - GERSHO THEORY

Rosencwaig-Gersho theory is a one-dimensional analysis of the production of PA signal from a sample kept in a cylindrical cell (PA cell) as shown in figure 2.1. Let D be the diameter and L be the length of the PA cell. It is assumed that the length L is small compared to the wavelength of the acoustic signal, and the microphone (not shown in figure) detects the average pressure produced in the cell. The sample of thickness l and diameter D is mounted on a poor thermal conductor of thickness l". The length of the gas in the cell is given by l' = L-l-l". It is also assumed that the gas and the backing materials are not light absorbing.

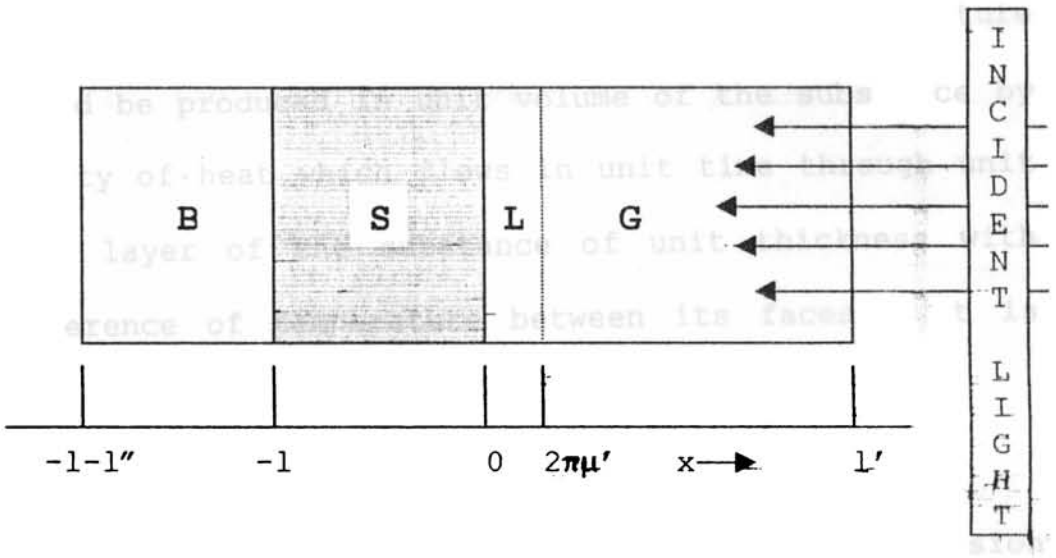

Fig. 2.1.: Cross sectional view of a cylindrical PA cell

B - Backing material; S - Sample;

L - Boundary layer of gas; G - Gas column

The three sample parameters that play the major role in determining the PA signal are the sample thickness l, the optical absorption length l_β, thermal diffusion length μ. Let us define the important parameters we use in the theoretical formulation.

K :thermal conductivity (cal / cm-sec-$^\circ$c)

ρ :the density (gm /cc)

c :the specific heat capacity (cal / gm-$^\circ$c)

α :thermal diffusivity (cm^2/sec)

[$\alpha = K / \rho c$. It is a measure of the change of temperature which would be produced in unit volume of the substance by the quantity of heat which flows in unit time through unit area of a layer of the substance of unit thickness with unit difference of temperature between its faces. It is also known as Thermometric conductivity.]

$\alpha = (\omega / 2 a \alpha)^{1/2}$: the thermal diffusion coefficient (cm^{-1})

$\mu = 1/a$: thermal diffusion length (cm)

[It is the distance over which a thermal wave is damped by 1/e of its initial amplitude.]

ω = chopping frequency (rad/sec)

β = optical absorption length

[It is the distance over which the light intensity is reduced to (1/e) of initial intensity.]

$\mu_\beta = 1/\beta$: optical absorption coefficient.

In the following treatment, the sample parameters are represented by unprimed symbols while the corresponding gas and backing materials by singly and doubly primed letters respectively.

Let I be the intensity of a sinusoidally chopped monochromatic radiation with wavelength λ incident on a solid given by

$$I = I_o (1+\cos \omega t) \qquad (2.1)$$

where I_o is the incident monochromatic light flux (W/cm^2) The heat density (H) produced at a point x due to the light absorbed at this point in the sample is given by

$$H = (1/2)\ \beta\ I_o e^{\beta x} (1+\cos \omega t) \qquad (2.2)$$

where x takes on negative values since the solid extends from x = 0 to x = -l, with the light incident at x = 0. Note also from figure 2.1 that the gas column extends from x = 0 to x = l′ and the backing from x = -l to x = -(l+l").

The thermal diffusion equation in the solid considering the distributed heat source due to illumination can be written as

$$(\partial^2\theta/\partial x^2) = (1/\alpha)(\partial\theta/\partial t) A e^{\beta t} (1+e^{i\omega t})$$

$$\text{for } -l \leq x \leq 0 \qquad (2.3)$$

with $$A = \beta I_o \eta \; / \; 2k \qquad (2.4)$$

where θ is the temperature and η is the efficiency with which the absorbed light is converted in to heat by non-radiative de-excitation process. For most of the solids at room temperature it is reasonable to take $\eta = 1$. The thermal diffusion equation for the backing material and gas are respectively given by

$$(\partial^2\theta/\partial x^2) = (1/\alpha'')(\partial\theta/\partial t) \qquad -l''-l < x < -l \qquad (2.5)$$

$$(\partial^2\theta/\partial x^2) = (1/\alpha)(\partial\theta/\partial t) \qquad 0 < x < -l \qquad (2.6)$$

The real part of the complex valued solution $\theta(x,t)$ of equations (2.3) to (2.6) is the solution of physical interest which represents the temperature in the cell relative to the ambient as a function of position and time. Thus the actual temperature field in the cell is given by

$$T(x,t) = Re.\theta(x,t) + \phi_o \qquad (2.7)$$

here Re denotes the "real part of" and ϕ_o is the ambient (room) temperature. To completely specify the solution of

(2.3), (2.5) and (2.6), appropriate boundary conditions are obtained from the requirement of temperature and heat flux continuing at the boundaries x = 0 and x = -1, and from the constraints that the temperature at the cell walls x = 1 and x = -1-1"is ambient.

The general solution for $\theta(x,t)$ in the cell neglecting transients can be written as

For $1-1'' \leq x < -1$

$$\theta(x,t)=(1/1'')(x+1+1'')W_0 + W\ e^{\sigma'(x+1)}e^{i\omega t} \qquad (2.8a)$$

For $-1 \leq x \leq o$

$$\theta(x,t)= b_1 + b_2x + b_3e^{\beta x} + (Ue^{\sigma x}+Ve^{-\sigma x}-Ee^{\beta x})e^{i\omega t} \qquad (2.8b)$$

For $0 \leq x \leq 1'$

$$\theta(x,t)= [1-(x/1')]F + \theta_0\ e^{-\sigma' x}\ e^{i\omega t} \qquad (2.8c)$$

where W, U, V, E and q are complex valued constants, b_1, b_2, b_3, W_0 and F are real valued constants, and $\sigma = (1+i)a$. θ_0 and W represent the complex amplitudes of the periodic temperatures at the sample-gas boundary (x = 0) and the sample-backing boundary (x = -1) respectively. The

quantities W_0 and F denote the d.c components of the temperature at the sample surface x =0 and x = -1 respectively. The quantities E and b, determined by the forcing function in eq.(2.3) are given by

$$b_3 = -A/\beta^2 \qquad (2.9)$$

$$E = A/(\beta^2-\sigma^2) = \beta I_0 / 2k(/(\beta^2-\sigma^2) \qquad (2.10)$$

The growing exponential components of the solutions to the gas and backing material are omitted in the general solution (2.8) because for all frequencies (ω) of interest, the thermal diffusion length is small compared to the length of the material and hence the sinusoidal components of these solutions are sufficiently damped so that they are effectively zero at the cell walls. Therefore, the growing exponential components of the solutions would have coefficients that are essentially zero so as to satisfy the temperature constraints at the walls.

By applying the boundary conditions all the constants of eq.(2.8)and hence the d.c and a.c components of the solutions can be obtained. Then the explicit solution for

θ_o , the complex amplitude of the periodic temperature at the solid-gas boundary (x = 0) is given by

$$\theta_o = [\beta I_o / 2K(\beta^2-\sigma^2)][(r-1)(b+1)e^{\sigma l} - (r+1)(b-1)e^{-\sigma l} + 2(b-r)e^{-\beta l}][(g+1)(b+1)e^{\sigma l} - (g-1)(b-1)e^{-\sigma l}]^{-1} \quad (2.11)$$

where

$$b = Ka''/Ka \; ; \; g = K'a'/Ka \; ; \; r = (1-I)\beta/2a \quad (2.12\text{-}2.14)$$

The periodic temperature variation at the sample surface as governed by eq.(2.11) causes thermal waves diffuse in to the gas. This periodic diffusion process produces a periodic temperature variation in the gas as given by the a.c component of the solution (2.8).

$$\theta(x,t) = \theta_o \, e^{\sigma' x} \, e^{i\omega t} \quad (2.15)$$

The time component of temperature in gas [eq.(2.15)] attenuates rapidly to zero with increasing distance from the surface of the solid. The periodic temperature variation in gas is effectively damped out at a distance $2\pi/a' = 2\pi\mu'$ where μ' is the thermal diffusion length of the gas. It can be assumed to a good approximation that only

this boundary layer of gas as sown in figure 2.1 whose thickness is $2\pi\mu'$ capable of responding thermally to the periodic temperature at the sample surface.

The spatially averaged temperature of the gas within this boundary layer as a function of time can be determined as,

$$\bar{\theta}(t) = (1/2\pi\mu') \int_0^{2\pi\mu'} \theta_{ac}(x,t)\, dx \qquad (2.16)$$

From eq.(2.15)

$$\bar{\theta}(t) = (1/2\pi\sqrt{2})\,\theta_0 e^{i(\omega t-\pi/4)} \qquad (2.17)$$

Due to the periodic heating of the boundary layer of gas, it expands and contracts which in turn exerts a periodic pressure on the rest of the gas column, there by producing an acoustic signal. The displacement of the boundary layer can be estimated by the ideal law as

$$\delta x(t) = 2\pi\mu'\ \theta(t)\ /\ T_o$$

$$= \mu'\ \theta_o\, e^{i(\omega t-\pi/4)}/\ T\sqrt{2} \qquad (2.18)$$

Assuming the expansion and contraction of gas to be adiabatic, the acoustic pressure in the cell can be determined from the adiabatic gas law, PV^{γ} = constant, where

P is the pressure, V is the volume of gas in the cell and γ is the ratio of specific heats. Then the incremental pressure is given by

$$\delta P(t) = \gamma (P_o/V_o)\delta V = \gamma\ (P_o/l')\delta x(t) \qquad (2.19)$$

where P_o and V_o are the ambient pressure and volume respectively and $-\delta V$ is the incremental volume. Substituting from eq.(2.18)

$$\delta P(t) = Q\ \theta_o\ e^{i(\omega t-\pi/4)} \qquad (2.20)$$

where $$Q = \gamma P_o \theta_o\ /\ I' a' T_o \sqrt{2} \qquad (2.21)$$

The actual physical pressure variation $\Delta P(t)$ is given by the real part of $\delta P(t)$ as

$$\Delta P(t) = Q_1 \cos(\omega t-\pi/4) - Q_2 \sin(\omega t-\pi/4) \qquad (2.22)$$

or $$\Delta P(t) = q \cos(\omega t-\psi-\pi/4) \qquad (2.23)$$

where Q_1 and Q_2 are the real and imaginary parts of Q and q and ψ are the amplitude and phase of Q, that is

$$Q = Q_1 + iQ_2 = q\, e^{i\psi} \qquad (2.24)$$

Thus Q satisfies the complex envelope of the sinusoidal pressure variation, and the explicit formula for Q is obtained by combining eq.(2.11) and eq.(2.21) we get

$$Q = [\beta I_o \gamma P_o / 2\sqrt{2}l' a' T_o K(\beta^2-\sigma^2)][(r-1)(b+1)e^{\sigma l} - (r+1)(b-1)e^{-\sigma l} + 2(b-r)e^{-\beta l}][(g+1)(b+1)e^{\sigma l} - (g-1)(b-1)e^{-\sigma l}]^{-1} \qquad (2.25)$$

This equation gives the amplitude and phase of the acoustic pressure wave generated in the cell by photoacoustic effect.

SPECIAL CASES :

The expression for Q can be made simple by considering various special cases. The special cases are determined by the relative magnitude of the optical absorption length $l_\beta = 1/\beta$, thermal length μ and the thickness l of the sample respectively. For all cases it is assumed that g < b and b~1. Also it is convenient to define

$$Y = I_o \gamma P_o / 2\sqrt{2} l' T_o \qquad (2.26)$$

which always appears as a constant factor in the expression for Q and the optical path length as

$$l_\beta = 1/\beta \qquad (2.27)$$

Case 1 :OPTICALLY TRANSPARENT SOLID ($l_\beta > l$)

In this case the light is absorbed throughout the length of the sample and some light is transmitted through the sample.

Case 1.a :Thermally thin solids [$\mu >> l$; $\mu > l_\beta$]

Here using the approximation $e^{-\beta l} \cong 1 - \beta l$, $e^{\pm\sigma l} \cong 1$ and $|r| > 1$ in eq.(2.25), we get

$$Q = (Y/2a'a''K'')(\beta - 2ab - i\beta)$$

$$= [(1-i)\beta l/2a'][\mu''/K''] \; Y \qquad (2.28)$$

The above equation shows that in this case the acoustic signal is proportional to βl and since (μ''/a') is

proportional to $1/\omega'$, the acoustic signal has a ω^{-1} dependence. For thermally thin case of $\mu.>> l$, the thermal properties of the backing material also come in to play in the expression for Q.

Case 1.b: Thermally thin solids ($\mu > l$; $\mu.< l_\beta$)

Setting $e^{-\beta l} \cong 1-\beta l$, $e^{\pm\sigma l} \cong (1+\sigma l)$ and $|r| <1$ in eq.(2.25) we get

$$Q = (\beta l Y/4Ka' a^3 b)(\beta^2+2a^2) + I(\beta^2-2a^2)$$

$$\approx [(1-i)\beta l/2a'][\mu''/K''] \; Y \qquad (2.29)$$

Here also the acoustic signal varies as ω^{-1}, since it is proportional to βl and depends on the thermal properties of backing material.

Case 1.c : Thermally thick solids ($\mu < l$; $\mu << l_\beta$)

Setting $e^{-\beta l} \cong 1-\beta l$; $e^{-\sigma l} \cong 0$ and $|r| <1$ in eq.(2.25) we get

$$Q = [-i\beta\mu/2a'][\mu/K] \; Y \qquad (2.30)$$

Here the acoustic signal is proportional to $\beta\mu$. The light absorbed with in the first thermal diffusion length contributes to the signal even though the absorption takes place through out the thickness of the solid. Since $\mu < l$, thermal properties of the backing material are replaced by those of the solid sample. The signal in this case varies as $\omega^{-3/2}$.

Case 2 : OPTICALLY OPAQUE SOLIDS

In this case most of the light is absorbed in a distance that is small compared to l and no light is transmitted.

Case 2.a : Thermally thin solids ($\mu >> l$; $\mu >> l_\beta$))

Taking $e^{-\beta l} \cong 0$; $e^{\pm\sigma l} \cong 1$ and $|r| < 1$.

$$Q \approx [(1-i)/2a'][\mu''/K''] \; Y \qquad (2.31)$$

In this case the acoustic signal is independent of β but depends on the thermal properties of the backing material and varies as ω^{-1}.

Case 2.b : Thermally thick solids ($\mu << 1$; $\mu > l_\beta$)

Setting $e^{-\beta l} \cong 0$; $e^{-\sigma l} \cong 0$ and $|r|<1$ in eq.(2.25) we get

$$Q \approx (Y/2aa'K\beta)\ (\beta-2a-i\beta)$$

$$\approx [(1-i\beta)/2a'][\mu/K]\ Y \qquad (2.32)$$

Here also the acoustic signal is independent of β and varies as ω^{-1}.

Case 2.c : Thermally thick solids ($\mu << 1$; $\mu < l_\beta$

Setting $e^{-\beta l} \cong 0$; $e^{-\sigma l} \cong 0$ and $|r| <1$ in eq.(2.25) we get

$$Q = (-i\beta Y/4a'a^3K)\ (2a-\beta-i\beta)$$

$$\approx (i\beta\mu/2a')(\mu/K) \qquad (2.33)$$

This is very important and interesting case because even though the sample is optically opaque it is not photoacoustically opaque as $\mu < l_\beta$, only the light absorbed within the first thermal diffusion length contributes to the acoustic signal. The PA signal is proportional to β and

depends on the thermal properties of the sample and varies as $\omega^{-3/2}$.

One of the most important prediction of the theory is that the PA signal is always linearly proportional to the power of the incident photon beam and that this dependence holds for any sample or cell geometry. RG theory also indicates that the PA effect primarily depends on the relationship between three length parameters of the sample: the thickness of the sample l, the optical absorption length $l_\beta = 1/\beta$ and thermal diffusion length $\mu = (2\alpha/\omega)^{1/2}$. Deviation from RG theory is observed at low chopping frequencies. This is due to the reason that RG theory is made on the assumption that the gas column in the PAS cell is always much larger than the gaseous thermal diffusion length, which is not valid at low chopping frequencies.

2.3. THERMAL DIFFUSIVITY MEASUREMENTS

2.3.1. INTRODUCTION

Thermal diffusivity α is of direct importance in thermal transport properties as it determines the rate of periodic or transient heat propagation through the medium.

Knowing thermal diffusivity, density and specific heat capacity the thermal conductivity of the material can be calculated since they are related through the relation $\alpha = K/\rho c$. Though thermal conductivity and thermal diffusivity are directly related, different experimental procedures are adopted for the measurement of these parameters. Thermal conductivity when measured directly by a steady state method requires the measurement of the thermal flux and temperature gradient. The thermal diffusivity requires the measurement of the time for a thermal disturbance to propagate to a known distance in the medium [18-21]. This shows the significance of thermal diffusivity measurements because the length and time intervals can be measured more easily and accurately than heat fluxes and temperature gradients.

Two kinds of techniques have been commonly used to determine thermal diffusivities: transient heat-flow method [15] and periodic heat-flow method [22]. In the transient heat-flow method, an addition or removal of thermal energy from the sample induces a transitory temperature change and α is determined by measuring temperature as a function of time at one or more points along the sample. In the periodic heat-flow method the thermal energy supplied to the sample is modulated at a fixed period. Consequently

the temperature at all points in the sample vary with the same period and α is then determined from the measurement of amplitude and phase of the thermal wave in the sample.

The PA technique, which belongs to the periodic heat-flow method, is an effective method to determining thermal parameters. Here the PA signal is measured as a function of chopping frequency. Charpentier et al [20] have presented a frequency analysis of the PA signal for the determination of thermal diffusivity by extending RG theory. They have also discussed the "drum effect", mechanical vibration of the sample due to its periodic dilation.

2.3.2. R.G THEORY OF THERMAL DIFFUSIVITY MEASUREMENTS

According to RG theory the pressure variation Q at the front surface of an optically thick sample depends on the thermal diffusivity a of the sample and can be written as

$$Q = qe^{-j\phi} = BA \qquad (2.34)$$

Where $q = |Q|$, ϕ is the phase shift between Q and excitation, and B and A are given by

$$B = (P_o \gamma W_a l \sqrt{\alpha'} / \; 2l' T_o K \sqrt{\alpha}) \qquad (2.35)$$

and

$$A = [1+g(d^+ + d^-)/(d^+ - d^-)] \; [g+(d^+ + d^-)/(d^+ - d^-)] (1/\sigma l)^2 \qquad (2.36)$$

where $d^+ = e^{\sigma l}$

$$d^- = e^{-\sigma l}$$

$$\sigma = (1+i) \; (\pi f/\alpha)^{1/2} \qquad (2.37)$$

and g, the ratio between effusivities of the backing material (e") and the sample (e) is given by

$$g = e''/e = (K''/K) \; (\alpha/\alpha'')^{1/2} \qquad (2.38)$$

In the above expression l, K and α are the thickness, thermal conductivity and thermal diffusivity respectively. T_o and P_o are the static temperature and static pressure of the gas, γ is the ratio of specific heats, W_a is the amount of light absorbed and l' and α' are the thickness and thermal diffusivity of the gas. The effusivity of the gas in the cell has been neglected compared to the effusivity

of the sample, the ratio being less than 1% always. The term A depends on the modulation frequency through the product σl which can be written as

$$\sigma l = (i+j)\ (\pi f/f_c) \qquad (2.39)$$

where f_c is the characteristic frequency, which can be obtained from eq.(2.37) and eq.(2.39) as

$$f_c = \alpha/l^2 \qquad (2.40)$$

The thermal diffusivity α can be determined by measuring the amplitude of the PA signal as a function of chopping frequency. One of the factors that determines the amplitude of the PA signal is the thermal diffusion length (μ) given by

$$\mu = (\alpha/\pi f)^{1/2} \qquad (2.41)$$

where f is the chopping frequency when the sample is thermally thin ($\mu > l$) the PA signal gets modified by the thermal properties of the backing material. In the thermally thick ($\mu < l$) regime the PA signal is independent of the thermal properties of the backing material. For a

given sample thickness, one can have a transition from thermally thin regime to thermally thick regime by increasing the chopping frequency. Hence in the log(amplitude) Vs log(frequency) plot a slope change occurs at the characteristic frequency (f_c). Knowing the characteristic frequency and thickness of the sample, the thermal diffusivity can be calculated from eq.(2.40) as

$$\alpha = l_s^2 f_c \qquad (2.42)$$

2.4. CONCLUSION

Rosencwaig-Gersho theory (one dimensional analysis) for the production of PA signal in a closed cell is described. Various special cases are also mentioned. The extension of the theory for thermal diffusivity measurements is also given.

REFERENCES

[1] A.G. Bell, Am. J. Sci., 20 (1880) 305.

[2] M.C. Viengero, Dokl. Akad Nauk, SSR, 19 (1938) 687,

[3] A.H. Pfund, Science, 90 (1939) 326.

[4] K.F. Luft, Tech Z, Phys., 24 (1941) 97.

[5] M.L. Viengerov, Dokal Akad Nauk, SSR, 54 (1946) 779.

[6] Lord Rayleigh, Nature, 23, (1881) 506.

[7] M.E. Mercardier, and C.R. Hebd, Serv. Aacd, Sci., 92 (1881) 409.

[8] W.H. Preece, Proc. R Soc. (Lond) 31 (1881) 506.

[9] J.G. Parker, Appl. Opt., 12 (1973) 2974.

[10] A. Rosencwaig, A. Gersho, Science, 190 (1975) 556.

[11] A. Rosencwaig, A. Gersho, J. Appl. Phys., 47 (1975) 64.

[12] F.A. Mac Donald and G.C. Wetsel. Jr., J. Acoust. Soc. Am. 60 (1976) S52.

[13] F.A. Mac Donald and G.C. Wetsel. Jr., J. Appl. Phys. 49 (1978) 4.

[14] G.C. Wetsel. Jr., and F.A. Mac Donald, Appl. Phys. Lett. 30 (1977) 252.

[15] W.J. Parker, R.J. Jenkins, C.P. Butler and G.L. Abdot, J. Appl. Phys., 32 (1961) 1679.

[16] L.C. Abdot J.C. Murphy and J.G. Parker,J. Appl. Phys. Lett., 30 (1977) 252.

[17] M.J. Adams and G.F. Kirkbright, Spectrosc. Let., 9 (1976) 255.

[18] A.C. Tam, Rev. Modern. Phys., 56 (1986) 2.

[19] C.L. Cesar, H. Vrgas, and L.C.M. Miranda, Appl. Phys. Lett., 32 (1978) 554.

[20] P. Charpentier, F. Lepoutre, and L. Bertrand, J. Appl. Phys., 53 (1982) 1.

[21] A. Hordvik and H. Scholssberg, Appl. Opt., 16 (1977) 101; 16 (1977) 2919.

[22] B. Ables, G.D. Cody and D.S. Beers, J. Appl. Phys, 31 (1960) 1585.

* * * * *

CHAPTER 3

INSTRUMENTATION

ABSTRACT

In this chapter we describe the experimental set-up employed in the present work. After a short general introduction to PA spectrometer, the design and fabrication details are given. The calibration of the experimental set-up using the materials of known thermal diffusivity values is also included in this chapter. The power dependence of the PA signal is also studied and is given in the last section.

3.1. GENERAL ASPECTS OF PHOTOACOUSTIC SPECTROMETER

The essential modules of a PA spectrometer are (i) a radiation source of sufficient intensity in the spectral range of interest (ii) intensity or frequency modulator (iii) PA cell in which the sample is placed which also incorporates the acoustic transducer (iv) signal processing unit. The block diagram of a PA spectrometer is shown in figure (3.1).

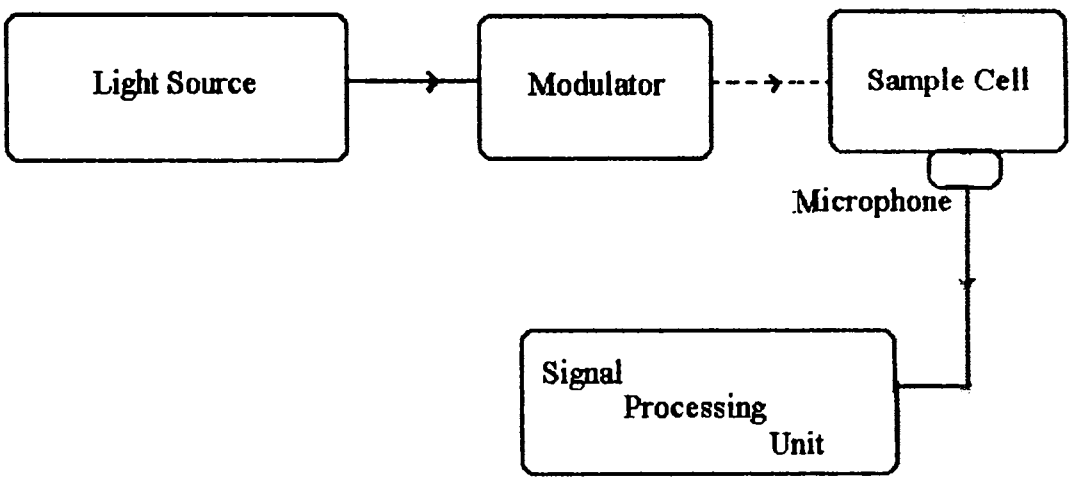

Fig.3.1: Gas-Microphone PA spectrometer

3.1.1. RADIATION SOURCE

Lasers and arc lamps are the two popular types of light sources currently in use for PA experiments. The lamp monochromator can provide continuous tunability over a wide spectral range from infrared to the vacuum ultraviolet. High pressure Xe arc lamp, Hg lamps, tungsten lamps etc are the commonly used incandescent sources. The major drawback with these sources is relatively low bandwidth. Lasers are widely accepted as the convenient radiation sources in the PA spectroscopy especially for measuring weak absorption. This is mainly due to their coherent and monochromatic nature. But the draw back with lasers is their limited tunability.

3.1.2. MODULATION

Modulation of the incident light beam is essential for the generation of PA signals. Amplitude or frequency modulation is the commonly used method. Amplitude modulation can be done by one of the several methods using mechanical, electrical or electro-optic devices. The most commonly used and inexpensive method is to use mechanical chopper, which is a disc with holes to allow light beam to pass through. Frequency of modulation can be varied by

controlling the rotation speed of the chopper and number of holes in it. Most mechanical choppers incorporate optocouplers to get reference signal for lock-in detection. The depth of modulation in this case is 100%. While using mechanical chopper, care should be taken to minimize the vibration noise as it may interfere with the PA signal and can not be filtered off even by lock-in detection. Frequency modulation can be employed to eliminate the PA signals generated due to wavelength independent absorption at the cell window. Frequency modulation is well suited for narrow line width absorbers such as atomic and diatomic species.

3.1.3. THE PHOTOACOUSTIC CELL

The heart of a PA spectrometer is the PA cell in which the sample is placed and the signal is generated. Proper design of the cell is very important for the generation of PA signal of detectable magnitude. Some of the important factors that decide the good response of a PA cell are given below.

(i) The cell should be acoustically isolated. For that the cell should be designed with good acoustic

seals and with walls of sufficient thickness to form good acoustic barriers.

(ii) The materials used for making cell windows and walls should not have absorption in the wavelength region of interest. This is to eliminate the contribution of the wall and window materials to the PA signal. To minimize the PA signal from walls due to their absorption of the incident radiation, the thermal mass of the walls should be quite large. The cell geometry should be such that the amount of the scattered light reaching the microphone is a minimum.

(iii) Since the PA signal varies inversely with the volume of gas inside the cell [1], its dimension should be so chosen that the volume of the cell is a minimum. Care should also be taken to avoid the dissipation of acoustic signal before reaching microphone. Hence it is advisable to optimize the cell volume so as to generate good signal strength.

(iv) The length l' of gas column between the sample and window should be greater than the thermal diffusion length μ' of gas at the lowest chopping frequency. Tam [2,3] has suggested the optimum gas

column to be $l' \cong 1.8\mu'$. In determining the passage way dimensions, thermo-viscous damping has to be taken in to account. The thermo-viscous damping effect varies exponential as $e^{-\varepsilon x}$, where ε is the damping coefficient given by

$$\varepsilon = (1/d\nu)\ (\eta_e \omega\ /\ 2\rho_o) \qquad (3.1)$$

where d is the closest distance between the cell boundaries in the passage way, ν is the velocity of sound, ω is the frequency ρ_o is the density of gas and η_e is the effective viscosity which depends on the ordinary viscosity and the thermal conductivity of the gas. Thermo-viscous damping coefficient varies as $\omega^{-1/2}$ and become prominent at high frequency where as thermal diffusion length which varies as $\omega^{-1/2}$ is predominant at low frequency. Considering these facts, the distance between the sample and window should be made minimum and the passage way dimensions also should be kept minimum (of the order of 1-3 mm) [4].

Depending on the nature of work, various types of cells are designed [5,6]. The most commonly used cell is cylindrical in shape with a bore at the center through which light beam is passed. Such cells can be operated

either in the resonant or in the non-resonant mode. The pressure variations produced due to the PA effect propagates radially outwards, perpendicular to the exciting beam. The hydrodynamic equation describing the time variation of pressure at a given point in the cell has been solved for cylindrical [7-10] and other cell geometries. The pressure distribution P with in a cylinder of length L and radius R is given by

$$P(r,\phi,z,t)=\cos(m,\phi)\ \cos(k\pi z/l)\ J_m(\alpha_{mn}\pi r/R)\ \exp(-i\omega t) \qquad (3.2)$$

where J_m is the Bessel function of the first kind of order m. The normal acoustic modes can be divided into pure longitudinal and pure radial. The lowest order radial mode has k=1 and m=n=0 , while the lowest order longitudinal mode has k= 1, m= 0, n= 1. The resonant frequency of the cell can be obtained from

$$f_{res} = (c_o/2)\,[(k/L)^2 + (\alpha_{m,n}/R)^2]^{-1/2} \qquad (3.3)$$

where c_o is the velocity of sound in gas $\alpha_{m,n}$ is the n^{th} root of the equation

$$(dJ_m/dr)_{r=R} = 0$$

Another cell geometry makes use of the Helmholtz resonator type in which the sample and microphone compartments of volumes v_1 and v_2 are connected by a narrow tube of length L and of cross sectional area A. Its resonance frequency is given by

$$2\pi f_{res} = c_o(A/Lv_r) \qquad (3.4)$$

where $$v_r = v_1v_2/v_1+v_2 \qquad (3.5)$$

The advantage of Helmholtz design is that the resonant frequency can be altered by changing the dimensions A and L of the channel. With this configuration, the properties of the sample at low as well as high temperature can be studied by using a sufficiently long connecting tube.

The PA cell also incorporates an acoustic transducer, usually a microphone, to detect the acoustic signal.

3.1.4. SIGNAL PROCESSING

Since the PA signal is very weak, often several orders of magnitude lower than the ambient noise, care must be taken in processing the microphone out put signal. In order to maximize the signal to noise ratio, the signal

from the microphone preamplifier should be processed by an amplifier tuned to the chopping frequency. The fact that the PA signal has the same frequency as that of modulation, enables one to use the lock-in detection technique [11]. The lock-in amplifier is also helpful in eliminating the noise from other sources. Also, by lock-in detection the amplitude and phase of the PA signal can be measured with high accuracy and much ease especially when both amplitude and phase vary simultaneously. When pulsed laser is used as the excitation source a boxcar averager is used instead of a lock-in amplifier.

In spectroscopic applications since the PA signal is proportional to the intensity of the incident beam, one has to normalize the PA spectrum with the power spectrum of the radiation source. The power spectrum of the source can be obtained by using a conventional power meter or another reference PA cell with a suitable absorber like carbon black as the sample. While using a reference PA cell, the modulated incident beam is allowed to fall in to the reference cell using a beam splitter. The signal from the sample cell is divided by that from the reference cell using a ratio meter and the spectrum is directly recorded.

3.2. EXPERIMENTAL SET-UP

A single beam PA spectrometer has been assembled for the investigations carried out. The block diagram of the experimental set-up is shown in fig (3.2). The essential parts of the set up are (1) an optical source (2) an electromechanical chopper (4) PA cell (5) a lock-in amplifier and (6) recorder.

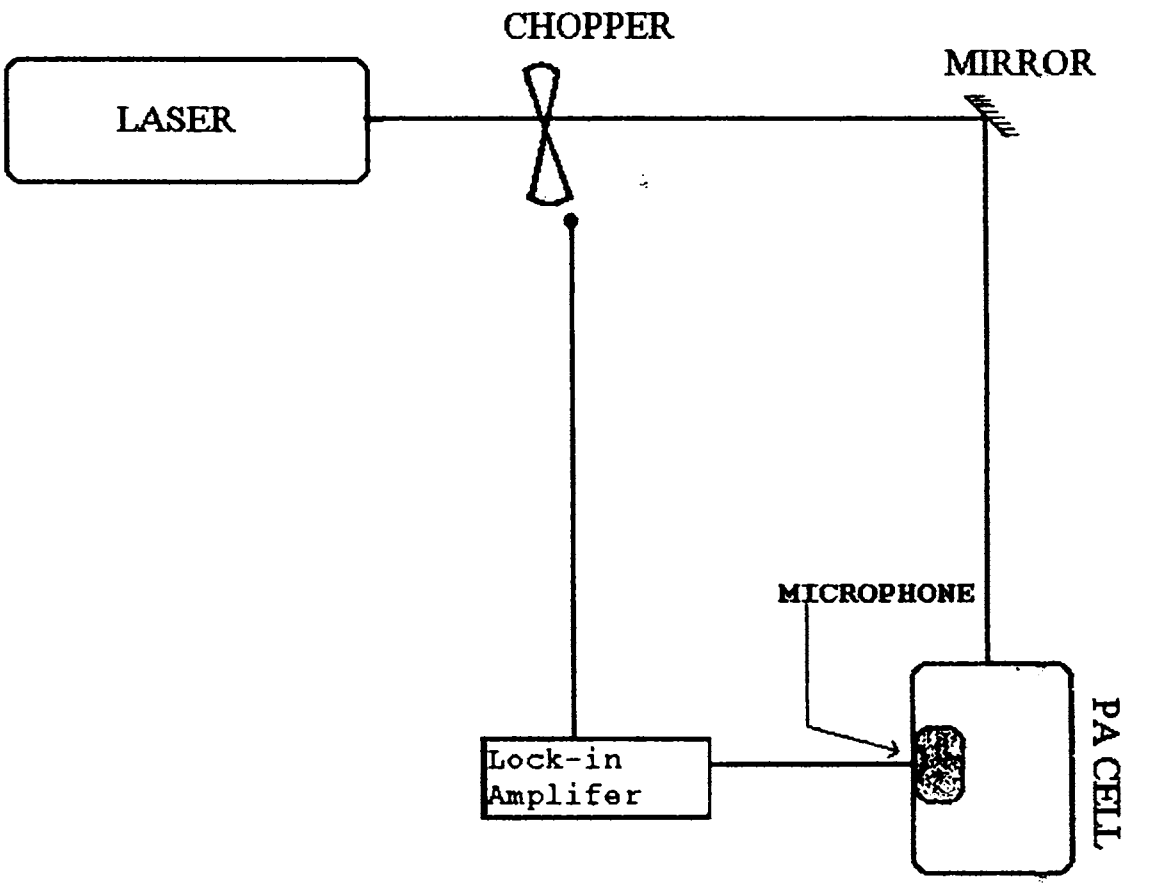

Fig.3.2: Experimental set-up.

In the present work, a cw argon ion laser (LiCONiX 5300 Series Water Cooled laser) has been used as the excitation or the pump source. It can be operated both in multi line and in single line mode. Prominent lines are 514, 488 and 476 nm, which can be used as the excitation wavelengths. To generate acoustic signal in the PA cell, as stated earlier, it is necessary to modulate the cw source before irradiating the sample. The laser beam is modulated using an electromechanical chopper (Stanford Research systems, INC, Model SR 540). The mechanical chopper is the simplest form of a modulator consisting of a rotating slotted disc placed in the path of the light beam. It can provide a modulation depth of 100% for the frequencies from a few Hz to 5 to 8 KHz. We have selected the chopping frequencies from 20 Hz to a maximum of 300 Hz.

The PA signal detected by the microphone is processed by means of lock-in amplifier (EG & G model 5208). It has sensitivity up to 100nV and phase sensitivity up to 0.025^{o}. Lock-in amplifier uses a technique known as phase-sensitive detection to single out the component of the signal at the reference frequency and phase. Noise signals at frequencies other than the reference frequencies are rejected and do not affect the measurements.

The PA cell is the most important part of any PA spectrometer. The description of the PA cell used for the room temperature measurement is given below.

A small volume non-resonant cell for room temperature measurement is made out of aluminium. The figure (3.3) depicts the cell with its various parts. The cell has an axial bore of about 0.5 cm. diameter. One side of the bore is closed by a glass window and to the other side we place the sample and closed air tightly. The bore provided at the back side of the cell helps us to study the effects on rear side illumination. The acoustical isolation of the cell volume from out side is achieved by using 'O' rings on the window holders.

The PA signal is detected using a microphone kept very close to the sample compartment in a separate port with provisions for electrical connections. A small size, high sensitive microphone has been used for the detection of the acoustic signal. The microphone output is fed to the lock-in amplifier through a BNC connector.

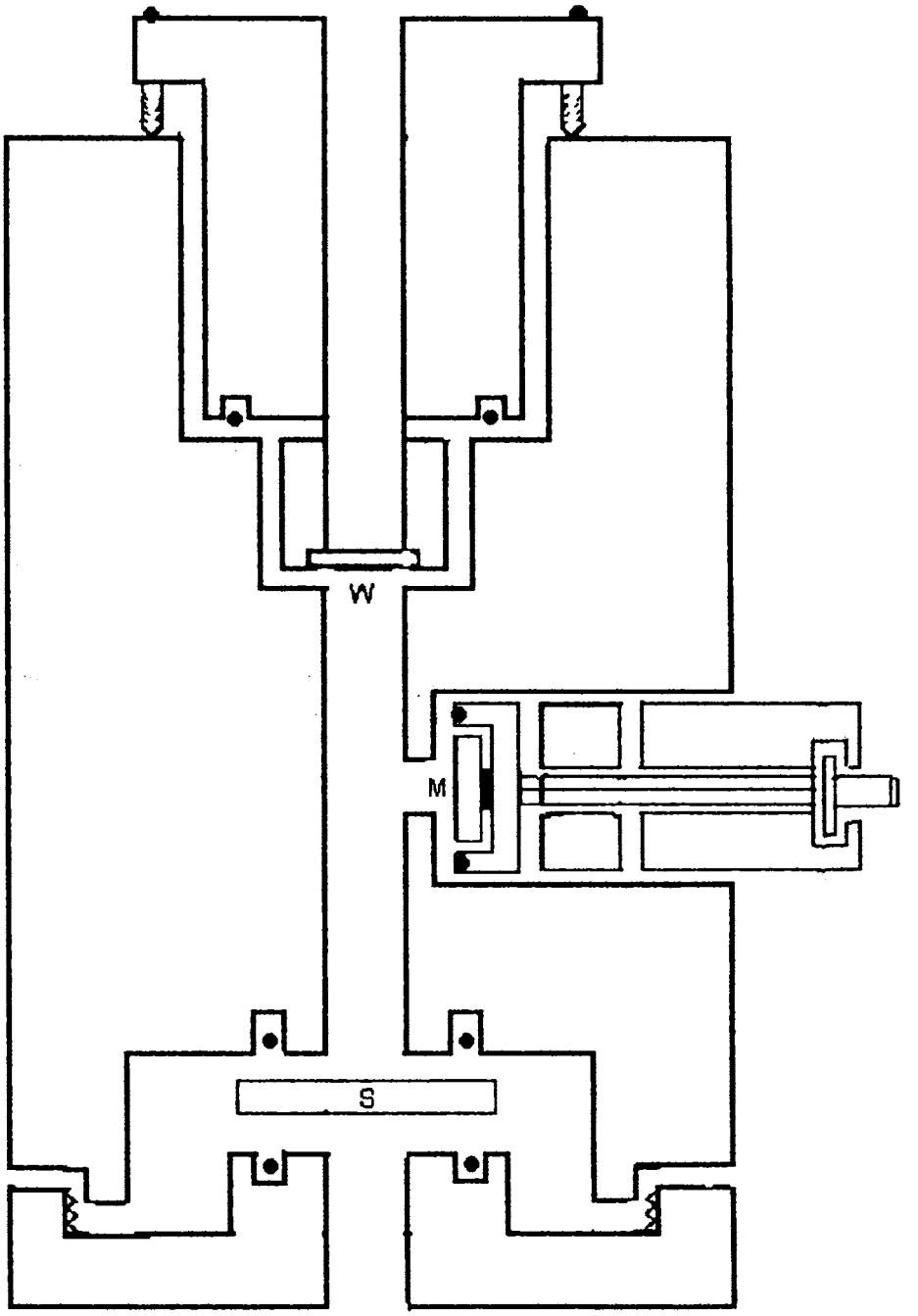

M - Microphone, W - Window, S - Sample

Fig. 3.3: Cross-sectional view of the PA cell used

3.3. STANDARDISATION OF THE EXPERIMENTAL SET-UP.

In order to standardise the experimental procedure, the thermal diffusivity of samples with known values of α have been determined. Copper, aluminium and iron were chosen as standard samples since their data are available from the literature. After standardising the set-up the work is extended to the samples whose thermal diffusivities are not known. The accuracy of the method depends on the accuracy with which the thickness and the characteristic frequency of the sample are measured. By measuring the thickness of the sample by optical methods, the accuracy of thermal diffusivity values comes up to the third decimal digit.

3.3.1. THERMAL DIFFUSIVITY MEASUREMENTS ON Cu, Al,AND Fe

For thermal diffusivity measurements the samples of appropriate thickness are taken such that the characteristic frequency, at which a cross over from thermally thin to thermally thick regime take place as the chopping frequency is varied. The thickness (l_s) of the

sample is accurately measured and the characteristic frequency (f_c) is noted from the log(amplitude) Vs log(frequency) plot.

Before thermal diffusivity measurement it is to be confirmed that the cell constructed for the investigation is non-resonant (ie. it should not produce any resonance in the frequency range used for the study). For that, keeping carbon black as sample the variation of PA signal amplitude with chopping frequency is studied.

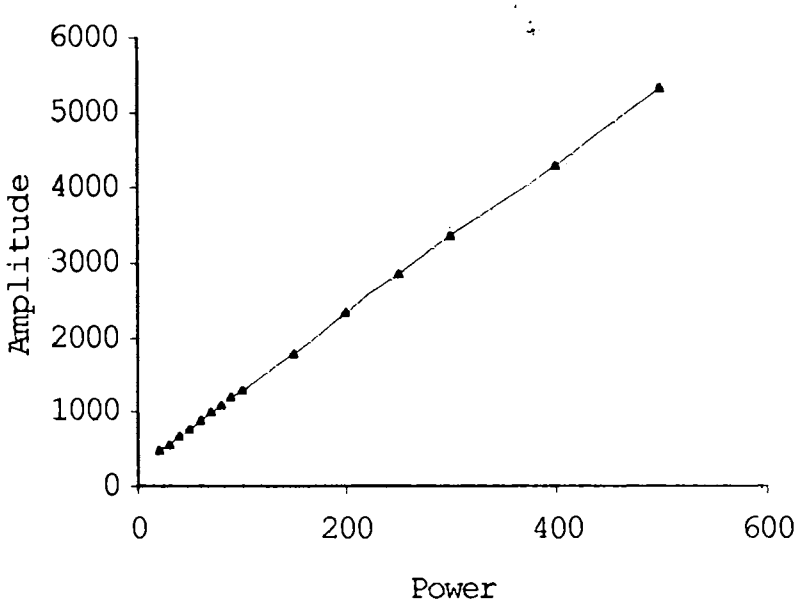

Fig. 3.4: Power dependence, Laser power(mW) Vs PA signal amplitude (mV)

Also the power dependence of the PA signal is studied. It is found that for laser powers used for the present investigation and the modulation frequencies, the PA signal varies linearly with laser power. It is shown graphically in figure 3.4

To determine the thermal diffusivity the sample is kept in the PA cell and the PA signal amplitude and phase are measured as functions of chopping frequency [Fig. 3.5 - 3.13]. Then a graph is drawn with log (amplitude) along the X axis and log (frequency) along the Y axis. The graph shows a change in its slope at a certain chopping frequency, which is the characteristic frequency (f_c) for the sample. Thus by knowing sample thickness (l_s) the thermal diffusivity α can be calculated using the relating $\alpha = l_s^2 f_c$ [eqn. 2.42]. The thickness, characteristic frequency and thermal diffusivity of copper, aluminium, and iron are shown in the table.

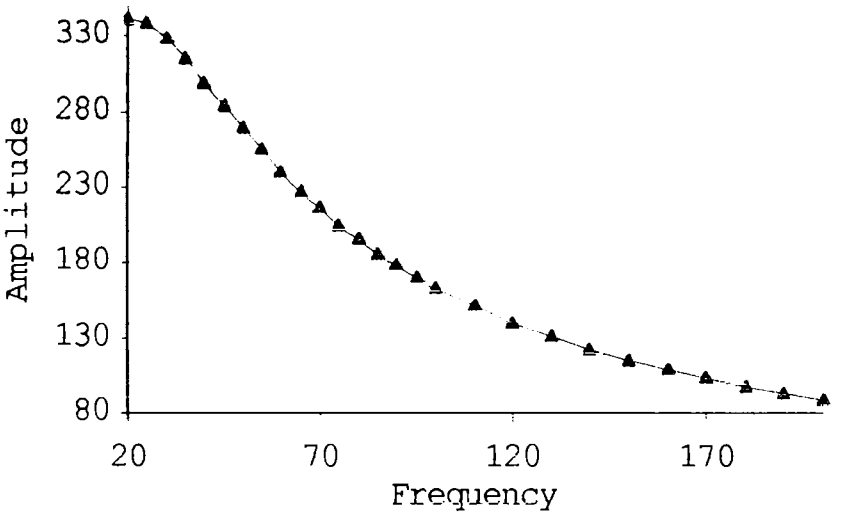

Fig. 3.5: Amplitude(μV) Vs Frequency (Hz) plot for copper

.

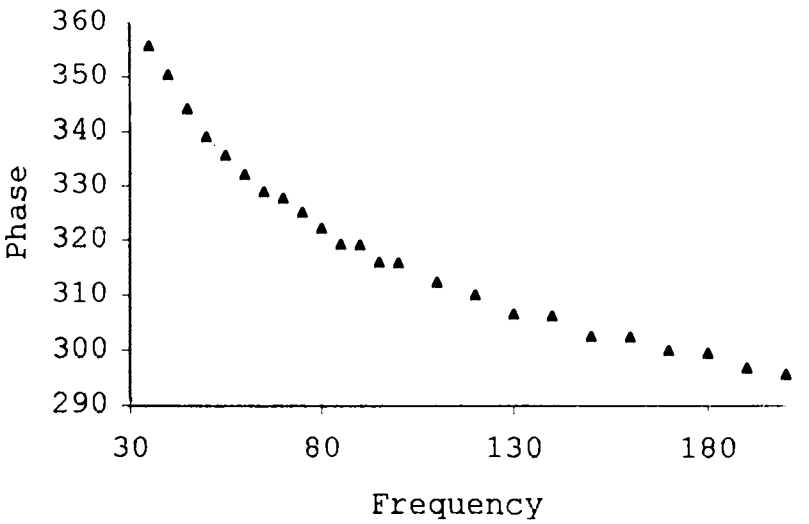

Fig. 3.6: Phase Vs Frequency (Hz) plot for copper.

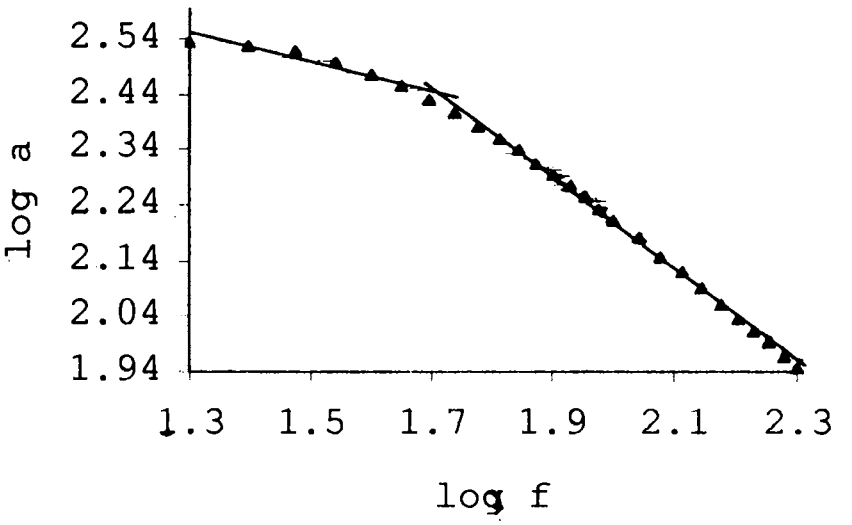

Fig.3.7: log amplitude(a) Vs log frequency(f) plot for copper

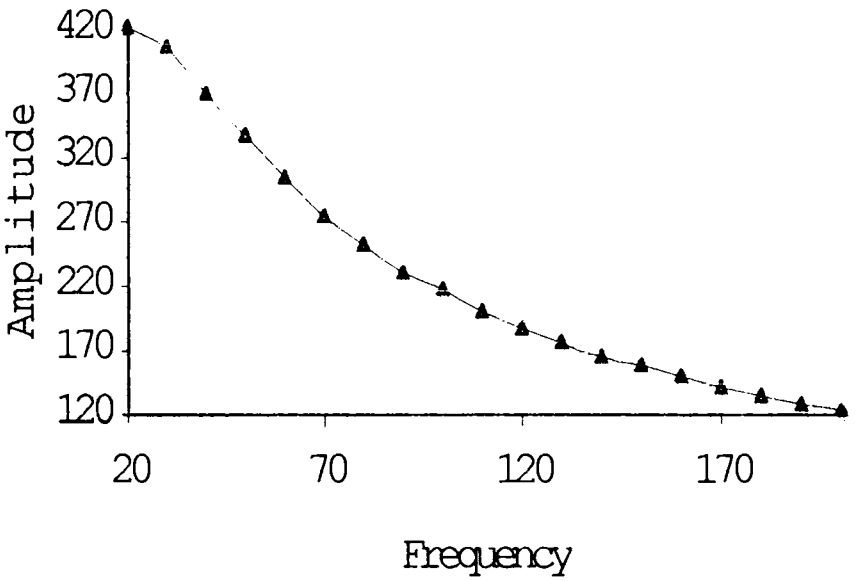

Fig 3.8: Amplitude(μV) Vs Frequency (Hz) plot for aluminium

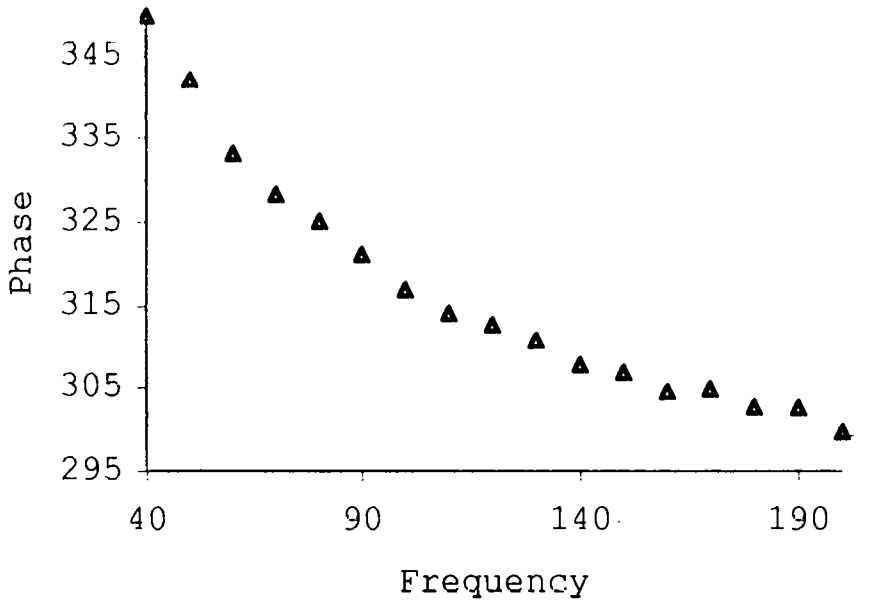

Fig. 3.9: Phase Vs Frequency (Hz) plot for aluminium

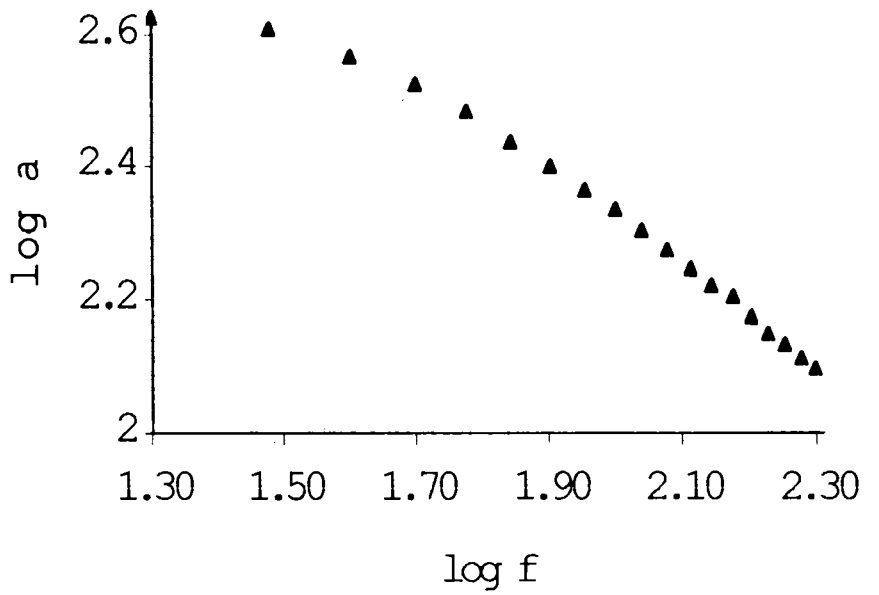

Fig. 3.10: log amplitude Vs log frequency plot for aluminium.

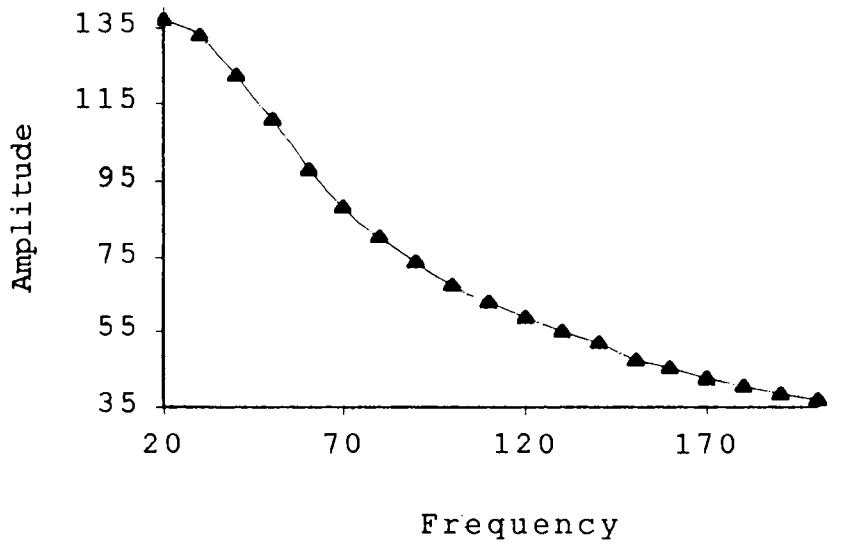

Fig. 3.11: Amplitude(μV) Vs Frequency (Hz) plot for iron.

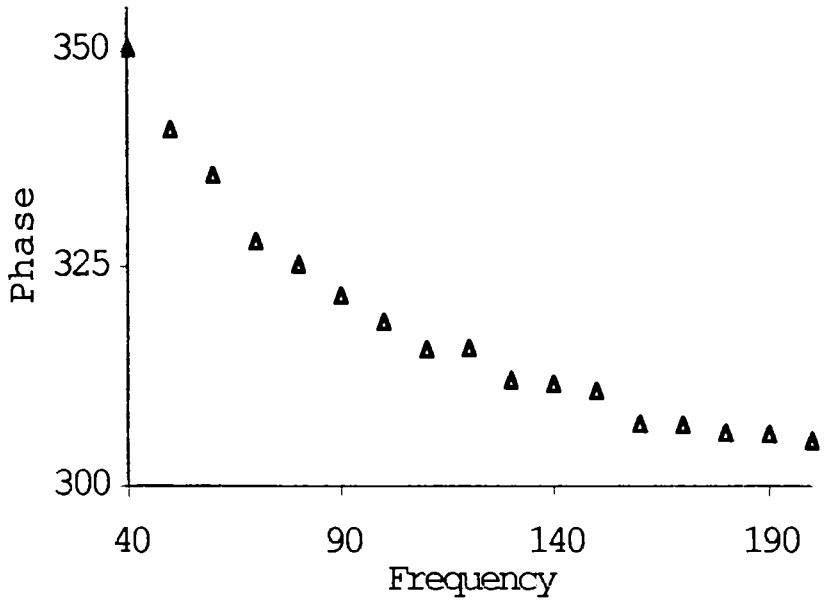

Fig. 3.12: Phase Vs Frequency (Hz) plot for aluminium.

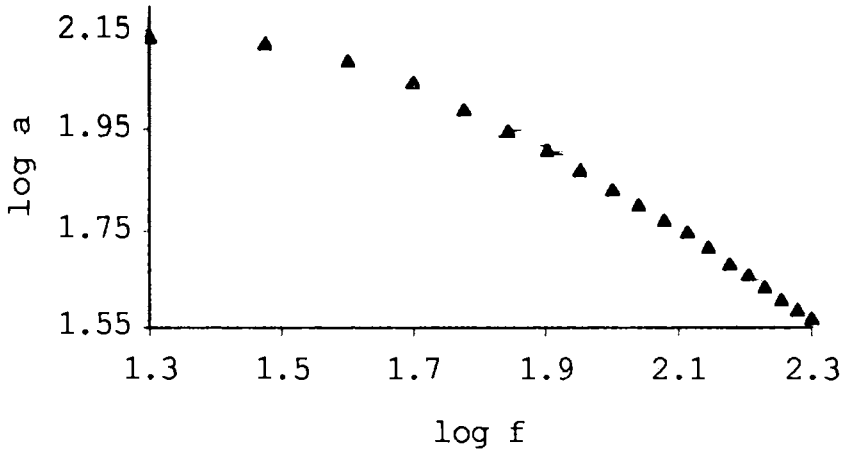

Fig. 3.13: log amplitude Vs log frequency plot for iron.

Table.1 Thermal diffusivity of certain metalic samples evaluated using PA technique.

Sample	l_s (mm)	f_c (Hz)	Thermal diffusivity (cm^2/s)	
			Calculated	Reported
Copper	1.56	48.8	1.180± 0.001	1.160 ± 0.001
Aluminium	1.28	59.8	0.979± 0.001	0.980 ± 0.001
Iron	0.64	55.3	0.234± 0.001	0.244 ± 0.001

3.4. SAMPLE SELECTION

The main objective of the present investigation is to measure thermal diffusivity of materials and to bring out

some the factors that can influence/govern the thermal properties of materials. With this intention some typical samples are selected from diverse class of materials that find applications in various fields of science and technology. The materials studied are significant in microelectronics, low temperature Physics, substrate and solid state technology (Alumina), an important rare earth oxide (Nd_2O_3) that finds applications in device fabrication, industry and chemical engineering and newly synthesised medically and industriallly important metal complexes (hlogeno benzimidazole complexes) and polymer bound metal complexes. Studies were also carried out in some of the metal Phthalocyanines that find applications in the fields of chemical technology, optical data storage etc.

3.5. CONCLUSION

General aspects of PA spectrometer with brief description of various components is given. The design and fabrication aspects of PA cell are also included. The experimental se-up is standardised by determining the thermal diffusivity of copper, iron and aluminium.

REFERENCES

[1] A. Rosencwaig and A. Gersho, J. Appl. Phys., 47(1976) 64.

[2] A.C. Tam, and H. Coufal, 1983b, J. Phys., (Paris) Colloq. C6, 9.

[3] A.C. Tam, 1983 in Ultrasensitive Laser Spectroscopy, edited by D. Kliger (Academic, NewYork), Chap.1.

[4] A. Rosencwaig, Rev. Sci. Instrum., 48 (1977) 1133.

[5] L.G. Rosengren, Appl. Opt., 14 (1975) 1960.

[6] C.F. Dewey, in Optoacoustic Spectroscopy and Detection, Ed: Y H Pao (Academic Press New York, 1977) P47.

[7] A. Rosencwaig, Photoacoustics and Photoacoustic Spectroscopy. (Wiley, New York, 1980).

[8] P.M. Morse, in Vibration and Sound, (Mc.Grawhil, New York, 1980).

[9] L.A. Farrow, and R.E. Richton, J. Appl. Phys., 48 (1977) 4962.

[10] C.F. Dewey Jr., R.D. Kamm and C.E. Hackett, Appl. Phys. Lett., 23 (1973) 633.

[11] M.L. Meady, Lock-in Amplifiers: Principles and Applications, Peter Peregrinus Ltd., London(1983).

* * * * *

CHAPTER 4

STUDY OF PHOTOACOUSTIC EFFECT IN γ-ALUMINA - THE INFLUENCE OF HYDROXYL ION ON THERMAL DIFFUSIVITY

ABSTRACT

Alumina is an important material in the field of low temperature Physics, microelectronics and in solid state technology as substrate material. The effect of the chemisorbed hydroxyl groups on the thermal diffusivity of γ-alumina is determined by evaluating the thermal diffusivity at various degassing temperatures and by doping it with rare earth oxide using photoacoustic technique. The thermal diffusivity is found to decrease with the increase in degassing temperature as well as with the increase in the doping concentration of rare earth oxide. This decrease has been attributed to the loss of hydroxyl ion from the γ-Al_2O_3.

4.1. INTRODUCTION

Metallic films on insulators are widely used in evolving technologies such as microelectronics, magnetic and optical devices and protective coatings. Excimer laser irradiation can modify the surface of various insulators, improving the properties relevant to packaging applications. For instance the adhesion between a ceramic substrate and a deposited metallic film is strongly enhanced if the substrate is laser-irradiated [1]. Thus a substantial increase in gold-alumina and copper-alumina adhesion strength has been achieved when the alumina substrates are irradiated with 308 nm wavelength pulsed - laser prior to deposition [1-3].

The interaction of UV light with wide band-gap materials is enhanced by the presence of structural defects. The light absorption in alumina (Al_2O_3) at 308-nm wavelength (4eV) occurs at grain boundaries and impurities. UV light absorption by these wide band-gap materials can also be enhanced through the accumulation of defects [4,5]. At a laser energy density of 0.7 J/cm^2 the polycrystalline Al_2O_3 melts. This implies not only that there is defects build up induced by these initial stages

but also that the damage is most likely photochemically induced.

As alumina has gained a significant place in microelectronics, low temperature Physics because of its juxtaposition of properties, substrate materials etc, a knowledge of its thermal parameters is valuable.

4.2. ALUMINA

Alumina (Al_2O_3) is an important material in adsorption and catalysis. Of a, wide variety of crystallographic modifications [1], the transition phases η and γ-Al_2O_3 are of special interest since they can provide high specific surface areas (typically between 100 and 200 m^2 /g). These modifications have a defect lattice of the spinal type and can be distinguished by their defect character and the distribution of the cations in tetrahedral and octahedral sites [1,2].

The alumina surfaces, on exposure to water vapour (moist air) are terminated by a monolayer of hydroxyl (OH) groups [3-5]. The rehydroxylation of dehydroxylated alumina surfaces on exposure to water vapour is accompanied by a

strong heat evolution [6,7] indicating the strong chemical interaction between surface and
water molecule.

On degassing the surface of γ-Al_2O_3 at 650 ^{o}C, Peri and Hannan [3] have observed three resolved OH stretching bands at 3698, 3737, and 3795 cm^{-1} which are assigned to "isolated", non-interacting, OH groups. Additional bands at 3733 and 3780 cm^{-1} were also observed by Peri [4]. The OH groups at various sites responsible for these bands are shown in fig. 4.1. When degassed below 500 ^{o}C, broad unresolved bands, due to the mutual interaction of OH groups, are obtained in the OH stretching region. At higher degassing temperatures, the isolated surface OH groups get progressively removed from the surface. Even after heat treatment at 800 ^{o}C, about 2% of the total OH content remains on the surface [4]. The removal of OH groups from the surface was postulated to generate "strained oxide linkages", a reaction that may be depicted as,

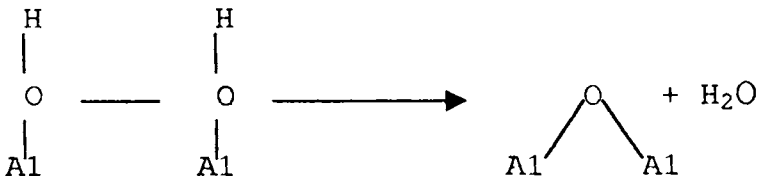

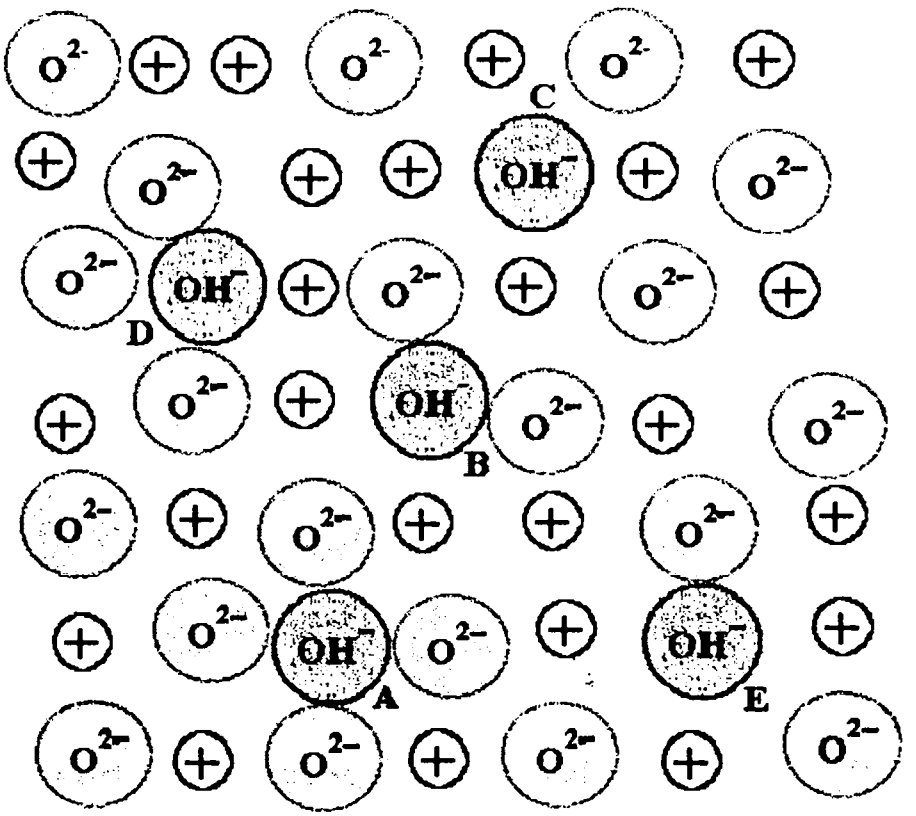

⊕ — '+' Al ion on the layer below the surface

A-3800 cm ; B -3744 cm ; C - 3700 cm ; D - 3780 cm ; E - 3733 cm

Fig. 4.1: The OH groups at various sites responsible for the bands in the IR spectrum of alumina.

The condensation of the two neighbouring OH groups leads to the formation of a water molecule that gets expelled from the surface. This process leaves an oxide

ion in the outer most surface layer and an exposed incompletely coordinated aluminium ion in the next lower layer. This exposed cation acts as a Lewis acid site. According to the model of Al_2O_3 developed by earlier workers [3,4], the dehydroxylation process is simulated by a statistical method. Assuming a random removal of OH pairs without the creation of "defects" (adjacent oxide ions or holes), a regular surface lattice can be maintained up to the stage where, about 67% of the OH monolayer has been removed at 500°C. Remaining hydroxyls can only be condensed to eliminate water with the creation of defects, which comprise adjacent aluminium and oxide ion. About 90% of OH content gets eliminated when degassed at 670 °C. When heated to 900 - 1000 °C the OH groups on the surface get expelled completely and leave coordinated O^{2-} on the outer surface layer.

The performance of the pure oxides can be considerably changed by supporting and/or mixing oxide systems. For example, addition of rare earth oxides promotes the effectiveness of alumina due to the formation of R-O-Al bond [$RalO_3$ phase] [8]. On the basis of TEM data, it is found that the presence of rare earth cations modifies the

crystal growth characteristics of Al_2O_3 and that the lanthanides hinder the reactivity of strong Lewis acid sites at the Al_2O_3 surfaces [9]. Thus, the OH content of alumina decreases on rare earth doping.

4.3. EXPERIMENTAL

Apart from the point of view of catalysis and adsorption studies, evaluation of thermal parameters of Al_2O_3 (like thermal diffusivity) are important means of thermal characterization. It has been well recognised that the photoacoustic (PA) effect is an effective technique for evaluating the thermal diffusivity of samples [10-20]. The basic principle behind PA effect is that when a sample is illuminated by intensity modulated (chopped) light, the resulting periodic optical absorption generates stress and thermal waves in the sample. The PA signal can be detected either directly by using a transducer in contact with the sample [21] or indirectly by keeping the sample in a cell and measuring the acoustic wave generated in the coupling gas with a sensitive microphone. By studying the chopping frequency dependence of the potoacoustic signal generated in the coupling gas at a fixed optical wavelength, the thermal diffusivity of the sample can be evaluated [19],

The present work deals with the study of the effect of OH ions on thermal diffusivity of alumina, by evaluating its thermal diffusivity after heating to various degassing temperatures and doping it with rare earth oxide. In the single beam PA spectrometer [21] assembled for the present investigation, the 488-nm line of an Argon ion laser (LiCONiX 5300) has been used as the pump source. To generate acoustic signal in the PA cell, the pump beam is modulated using an electromechanical chopper. The PA cell used is a cylindrical, small volume (~3 cc), non-resonant cell made out of aluminium. The cell has an axial bore of about 0.5-cm diameter. One side of the bore is closed by a glass window, to the other side we place the sample, and the cavity is closed tightly. To detect the acoustic signal generated in the coupling medium, a small highly sensitive (100 μV/Pa) microphone is kept close to the sample compartment in a separate port. The microphone output is processed by means of a lock-in amplifier (EG & G Model 5208). The experimental set-up is described in detail in chapter 3.

As mentioned earlier thermal diffusivity can be evaluated from the chopping frequency dependence of the PA signal [18]. For a given sample thickness (l_s), one can have a transition from thermally thin regime to thermally

thick regime by increasing the chopping frequency. The transition appears as a slope change at the characteristic frequency (f_C) in the log (amplitude) Vs log (frequency) plot. Knowing the actual thickness of the sample (l_S), the thermal diffusivity (α) can be calculated using the relation, $\alpha = l_S^2 f_C$ [18,19].

4.3.1. PREPARATION OF γ -Al_2O_3

In our experiment, γ-Al_2O_3 is prepared by the dehydroxylation of hydrous oxides at low temperature (350 ^oC). Nitrate solution of the sample (250 ml) containing 0.5g of Al_2O_3 is heated to boiling and 1:1 ammonium hydroxide solution is added dropwise with stirring until the precipitation is complete. It is then allowed to digest on a steam bath until the precipitate is flocculated and settled. The precipitate is filtered on a whatmann No.41 filter paper and washed with small portion of an aqueous solution containing 2g of ammonium chloride and 10 ml of concentrated ammonium hydroxide in 100 ml until the precipitate is free of Cl^{-1}. The precipitate is kept in an air oven at 450 ^oC for 3 h.

4.3.2. PREPARATION OF MIXED OXIDES

The mixed oxide is prepared by co-precipitation from a nitrate solution. Aqueous ammonia solution is added to a mixed aqueous solution containing rare earth nitrate and aluminium nitrate. It is then dried overnight at 110 ^{o}C and then calcined at 400 ^{o}C for three hours to form the mixed oxide.

4.3.3. THERMAL DIFFUSIVITY MEASUREMENT

To determine the thermal diffusivity, 0.1 g of the sample (with specific surface area [1,2] ~80m^2) is pelletised under high pressure (6 tons/cm^2) using hydrolic press. Placing the sample (in the form of a pellet) in the PA cell, the frequency dependence of the acoustic signal amplitude is studied (Fig.4.2). Knowing the thickness (l_s) of the sample and the characteristic frequency (f_c) from the log-log plot, the thermal diffusivity can be calculated. The log-log plot for these various samples are shown in figures 4.3-4.16. After the measurements the Al_2O_3 sample is kept in an oven at 500 ^{o}C or 1000 ^{o}C for about three hours in order to degas it and eliminate the OH ions. The thermal diffusivity of Al_2O_3 degassed at different

temperatures is shown in Table 4.1 [21] and pictorially in 4.17. The accuracy of the measurements depends on the

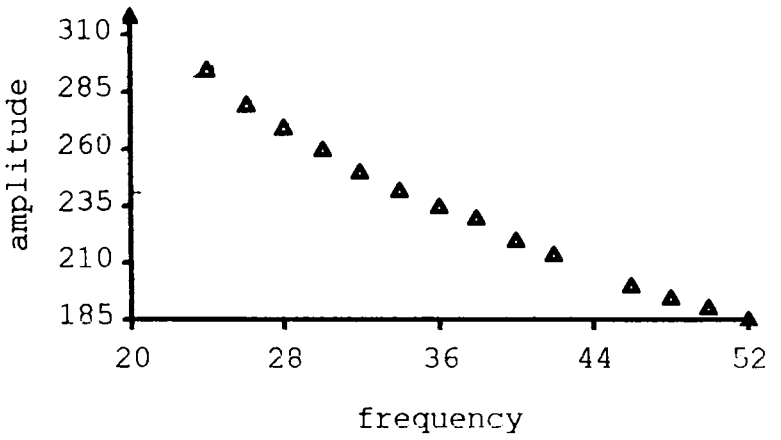

Fig. 4.2: Amplitude(μV) Vs Frequency (Hz) plot for Al_2O_3 - 100% and Nd_2O_3 0% at 30°C

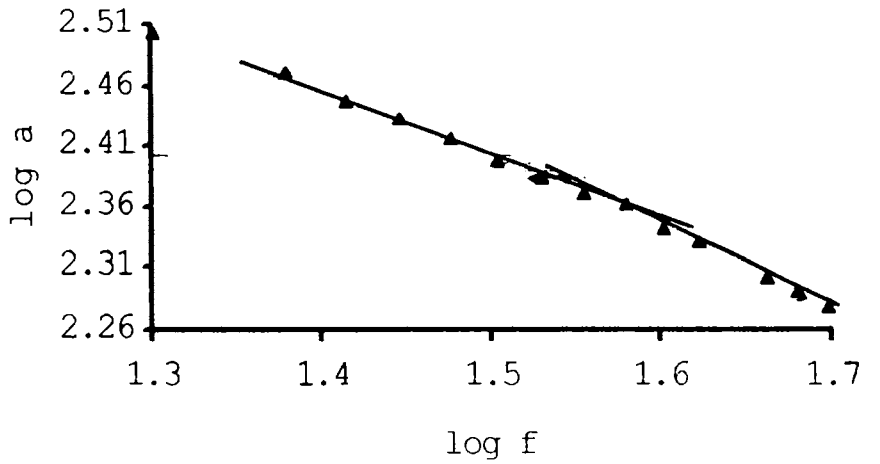

Fig. 4.3:log amplitude Vs log frequency plot for Al_2O_3 -100% and Nd_2O_3 0% at 30°C

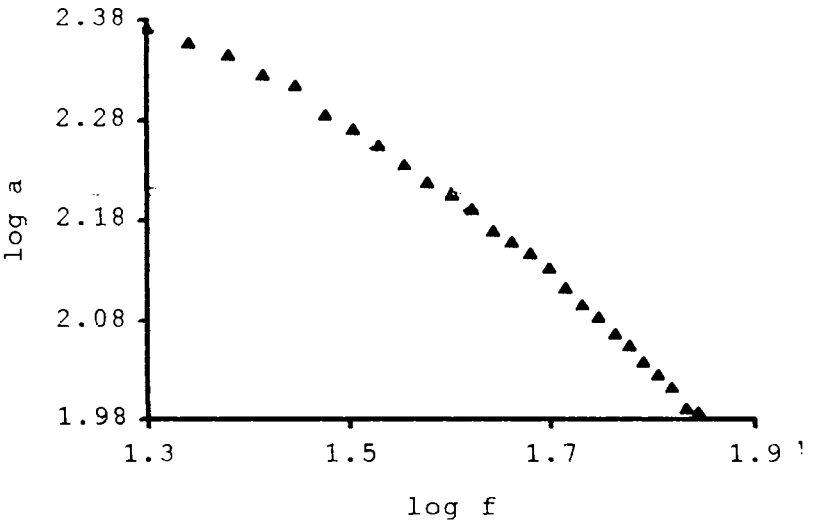

Fig. 4.4: log amplitude Vs log frequency plot for Al_2O_3 -95% and Nd_2O_3 5% at 30°C

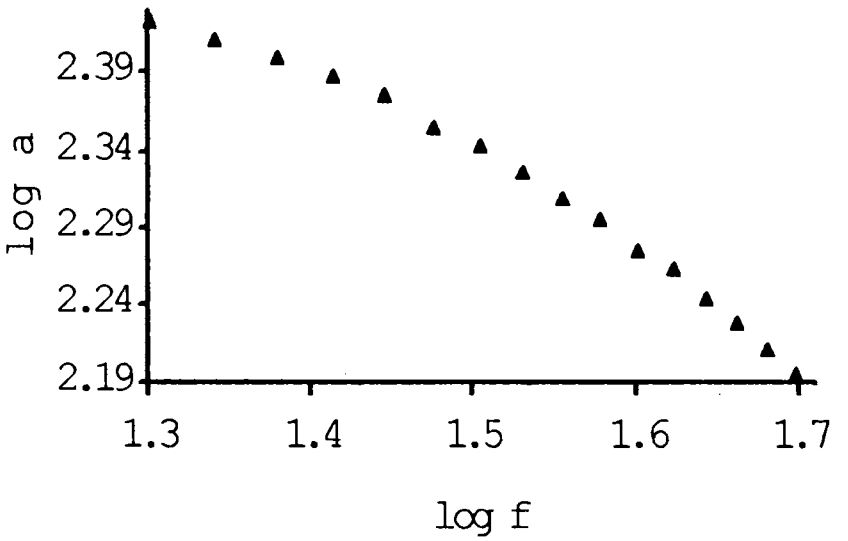

Fig. 4.5: log amplitude Vs log frequency plot for Al_2O_3 -90% and Nd_2O_3 10% at 30°C

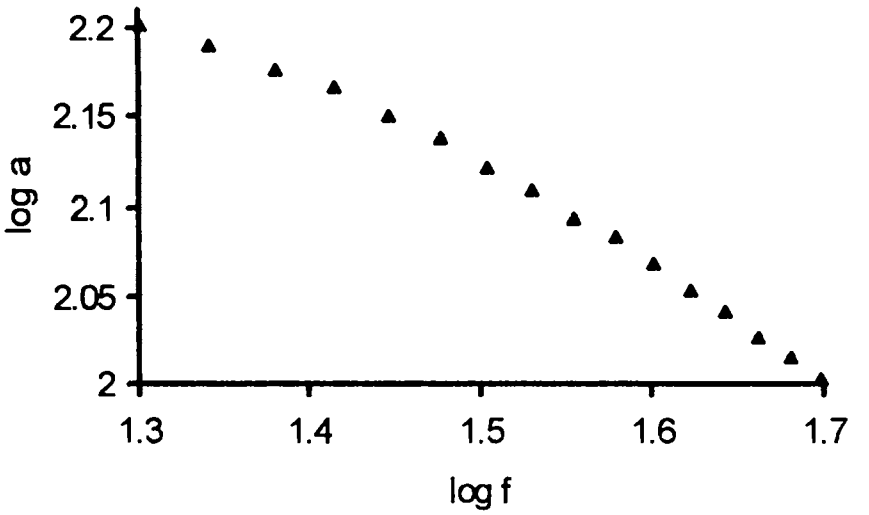

Fig. 4.6: log amplitude Vs log frequency plot for Al_2O_3 -80% and Nd_2O_3 20% at 30°C

Fig. 4.7: log amplitude Vs log frequency plot for Al_2O_3 -40% and Nd_2O_3 60% at 30°C

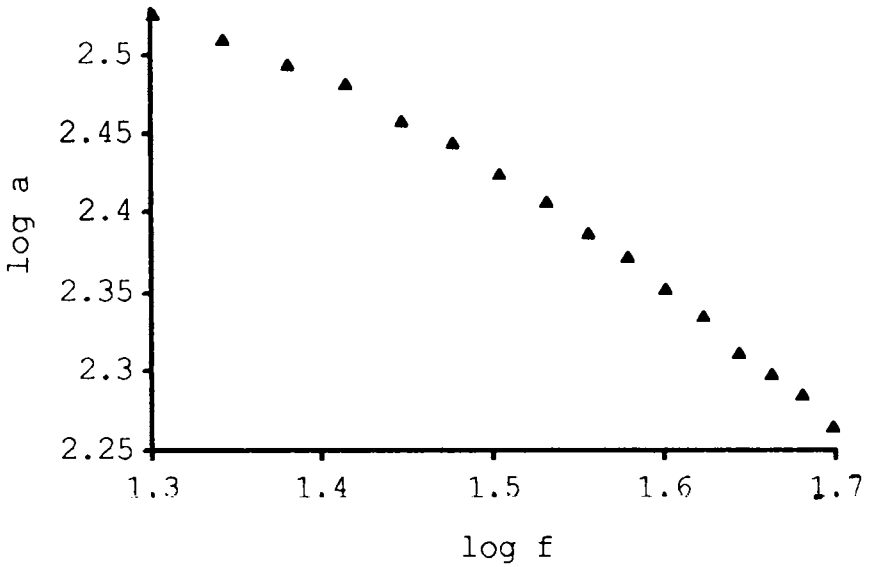

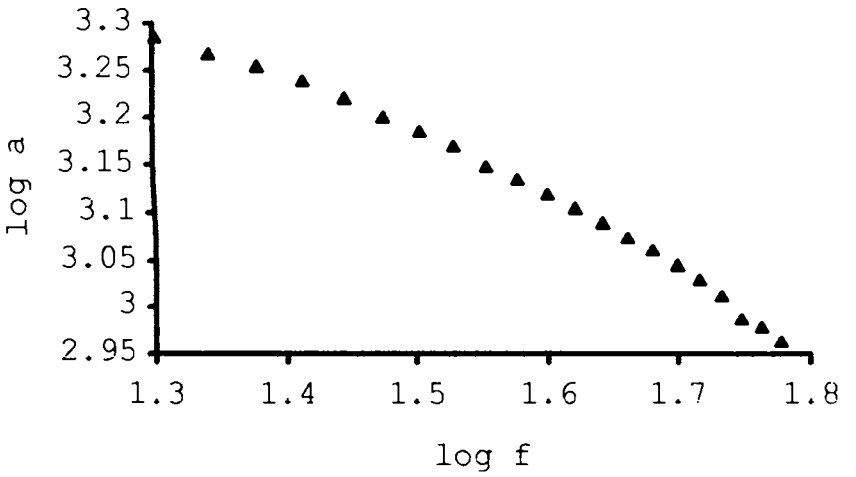

Fig. 4.8: log amplitude Vs log frequency plot for Al_2O_3 -20% and Nd_2O_3 80% at 30°C

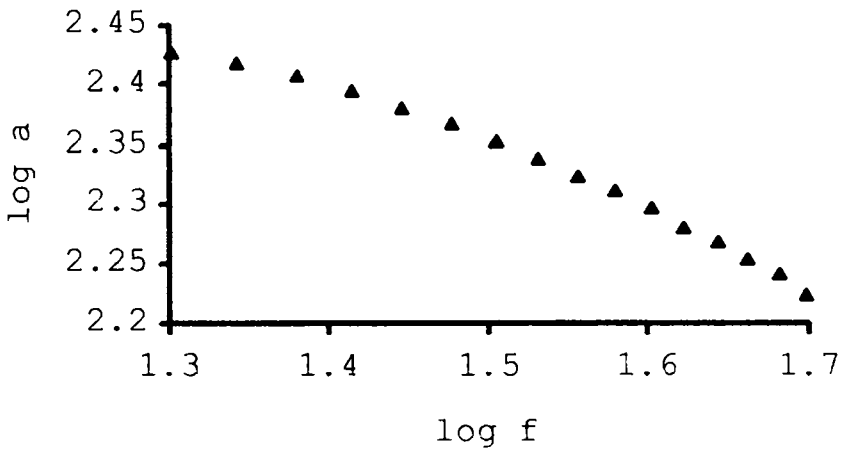

Fig. 4.9: log amplitude Vs log frequency plot for Al_2O_3 -0% and Nd_2O_3 100% at 30°C

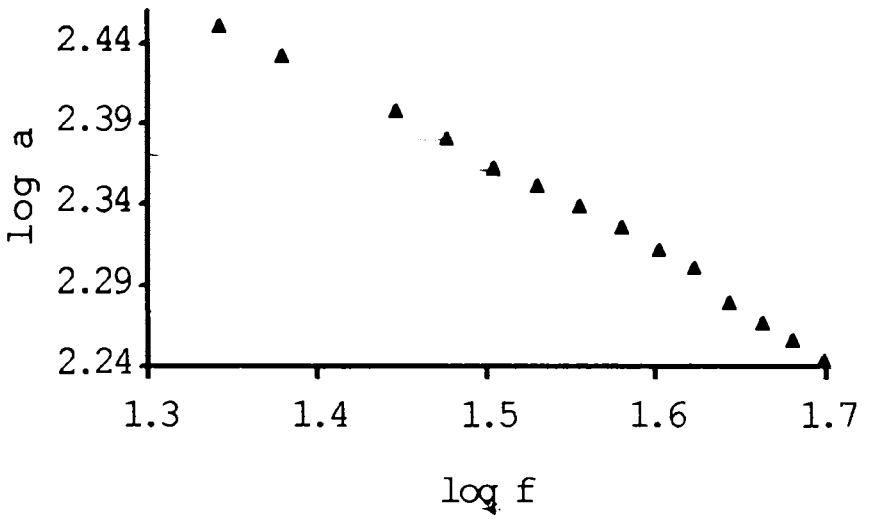

Fig. 4.10:log amplitude Vs log frequency plot for Al_2O_3 - 100% and Nd_2O_3 0% at 500°C

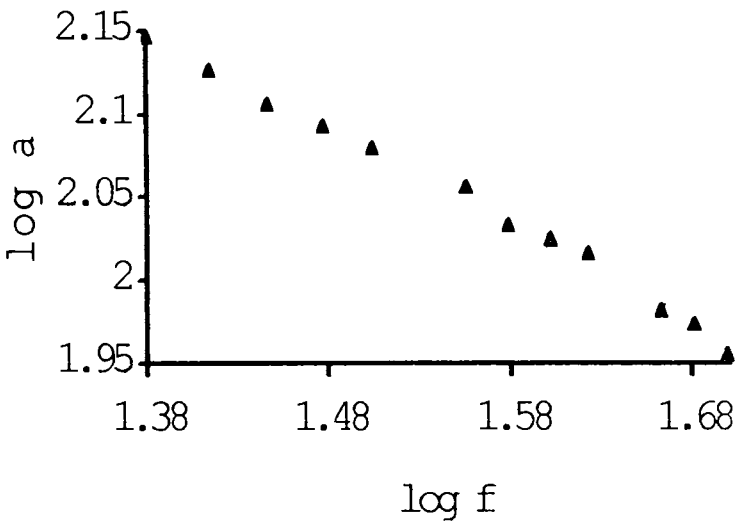

Fig. 4.11: log amplitude Vs log frequency plot for Al_2O_3 - 95% and Nd_2O_3 5% at 500°C

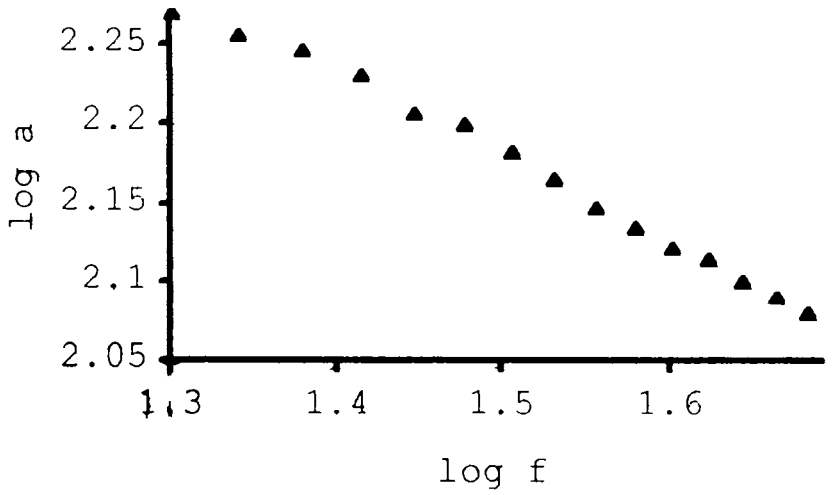

Fig. 4.12: log amplitude Vs log frequency plot for Al_2O_3 - 90% and Nd_2O_3 10% at 500°C

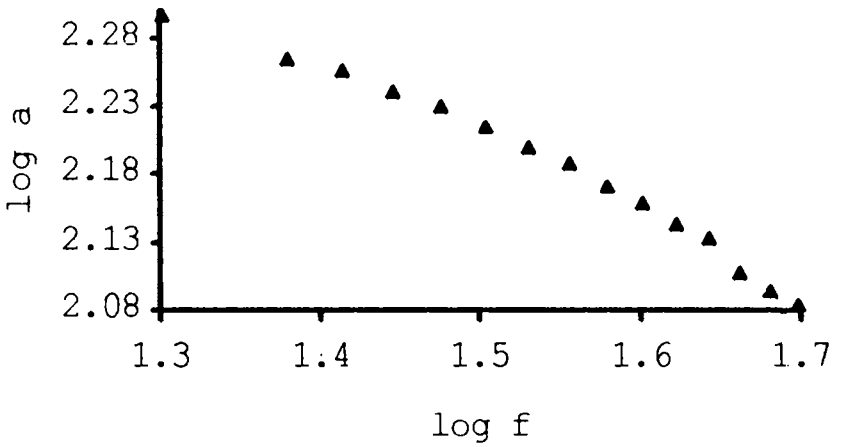

Fig. 4.13: log amplitude Vs log frequency plot for Al_2O_3 - 80% and Nd_2O_3 20% at 500°C

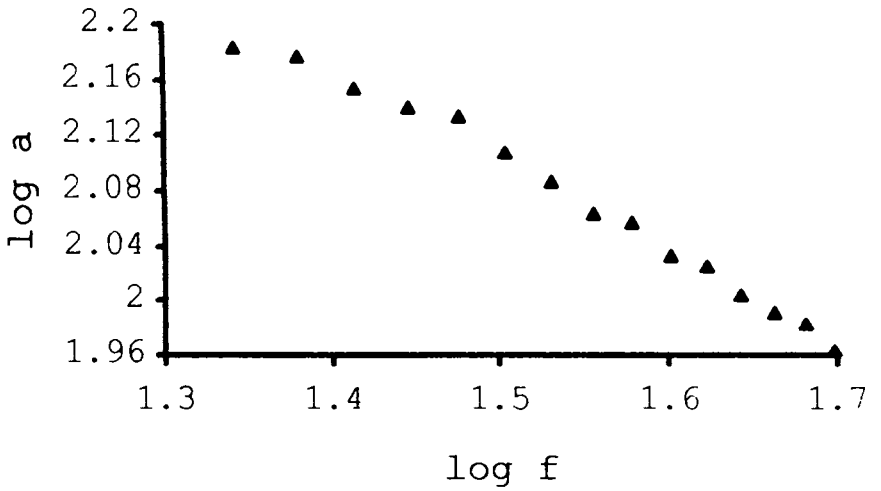

Fig. 4.14: log amplitude Vs log frequency plot for Al_2O_3 - 40% and Nd_2O_3 60% at 500°C

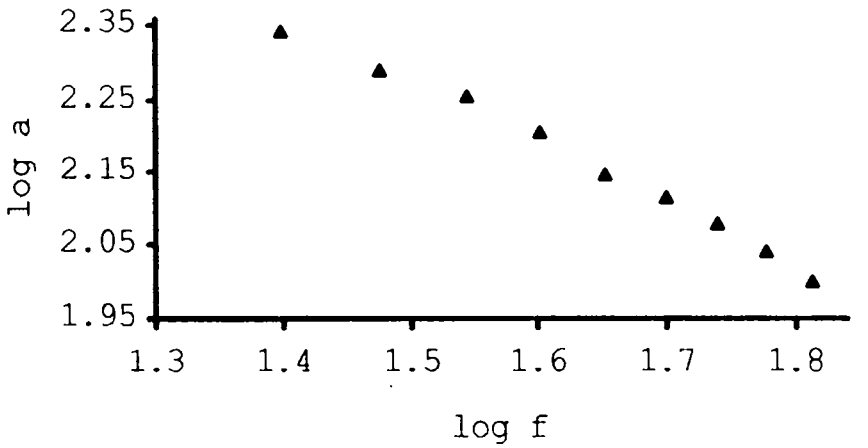

Fig. 4.15: log amplitude Vs log frequency plot for Al_2O_3 -0% and Nd_2O_3 100% at 500°C

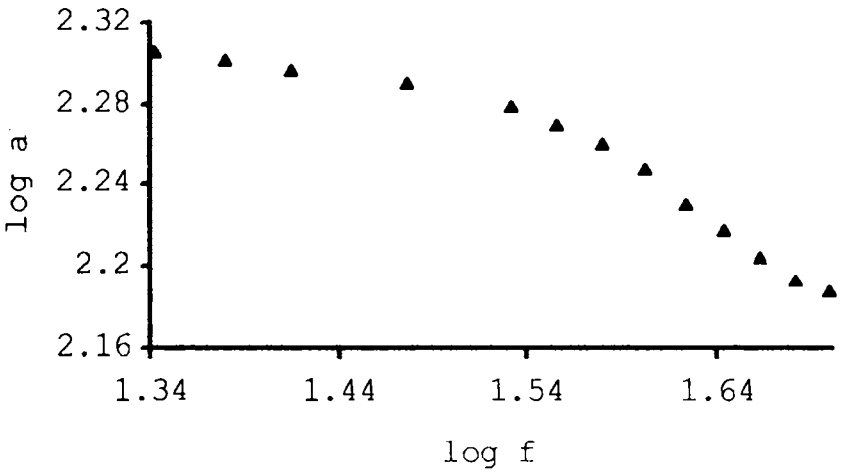

Fig. 4.16: log amplitude Vs log frequency plot for Al_2O_3 - 100% and Nd_2O_3 0% at 1000°C

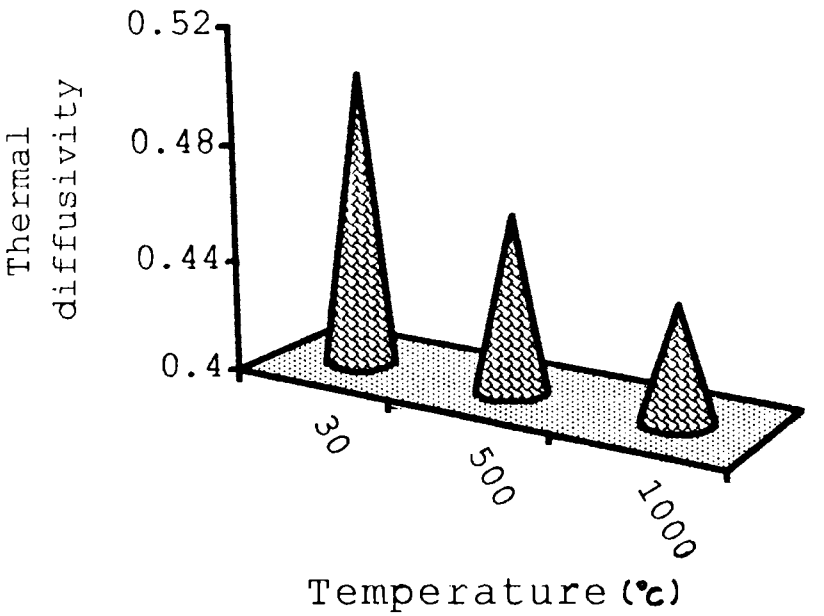

Fig. 4.17: Thermal diffusivity of Al_2O_3 at different temperatures

determination of sample thickness (l_s) and characteristic frequency (f_c). The values of thermal diffusivity are correct up to third digit.

The experiment is repeated after doping Al_2O_3 with Nd_2O_3. It is seen that the doping causes a decrease in the thermal diffusivity of Al_2O_3. The doped samples are then degassed at 500 ^{o}C and the thermal diffusivity is found to decrease further. Results are given in Table 4.2(a & b) [22,23] and the variation of thermal diffusivity with the percentage of alumina in the sample is graphically shown in figure 4.18.

TABLE 4.1 Thermal diffusivity of Al_2O_3 degassed at different temperatures. (l_s= 1.15 X 10^{-3} m)

Temperature (^{o}C)	Characteristic Frequency(f_c) (Hz)	Thermal diffusivity (α) (cm^2/s)
30	37.9	0.502 ± 0.001
500	34.8	0.461 ± 0.001
1000	33.3	0.440 ± 0.001

TABLE 4.2 Thermal diffusivity of Al_2O_3 doped with Nd_2O_3.

(a) At room temperature(30 °C)

l_s (mm)	f_c (Hz)	Al_2O_3 (%)	Nd_2O_3 (%)	Thermaldiffusivity (α) (cm^2/s)
1.15	37.9	100	0	0.502 ± 0.001
0.89	45.6	95	5	0.361 ± 0.001
0.93	30.5	90	10	0.264 ± 0.001
0.87	33.9	80	20	0.257 ± 0.001
0.86	33.3	40	60	0.246 ± 0.001
0.82	33.9	20	80	0.228 ± 0.001
0.54	33.9	0	100	0.099 ± 0.001

(b) At 500 °C

l_s (mm)	f_c (Hz)	Al_2O_3 (%)	Nd_2O_3 (%)	Thermaldiffusivity (α) (cm^2/s)
1.15	34.8	100	0	0.461 ± 0.001
0.89	38.9	95	5	0.262 ± 0.001
0.93	34.5	90	10	0.243 ± 0.001
0.87	30.6	80	20	0.211 ± 0.001
0.86	29.6	40	60	0.209 ± 0.001
0.82	28.1	20	80	0.189 ± 0.001
0.54	32.5	0	100	0.095 ± 0.001

4.4. RESULTS AND DISCUSSIONS

From the photoacoustic measurements it is seen that when the sample is degassed at 500 °C, α falls by 8.2% of its value before degassing, when it had a monolayer[3-5] of OH ions. When the sample is degassed further at 1000 °C the thermal diffusivity falls by 12.4% of its initial value. The reason for selecting 500 and 1000 °C is that at 500 °C about 67%, and at 1000 °C more than 98% of OH ions are removed from the sample.

From Table I, it is evident that the degassing temperature has pronounced effect on thermal diffusivity. The heating of Al_2O_3 decreases the amount of OH ions at various sites [3]. The observed decrease in the thermal diffusivity of Al_2O_3 at increasing degassing temperature is therefore due to the loss of OH ions from Al_2O_3.

It has been found from the IR spectrum that the doping of Al_2O_3 with Nd_2O_3 also decreases the OH content [8,9]. This implies that Nd has interacted extensively with the OH groups on the surface. The calcination of these doped samples further reduces the OH content [9]. As expected, the thermal diffusivity of Al_2O_3 is also found to decrease with the increase of Nd_2O_3 (Table II). These results

further suggest that the observed variation of thermal diffusivity is due to the loss of OH ions [3-5],

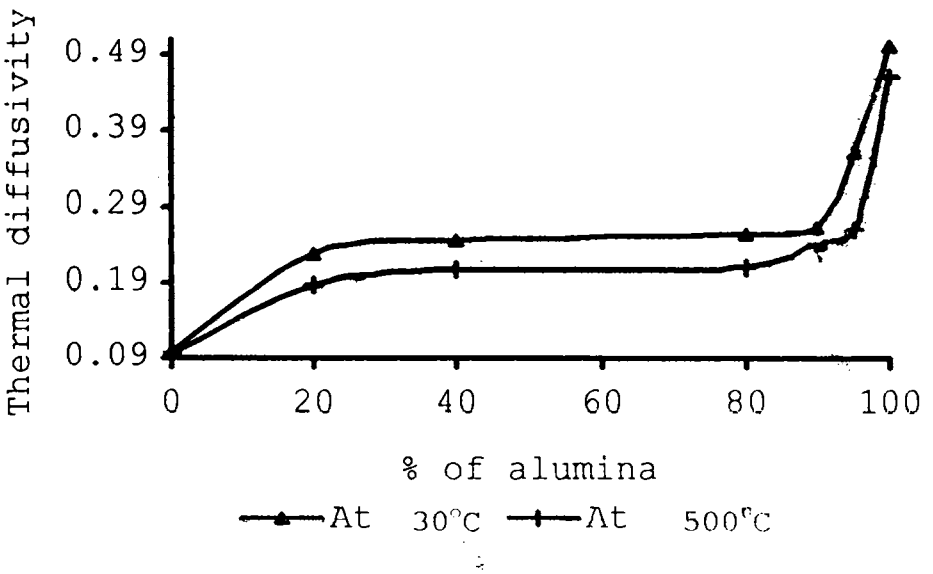

Fig.4.18: Variation of thermal diffusivity with % of alumina at 30°C and 500°C.

Due to the larger surface area, Al_2O_3 has more adsorbed OH ions than Nd_2O_3. If we compare the thermal diffusivity of Al_2O_3 and Nd_2O_3 before and after degassing, it can be seen that the decrease in the thermal diffusivity of Nd_2O_3 is much less than that of Al_2O_3. This further confirms the role of OH ions on the thermal properties of Al_2O_3.

With these supporting evidences, we can conclude that the OH ions have significant effect on the thermal diffusivity of alumina.

REFERENCES

[1] B.C. Lippens and J.J. Steggerda in Physical and Chemical Aspects of Adsorbents and Catalysts, edited by B.G. Linsed Academic press, New York, 1970), p. 171.

[2] A.J. Leonard, F. Van Cauweleert, and J.J. Fripiat, J. Phys. Chem., 71 (1967) 695.

[3] J.B. Peri and R.B. Hannan, J. Phys. Chem., 64 (1960) 1526.

[4] J.B. Peri, J. Phys. Chem., 69 (1965) 211.

[5] J.L. Carter, P.J. Lucchesi, P. Corncil, D.J.C. Yates, and J.H. Sinfelt, J. Phys. Chem., 69 (1965) 3070.

[6] E.B. Cornelius, T.H. Milliken, G.A. Mills, and A.G. Oblad, J. Phys. Chem., 59 (1955) 809.

[7] R.L. Venable, W.H. Wade, and N. Hackerman, J. Phys. Chem., 69 (1965) 317.

[8] M.J. Capitan, P. Malet, and J.A. Odinozole, J. Phys. Chem., 97 (1993) 9233.

[9] J.W. Cui and I.E. Massoth, J. Catal., 136 (1992) 361.

[10] A.G. Bell, Am. J. Sci., 20 (1880) 305.

[11] A.G. Bell, Philoss. Mag., 11 (1881) 510.

[12] A. Rosencwaig and A. Gersho, J. Appl. Phys., 47 (1975) 64.

[13] A. Rosencwaig, Rev. Sci. Instrum., 48 (1977) 1133.

[14] G.C. Wetsel. Jr and F.A. Mac Donald, Appl. Phys. Lett. 30, (1977) 252.

[15] A.C. Tam, C.K.N. Patel, and R.J. Kerl, Opt.,Lett. 4 (1979) 81.

[16] A.C. Tam, Rev. Modern Phys., 56 (1986) 2.

[17] C.L. Cesar, H. Vrgas, and L.C.M. Miranda, Appl. Phys., Lett. 32 (1978) 554.

[18] P. Charpentier, F. Lepoutre, and L. Bertrand, J. Appl. Phys., 53 (1982) 1.

[19] F.A. Mac Donald and G.C. Wetsel. Jr, J.Appl. Phys., 49 (1978) 4.

[20] A. Hordvik and H. Scholssberg, Appl. Opt., 16 (1977) 101 and 16 (1977) 2919.

[21] S. Sankara raman, V.P.N. Nampoori, C.P.G. Vallabhan, G. G. Ambadas and S. Sugunan, Appl. Phys. Lett., 67 (1995) 2939.

[22] S. Sankara raman, V.P.N. Nampoori, C.P.G. Vallabhan, G. Ambadas and S. Sugunan, J. Appl. Phys., 85(1999) (In press).

[23] S. Sankara raman, V.P.N. Nampoori, C.P.G. Vallabhan, G. Ambadas and S. Sugunan, Proceedings of 8th Kerala Science Congress-Jan. 1996 p. 333

* * * * *

CHAPTER 5

INFLUENCE OF SAMPLE PREPARATION ROUTE ON THERMAL DIFFUSIVITY

ABSTRACT

Knowledge of thermal and optical properties of rare earth (RE) oxides is important in the context of electronic component and device development and piezo, pyro and electrooptic applications. For example, from the point of view of laser based studies Nd_2O_3 is one of the important RE oxides which can be prepared by two different methods viz. oxalate and hydroxide methods. The thermal diffusivity of these differently prepared Nd_2O_3 is determined by laser induced photoacoustic technique. The method is standardised by determining the thermal diffusivity of copper and aluminium. The effect of preparation method on thermal diffusivity of Nd_2O_3 is studied details of which are given in this chapter.,

5.1. INTRODUCTION

The photoacoustic (PA) effect has been recently revived as a very useful technique for measuring the optical [1-7] and thermal [8-10] properties of materials because of its high sensitivity and non-destructive nature. In the energy conversion process (optical to acoustical) involved in this effect, the thermal properties of the sample play a significant role. Hence photoacoustic effect can be used for the study of thermal properties of solids such as thermal diffusivity, phase transition etc. By studying the chopping frequency dependence of the photoacoustic signal generated in the coupling gas at a fixed optical wavelength, the thermal diffusivity of the sample can be evaluated [9].

The method of preparation of a sample has profound effect on its physical as well as chemical properties [12,13]. Hence a material prepared by two different methods show slightly different surface as well as chemical properties. Kuo et al has shown [14] by mirage-effect that the thermal diffusivities of differently prepared specimens of SiC differ. In this chapter, the effect of method of preparation on thermal diffusivity of Nd_2O_3 has been determined by photoacoustic technique.

5.2. RARE EARTH OXIDES

The rare earth oxides are industrially very important, and find applications in electronic component and device fabrications. All rare earth oxides are found to be basic [15]. They are generally prepared by the decomposition of their trihydroxides $LaOH)_3$ when precipitated with aqueous ammonia from solutions of their corresponding nitrate chloride or sulphate.

From the study of the surface characterization of LaO_3 as a typical example it is found that the trihydroxide decomposes in to the sesquioxide by passing through an oxyhydroxide [LaO(OH)] intermediate. The first true stage of $LaOH)_3$ occurs in the temperature range 250 - 350 ^oC and results in the formation of a well-defined LaOOH intermediate. Subsequent dehydration of oxyhydroxide to lanthanum oxide of occurs at 350 - 420 ^oC and is complete at the latter temperature. At the temperature range 450 - 500 ^oC decomposition of a carbonate layer that invariably exist on the oxide surface as a result of interaction of the highly basic trioxide precursor with atmospheric CO_2 during preparation and handling is observed. The two stages of dehydration that occurs at 200 and 300 ^oC cause small decrease in surface area due to particle size shrinkage

after which little further change occurs up to about 500 ^{o}C. The decline in surface area at temperature 500 ^{o}C is due to the macropore structure and `annealing' of the surface irregularities.

Above 400 ^{o}C decomposition of the oxyhydrousoxide is complete and exposed La^{3+} and O^{2-} ions in various normal or defective surface environment becomes available for participation as component of active site [16].

It has been suggested that at higher activation temperature, the donor sites consist of an oxygen ion in the surface specifically a co-ordinatively unsaturated oxygen ion (O^{2-}) associated with a nearby OH group and the concentration of these donor cites on the surface is related to basic strength of the surface [17].

5.3. EXPERIMENTAL

In our experiment Nd_2O_3 has been prepared by (1) hydroxide method and (2) Oxalate method as described below.

5.3.1. PREPARATION OF Nd_2O_3 BY HYDROXIDE METHOD:

The sulphate solution of the sample (250 ml) containing 0.5 g of Nd_2O_3 is heated to boiling and 1:1 ammonium hydroxide solution is added drop wise with stirring until the precipitation is complete. It is then allowed to digest on a steam bath until the precipitate is settled. The precipitate is then filtered on a whatman No.41 filter paper and washed with small portion of an aqueous solution containing 2g ammonium chloride and 10 ml of concentrated ammonium hydroxide in 100 ml until the precipitate is free from Cl^-. The precipitate is then kept in an air oven at 100 ^oC overnight and is ignited in a china dish at 300 - 400 ^oC for two hours.

5.3.2. PREPARATION OF Nd_2O_3 BY OXALATE METHOD:

The chloride solution of Nd (250 ml) is heated to boiling and 60 ml of 12% oxalic acid solution is added slowly with constant stirring and allowed to stand over night. The precipitate is filtered on whatman No.42 filter paper and washed with 2% oxalic acid in 1:99 HCl. The precipitate is then kept in an air oven at 100 ^oC for one day and then ignited in china dish at 850-900 ^oC to constant

weight. The weight obtained represent rare earth oxide present.

5.3.3. THERMAL DIFFUSIVITY MEASUREMENTS

In the single beam PA spectrometer [18-20] assembled for the present investigation, the 488 nm line of an Argon ion laser (LiCONiX 5300) has been used as the pump source. To generate acoustic signal in the PA cell, the pump beam is modulated using an electromechanical chopper. The acoustic signal generated in the coupling medium is detected by a small, highly sensitive (100-μV/Pa) microphone is kept close to the sample compartment and its output is processed by means of a lock-in amplifier (EG & G Model 5208). The experimental details are given in chapter 3.

To determine the thermal diffusivity, about 0.5 g of the sample is pelletised under high pressure (6 tons/cm^2). Keeping the sample in the PA cell and the frequency dependence of the acoustic signal is studied. The variation of signal amplitude with frequency is shown in figure 5.1-5.6. Knowing the thickness (l_s) of the sample and characteristic frequency(f_c) from the log(amplitude) Vs log(frequency) plot, the thermal diffusivity can be calculated using the relation $\alpha = l_s^2 f_c$ [eqn 2.42].

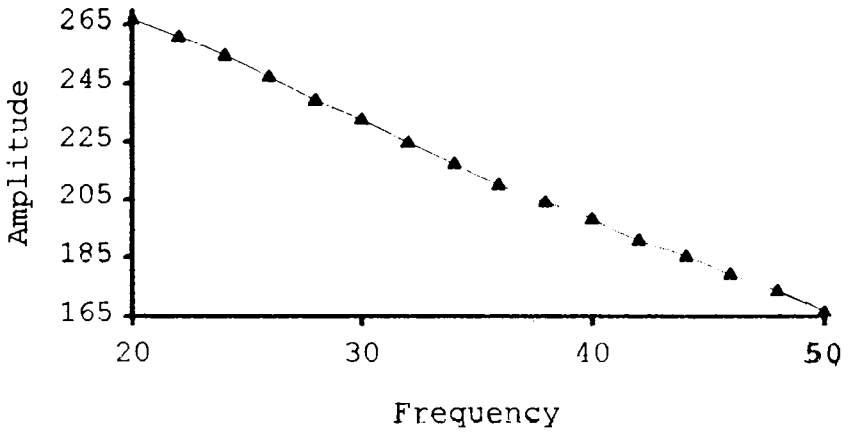

Fig. 5.1: Amplitude(μV) Vs Frequency (Hz) plot for Nd_2O_3 at 30°C, prepared by oxalate method

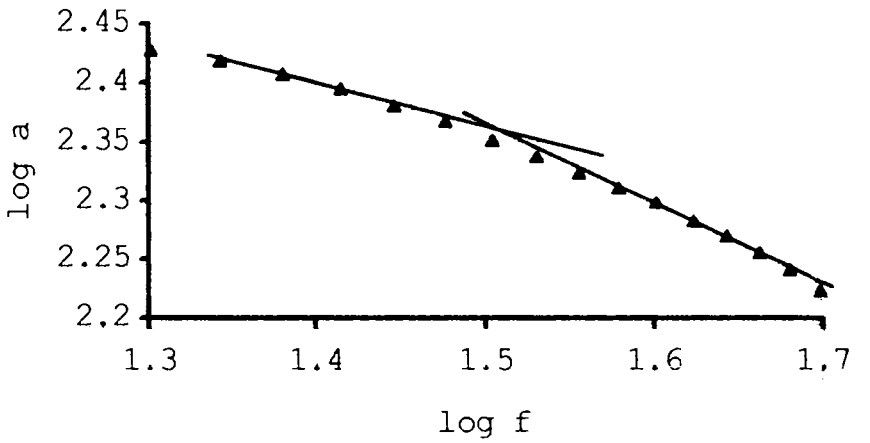

Fig. 5.2: log amplitude Vs log frequency plot for Nd_2O_3 at 30°C, prepared by oxalate method

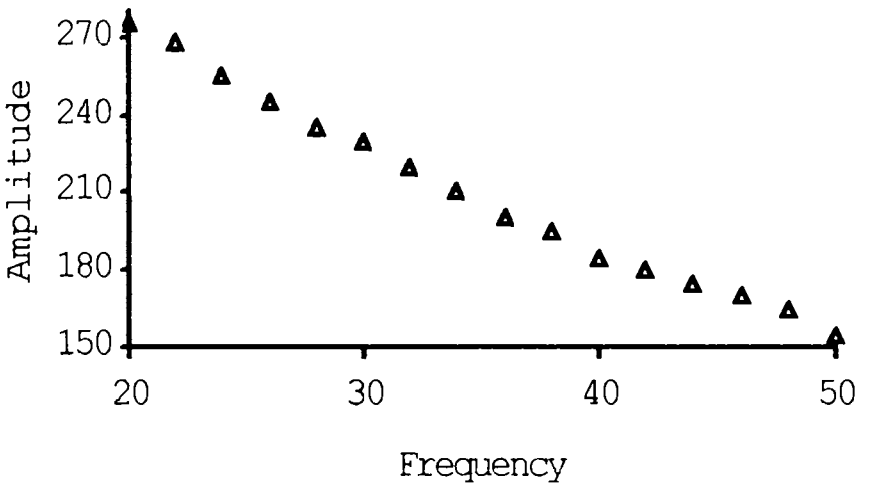

Fig. 5.3: Amplitude(μV) Vs Frequency (Hz) plot for Nd_2O_3 at 30°C, prepared by hydroxide method

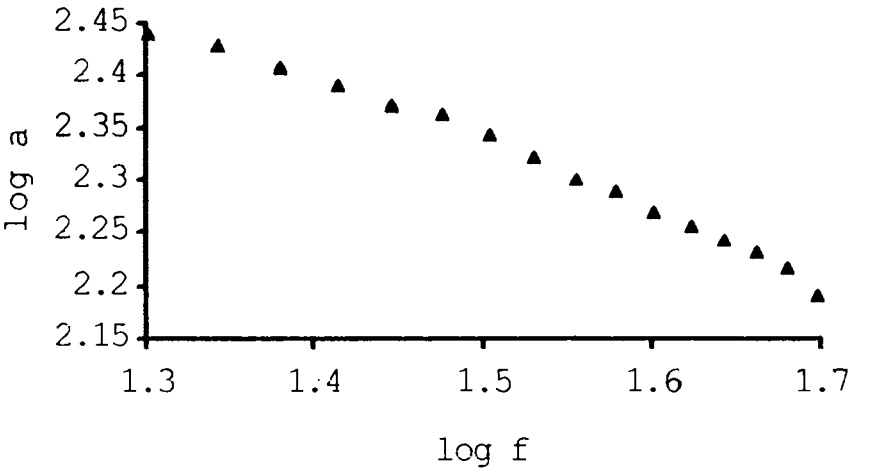

Fig. 5.4: log amplitude Vs log frequency plot for Nd_2O_3 at 30°C, prepared by hydroxide method

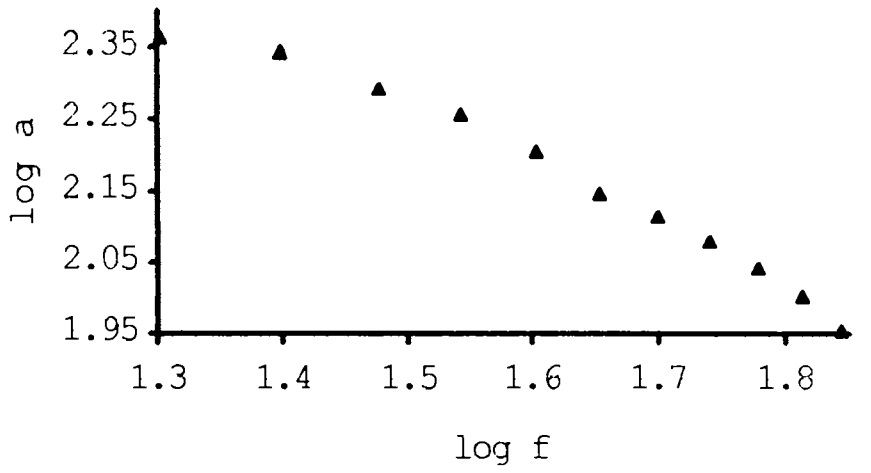

Fig. 5.5: log amplitude Vs log frequency plot for Nd_2O_3 at 500°C, prepared by oxalate method

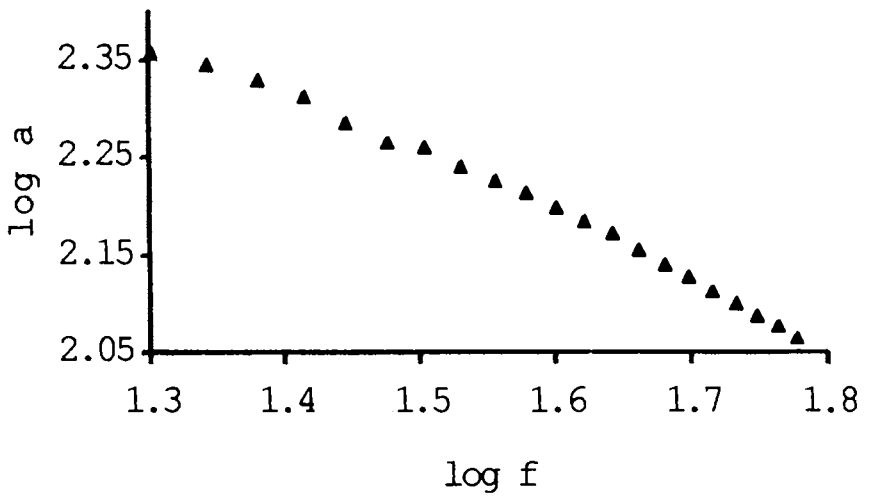

Fig. 5.6: log amplitude Vs log frequency plot for Nd_2O_3 at 500°C, prepared by hydroxide method

The accuracy of the measurement depends on the determination l_s and f_c. The values obtained are accurate up to third digit. Then the thermal diffusivities of pelletised samples of Nd_2O_3 are determined before and after degassing the sample at 500 °C. The thermal diffusivities of Nd_2O_3 prepared by oxalate method and hydroxide method at room temperature and at 500 °C are given in Table 5.1 respectively.

Table 5.1. Thermal diffusivity of Nd_2O_3 .

Preparation method	Thermal diffusivity (cm^2/s)	
	At 30 °C	At 500 °C
Oxalate method	0.099 ± 0.001	0.095 ± 0.001
Hydroxide method	0.119 ± 0.001	0.103 ± 0.001

5.3.4. INFRARED SPECTRA

The infrared spectra of these samples are taken before degassing so as to get an information about the surface hydroxyl groups, a characteristic of oxides.

Table5.2: IR spectral data of Nd_2O_3- oxalate method

No.	Abscissa (cm^{-1}) ν	% Transmittance
1	3668.7	6.86
2	3852.3	6.8
3	**3819.5**	6.97
4	**3748.1**	7.33
5	**3673.9**	6.96
6	2854.0	1.20
7	1699.5	11.91
8	1652.2	9.94
9	1575.1	7.56
10	1568.3	7.09
11	1563.5	7.03
12	1557.7	5.45
13	1553.8	5.78
14	1549.0	5.3
15	1538.4	3.44
16	1532.6	3.46
17	1520.1	2.56
18	1516.2	2.75
19	1505.6	2.14
20	1495.0	2.52
21	1436.2	2.3
22	1418.8	3.42
23	1081.2	9.55
24	816.0	8.61
25	726.3	5.37
26	435.0	9.41
27	420.5	8.4
28	417.6	8.12

Table5.3: IR spectral data of Nd_2O_3- hydroxide method

No.	Abscissa (cm^{-1}) ν	% Transmittance
1	**3745.2**	1.02
2	**3676.8**	1.09
3	**3671.9**	1.34
4	**3612.1**	4.74
5	**3606.4**	4.40
6	2954.3	4.66
7	2923.5	3.90
8	2854.0	4.65
9	1735.2	7.95
10	1718.8	7.70
11	1701.4	8.15
12	1696.6	8.59
13	1685.0	8.22
14	1654.2	7.68
15	1648.4	7.97
16	1464.1	8.10
17	1456.4	8.21
18	1377.3	0.06
19	1070.6	9.47
20	673.2	0.35
21	667.5	9.95
22	443.7	3.94
23	437.9	3.79
24	430.2	3.51
25	418.6	1.89

The IR data of Nd_2O_3 at room temperature prepared by oxalate method and hydroxide method are given in Table 5.2 and 5.3 respectively

5.4. RESULTS AND DISCUSSION

A search through literature reveals that oxides like Al_2O_3, Nd_2O_3 etc on exposure to water vapour (moist air) is terminated by a layer of hydroxyl groups at the surface [21,22]. The presence of hydroxyl groups at the surface has been shown by deuterium exchange and infrared spectroscopy and chemical methods [21-23]. The IR spectrum of the oxides show bands between 3300 and 3800 cm^{-1}, typical of surface OH groups [23]. These surface hydroxyl groups get expelled as the sample is heated to higher temperatures [21,22].

The IR spectrum shows more number of peaks between 3300 and 3800 cm^{-1} for the Nd_2O_3 prepared by oxalate method than the Nd_2O_3 prepared by hydroxide method. (The peaks are observed at 3673.9, 3748.1, and 3819.5 cm^{-1} for the Nd_2O_3 prepared by oxalate method and at 3606.4, 3612.1, 3671.9, 3676.8, and 3745.2 cm^{-1} for the Nd_2O_3 prepared by hydroxide method). This shows that Nd_2O_3 prepared by hydroxide method has greater hydroxyl groups. This may be due to the fact that method of preparation alters the surface properties [12,13]. From Table 1 it can be seen that, thermal diffusivity of Nd_2O_3 prepared by oxalate method is lower than that prepared by hydroxide method. Correlating the IR

data and thermal diffusivity values it seems to have a relation with the amount of surface hydroxyl groups. From IR data and thermal diffusivity values we can come to a conclusion that greater the surface hydroxyl groups greater is the thermal diffusivity.

It has been reported that as the degassing temperature increases the thermal diffusivity of γ-Al_2O_3 decreases. The reason for which is attributed to the loss of surface OH groups [16].

Table. 4.1 shows a decrease in thermal diffusivity with the increase of degassing temperature for both the samples. The variation in thermal diffusivity is very small in comparison with that of γ-Al_2O_3 [16]. This is due to the fact that the specific surface area and hence the number of surface hydroxyl groups is very much lower than that in γ-Al_2O_3.

Thus it can be concluded that, with the method of preparation, the amount of surface hydroxyl groups also changes. This in turn may be the reason for the difference in thermal diffusivity for the sample prepared by the two methods. The values at 500 ^{o}C further confirm the above conclusion. In other words, the difference in the thermal

diffusivity values may be attributed to the difference in the preparation method,

5.5. CONCLUSION

The influence of preparation route on the thermal diffusivity of a material is clearly understood. The rare earth oxide Nd_2O_3 is prepared by oxalate and hydroxide method. Its thermal diffusivity values are determined at 30 and 500 ^{o}C. To understand the difference in the amount of hydroxyl groups in these two samples the IR spectrum is recorded. The studies reveals the reason for the difference in thermal diffusivity to be the difference in the amount of OH groups in the sample which in turn is the result of preparation method.

REFERENCES

[1] A.G. Bell, Am. J. Sci., 20 (1880) 305.

[2] A.G. Bell, Philoss. Mag., 11 (1881) 510.

[3] A. Rosencwaig and A. Gersho, J. Appl. Phys., 47 (1975) 64.

[4] A. Rosencwaig, Rev. Sci. Instrum., 48 (1977) 1133.

[5] G.C. Wetsel.Jr and F.A. Mac Donald, Appl. Phys. Lett., 30 (1977) 252.

[6] A.C. Tam, C.K.N. Patel and R.J. Kerl, Opt. Lett., 4 (1979) 81.

[7] A.C. Tam, Rev. Modern Phys., 56 (1986) 2.

[8] C.L. Cesar, H. Vrgas and L.C.M. Miranda, Appl. Phys. Lett., 32 (1978) 554.

[9] P. Charpentier, F. Lepoutre and L. Bertrand, J. Appl. Phys., 53 (1982) 1.

[10] F.A. Mac Donald, and G.C. Wetsel.Jr, J. Appl. Phys., 49 (1978) 4.

[11] A. Hordvik and H. Scholssberg, Appl. Opt., 16 (1977) 101; 16 (1977) 2919.

[12] S. Sugunan, G. Devika Rani and K.B. Sherly, React. Kinet. and Catal. Lett., 43 (1991) 375.

[13] S. Sugunan and G. Devika Rani, J. Mat. Sci. Lett., 10 (1991) 887.

[14] P.K. Kuo, M.J. Lin, C.B. Reyes, L.D. Favro, R.L. Thomas, D.S. Kim and Shu-yi Zhang, Can. J. Phys. 64 (1986) 1165.

[15] K. Tanabe, `Solid acids and bases', Academic pres, New York, 1970.

[16] M.P. Rosynek and D.T. Magnuson, J. Catal., 40 (1977) 402.

[17] D. Cordischi and V. Indovina, J. Chem. Soc. Faraday Tran., 72(10) (1976) 2341.

[18] S. Sankara raman, V.P.N. Nampoori, C.P.G. Vallabhan, N. Saravanan, and K.K. Mhammed Yusuff, J. Mat. Sci. Lett., 15 (1996) 230.

[19] S. Sankara raman, V.P.N. Nampoori, C.P.G. Vallabhan, G. Ambadas, and S. Sugunan, Appl. Phys. Lett., 67 (1995) 2939.

[20] S. Sankara raman, V.P.N. Nampoori, C.P.G. Vallabhan, G. Ambadas, and S. Sugunan, J. Appl. Phys.(In press).

[21] J.B. Peri and R.B. Hannan, J. Phys. Chem., 64 (1965) 1526.

[22] J.B. Peri, J. Phys. Chem., 69 (1965) 211.

[23] J.L. Carter, P.J. Lucchesi, P. Corncil, D.J.C. Yates, and J.H. Sinfelt, J. Phys. Chem., 69 (1965) 3070.

[24] P.O. Sockart and P.G. Rouxhet, J. Coll. and Interf. Sci., 86 (1982) 1.

* * * * *

CHAPTER 6

THERMAL DIFFUSIVITY MEASUREMENTS ON SOME HALOGENO BENZIMIDAZOLE COMPLEXES

ABSTRACT

The thermal diffusivity of some halogeno benzimidazole complexes of cobalt (II), copper (II), and copper (I) with the ligand, 1-nitrobenzyl-2-nitrophenyl benzimidazole (NBPBI) have been determined by laser induced photoacoustic technique. The effects of the metal as well as the halogen part on thermal diffusivity of the complexes have been studied. The structure of the complex is determined from the electronic spectral data and magnetic susceptibility values. Thermal stability of the complexes is studied by thermogravimetric analysis. It is confirmed that the structure of the complex does not change on metal and/or halogen part replacement.

6.1. INTRODUCTION

Complexes of benzimidazoles have attracted considerable attention in recent years. Benzimidazole derivatives have been reported to have antibacterial, antifungal, antiviral, anti-tumour, anticancer, anti-inflammatory, analgesic, antipyretic, antineoplastic, antihelmentic, germicidal and immuno-chemical agents activities. Complex compounds of transition metal ions with imidazole, benzimidazole and their substituted ligands have been studied extensively [1-5]. Recently, many low molecular weight complexes of Cu (II) containing imidazole ligand have been proposed as models of active sites of Cu-proteins [6-9]. Incorporation of nitro group in the azole compounds makes them to have antiamoebic activity also [9]. Some of the Co (II) and Cu (II) complexes reported have shown better catalytic activity, particularly synthetically important reaction of oxidation of substituted phenols, in which Co (II) and Cu (II) play a major role in catalysing these types of reactions. The structure of the ligand and the complex is shown in figure 6.1 and 6.2. A search through the literature reveals that very few PA studies have been carried out on metal complexes and that no work has been reported on benzimidazole complexes.

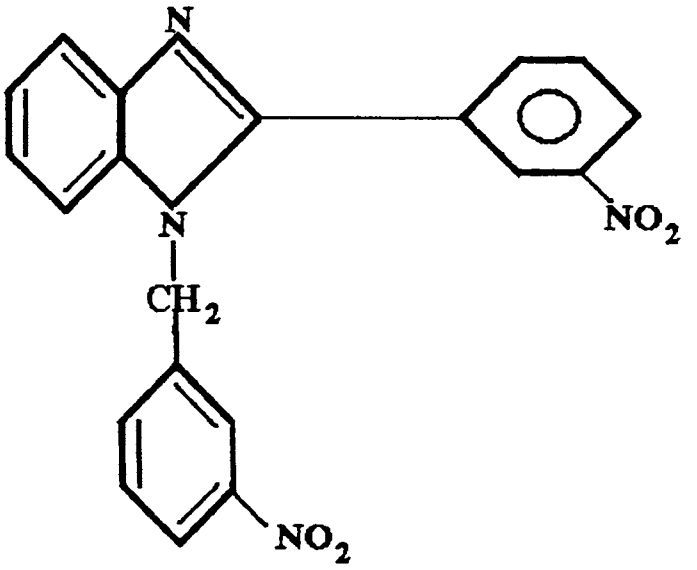

Fig.6.1: Structure of the ligand (NBPBI)

6.2. EXPERIMENTAL

6.2.1. PREPARATION OF THE COMPLEXES

The materials used for the preparation of the complexes are nitrobenzaldehyde (CDH), phenylenediamine (CDH), cobalt (II) chloride hexahydrate (Merk), copper (II) dihydrate (BDH), cobaltous carbonate and cupric carbonate (Reidel Chemicals) and other chemicals were of Analar grade purity. Solvents employed were distilled before use.

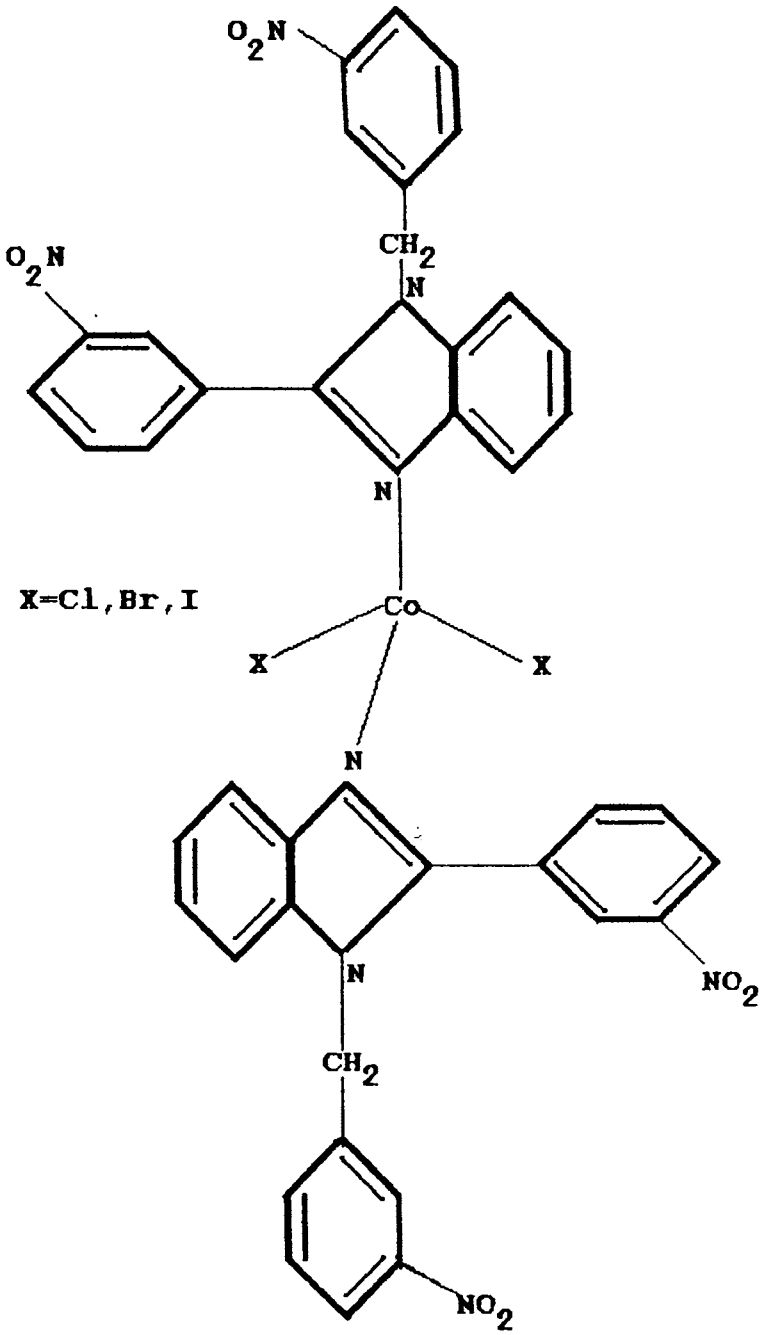

Fig.6.2a: Structure of the Cobalt complex

The ligand, 1-nitrobenzyl-2-nitrophenyl benzimidazole (NBPBI) was prepared according to the procedure

reported in the literature [10] by changing the reaction time from 12h to 24h.

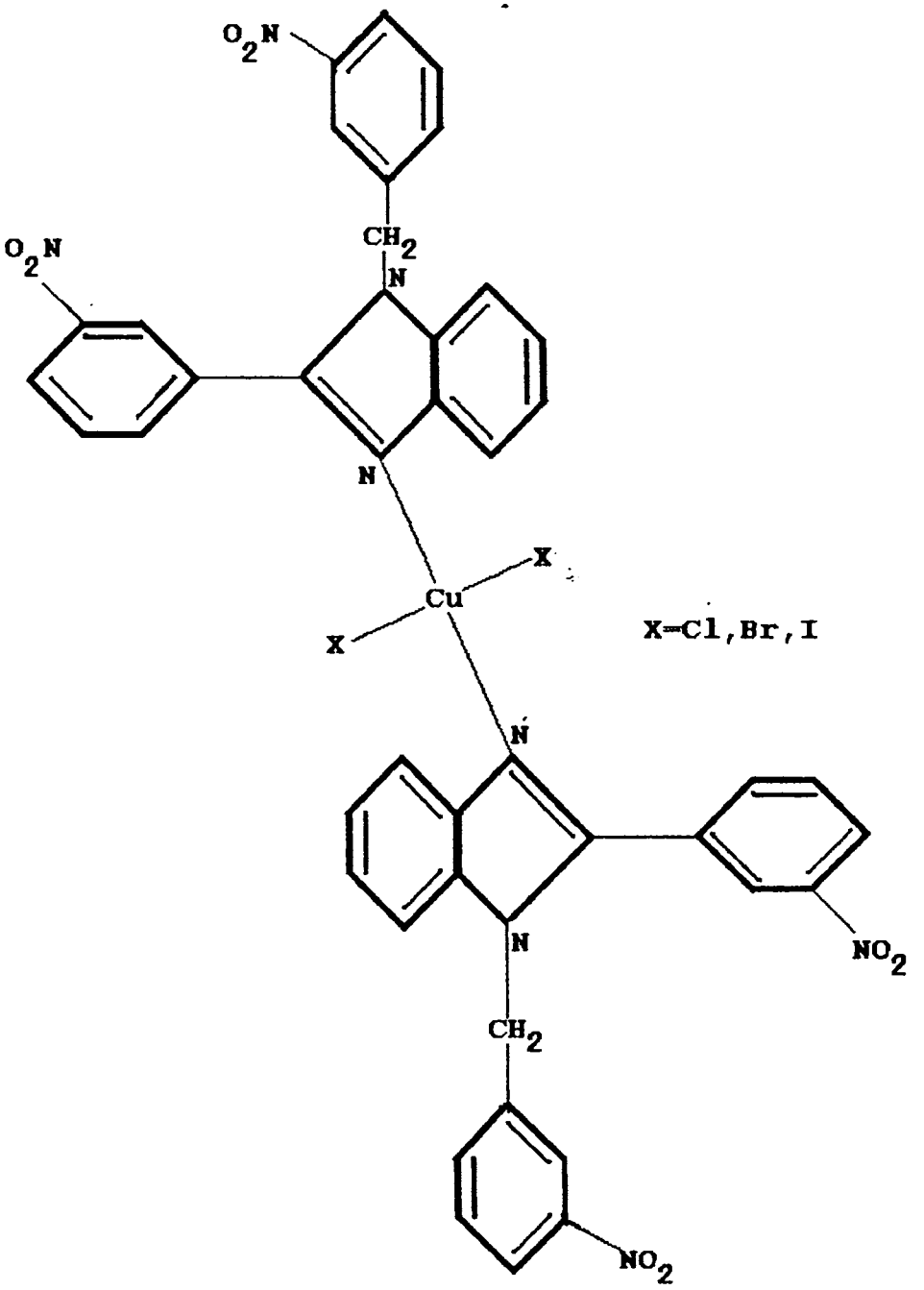

Fig.6.2b: Structure of Copper complex

CoL_2Cl_2: Hot ligand solution of NBPBI (3.74g, 0.01 mol dissolved in 75ml ethanol) is added slowly to cobalt (II) chloride hexahydrate (1.18g, 0.005 mol in minimum volume of ethanol). The green solution appeared is refluxed for about 2-3h over a water bath. Blue crystals obtained during refluxion are filtered, washed with hot ethanol and chloroform. This is dried in air and also under vacuum over anhydrous $CaCl_2$.

CoL_2Br_2: Cobalt (II) bromide salt (1.09 g, 0.005 mol in 20 ml acetone is added to the ligand (3.74g, 0.01 mol) and the resulting green solution is kept over a water bath for refluxion for about 2h only. Then volume of the solution is reduced to half the volume. Greenish blue crystals formed are collected, washed with chloroform and dried under vacuum over anhydrous $CaCl_2$.

CuL_2Cl_2: Hot ligand solution of NBPBI (3.74g, 0.01 mol dissolved in 75ml ethanol) is added slowly to cobalt (II) chloride dihydrate (1.18g, 0.005 mol in 5ml ethanol) and the solution appeared is refluxed for about 1h over a water bath. Greenish grey crystals obtained during refluxion are filtered, washed with hot ethanol and chloroform. This is dried in air and also under vacuum over anhydrous $CaCl_2$.

CuL_2Br_2: Hot ethanolic solution of the ligand (3.74g, 0.01 mol in 75 ml ethanol) is added to copper (II) bromide solution (0.6g of copper (II) carbonate dissolved in HBr, 0.005 mol) and the refluxion is carried out over a water bath for about 1h. Greenish yellow crystals thus formed during refluxion were filtered, washed with hot ethanol over anhydrous $CaCl_2$.

CuL_2I_2 and CoL_2I_2 are also prepared by a similar procedure.

6.2.2. THERMOGRAVIMETRIC ANALYSIS

In order to get an information about the thermal stability of the material against decomposition thermogravimetric study is essential. The study was carried out using Shimadzu TGA 50 thermogravimetric analyser at a heating rate of 20 °C/minute in air using platinum crucible in the temperature range between room temperature and 1000 °C. The amount of sample used for the study is about 5-12mg.

The thermogravimetric analysis shows that the sample does not decompose at temperatures lower than 280 °C. Hence, the exposure to the intensity modulated (chopped)

laser beam of the power level used in the present experiment (~100 mW) does not decompose the samples [11].

6.2.3. MAGNETIC SUSCEPTIBILITY MEASUREMENT

Magnetic susceptibility measurements of the complexes at room temperature were determined by the Gouy's method using Hg[Co (SCN)] as calibrant. The room temperature magnetic moment of the cobalt complexes are in the range 4.1 to 4.4 B.M. which are characteristic of tetrahedral geometry of these complexes. Magnetic moment of 2.19 - 2.2 B.M. for the copper complexes suggest the tetrahedral structure for these complexes [11].

6.2.4. ELECTRONIC SPECTRA

All the cobalt (II) complexes exhibit a broad absorption band with intensity around the region, 17500-14500 cm^{-1}. This band can be assigned to $^4A_2 \longrightarrow {}^4T_1$ (P) electronic transition. An additional band observed for the complexes in this region is the characteristic of tetrahedral structure and arises due to spin-orbit coupling of the T state. Apart from this, an additional band in near IR region is also observed in the range between 7200

and 6900cm^{-1} and this band can be accounted to $^4A_2 \longrightarrow {}^4T_1(F)$ transition.

All the copper (II) complexes show a broad band in the region 24500-15000 cm^{-1} and this band can be assigned to the transition $^2T \longrightarrow {}^2E$. All complexes exhibit strong bands between 34000 -29000 cm^{-1} corresponding to infra-ligand transition. Further, the molar extinction coefficient values for both the Co (II) and Cu (II) complexes fall in the range between 200 - 300, which supports tetrahedral structure for these complexes.

6.3. RESULTS AND DISCUSSION

To determine the thermal diffusivity, the sample is pelletised under high pressure. Keeping the sample in the PA cell, the frequency dependence of the acoustic signal is studied [12-14]. The variation of signal amplitude with frequency for these samples is shown in figure 6.3-6.10. Knowing the thickness of the sample and the characteristic frequency from the log-log plot of signal strength Vs chopping frequency, the thermal diffusivity can be calculated using the relation, $\alpha = l_s^2 fc$ [15,16]. The metal part of the complex viz. cobalt is replaced by copper and the thermal diffusivities of CuL_2X_2 are also determined.

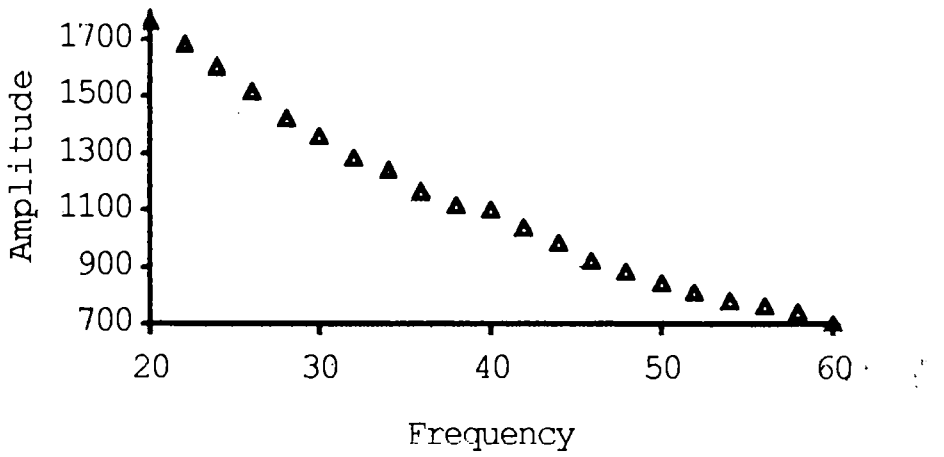

Fig. 6.3: Amplitude(μV) Vs Frequency (Hz) plot for the ligand (NBPBI)

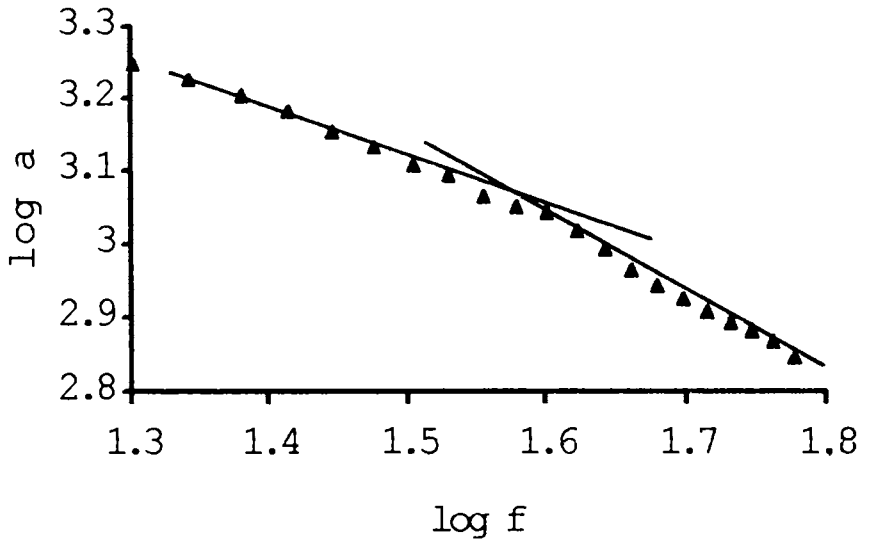

Fig. 6.4: log amplitude Vs log frequency plot for ligand

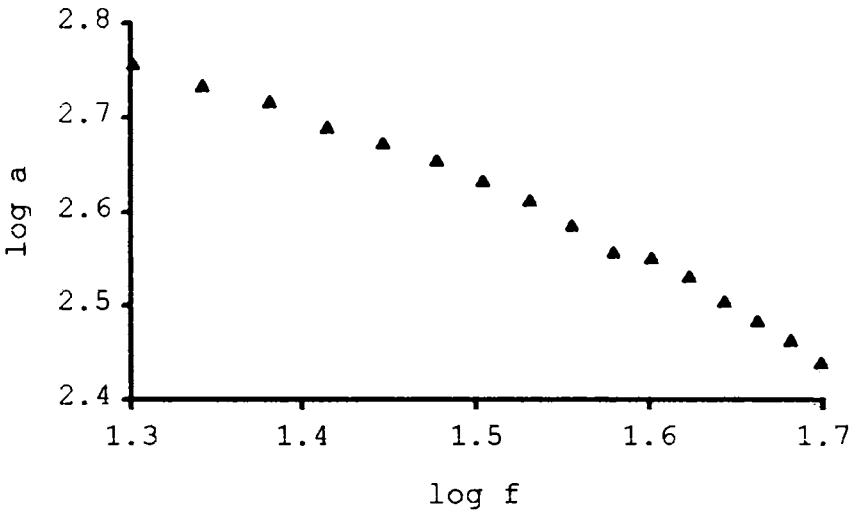

Fig. 6.5: log amplitude Vs log frequency plot for CoL_2Cl_2

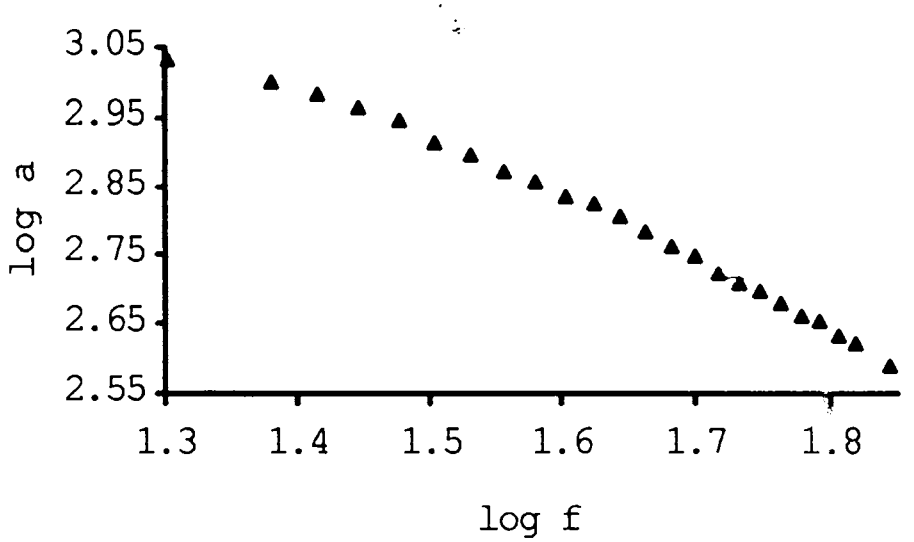

Fig. 6.6: log amplitude Vs log frequency plot for CoL_2Br_2

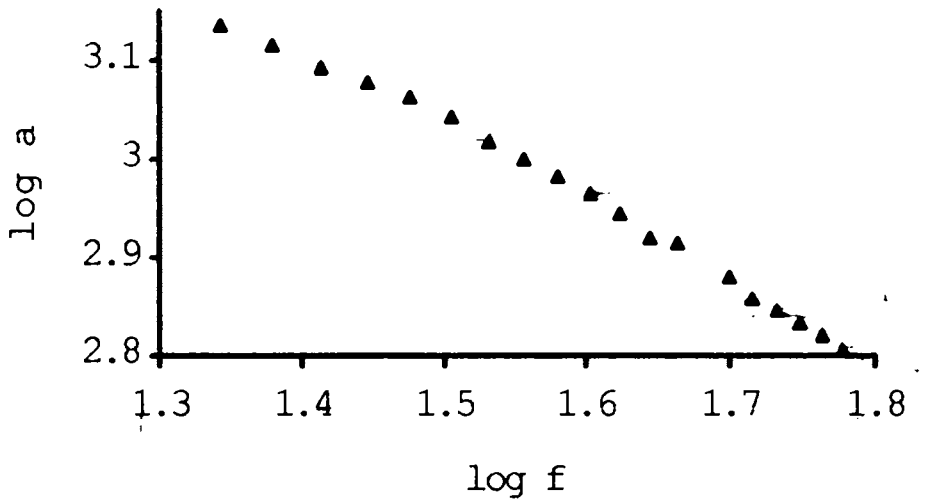

Fig. 6.7: log amplitude Vs log frequency plot for CoL_2I_2

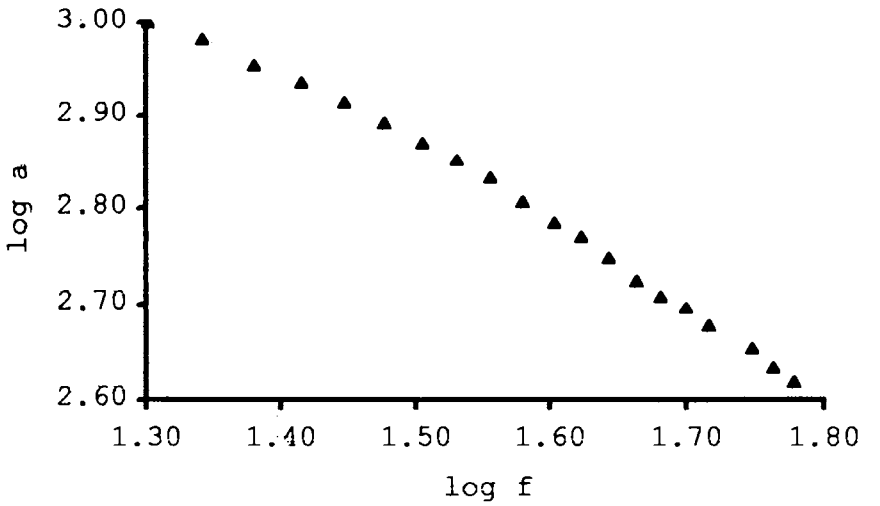

Fig. 6.8: log amplitude Vs log frequency plot for CuL_2Cl_2

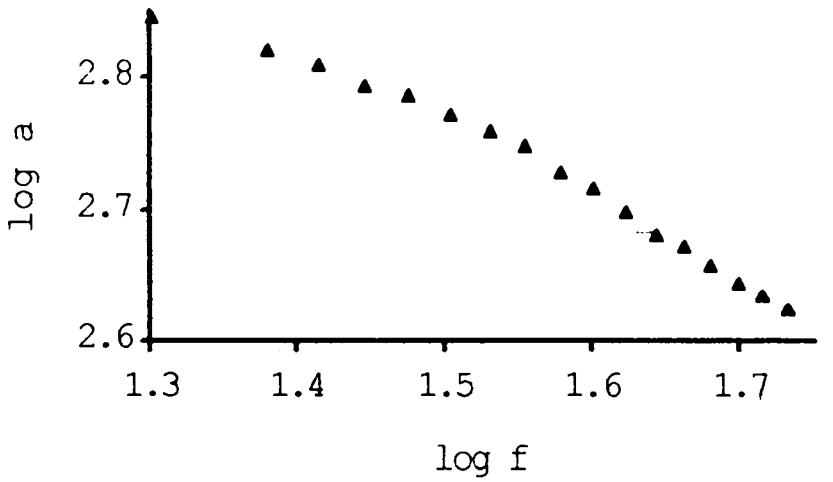

Fig. 6.9: log amplitude Vs log frequency plot for CuL_2Br_2

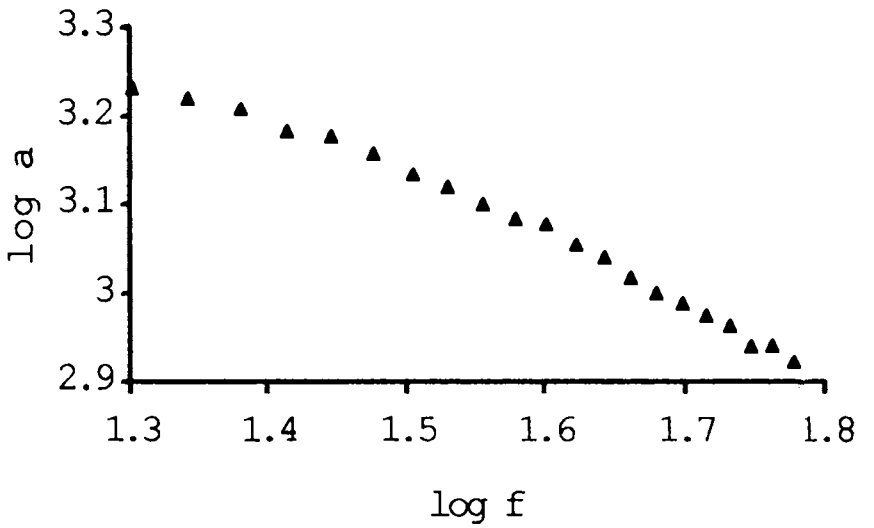

Fig.6.10: log amplitude Vs log frequency plot for CuL_2I_2

Table 1. Thermal diffusivities of Co(II), Cu(II), and Cu(I) halogeno benzimidazole complexes.

Sl. No	Sample	Thermal diffusivity(cm^2/s)
1	Ligand	0.209 ± 0.001
2	CoL_2Cl_2	0.193 ± 0.001
3	CoL_2Br_2	0.383 ± 0.001
4	CoL_2I_2	1.410 ± 0.001
5	CuL_2Cl_2	0.458 ± 0.001
6	CuL_2Br_2	0.203 ± 0.001
7	Cu*L2I2	0.189 ± 0.001

* +1 oxidation state

The results obtained from the present study are given in Table 1 [12]. In the case of CoL_2X_2, thermal diffusivity(α) increases in the order of X = Cl, Br, and I while reverse is the case for CuL_2X_2. Thus, the thermal diffusivity of the halogeno complexes depends on the metal part as well as on the halogen part. Though the structure of the complexes seem to be tetrahedral, a detailed single crystal study is essential for the confirmation of the structure. The complexes being newly synthesized and reported other relevant physical as well as chemical data

that are required for the analysis of our results are not available.

6.4. CONCLUSION

The thermal diffusivity of CuL_2X_2 and CoL_2X_2 (where, X = Cl, Br, or I) are determined by PA technique and the effect of replacement of cobalt by copper on the thermal diffusivity of these complexes have clearly been brought out. The thermal stability of these compounds is also studied [12]. As the compounds are new, no relevant physical and chemical data are available for the analysis and finding out the reason for the thermal diffusivity variations with halogen part and metal part.

REFERENCES

[1] S.P. Gosh, J. Indian Chem. Soc. 28 (1951) 710.

[2] S.P. Gosh and H.M. Gosh, J. Indian Chem. Soc. 33 (1956) 894.

[3] G. Goodgame and F.A. Cotton, J. Am. Chem., Soc. 84 1962) 1543.

[4] D.M.L. Goodgame and M. Goodgame, Inorg. Chem. 4 (1965) 139.

[5] J. Reedijik, J. Inorg. Nucl. Chem. 35 (1973) 239.

[6] K. Nakamoto, "Infrared and Raman spectra of Inorg. and Coordn. compounds", 3rd Edn (Wiley, New York, 1978) p.314.

[7] J.R. Dyer, "Applications of Absorption Spectroscopy of organic compounds", (Prentice Hall, New Jersey, 1965) p.33.

[8] B.J. Hathaway, J. Chem. Soc., Dalton Trans. (1972) 1196.

[9] G. Vasilev and K. Davarski, Dokl. Bolg. Acad. Nauk. 35 (1982) 1717.

[10] N.V Subba Rao and C.V Rtnam, Proc. Indian Acad. Sci., 43A (1956) 174.

[11] N. Saravanan, Ph.D thesis , Cochin University (1996).

[12] S. Sankara raman, V.P.N. Nampoori, C.P.G. Vallabhan, N. Saravanan, and K.K. Mhammed Yusuff, Mat. Sci. Lett., 15 (1996) 230.

[13] S. Sankara raman, V.P.N. Nampoori, C.P.G. Vallabhan, G. Ambadas, and S. Sugunan, Appl. Phys. Lett., 67(1995) 2939.

[14] S. Sankara raman, V.P.N. Nampoori, C.P.G. Vallabhan, G. Ambadas, and S. Sugunan, J. Appl. Phys.,85 (1999) In press.

[15] P. Charpentier, F. Lepoutre and L. Bertrand, J. Appl. Phys. 53 (1982) 1.

[16] F.A. Mac Donald, G.C. Wetsel: Jr, J. Appl. Phys. 49 (1978) 4.

* * * * *

CHAPTER 7

THERMAL DIFFUSIVITY OF SOME POLYMER SUPPORTED METAL COMPLEXES

ABSTRACT

The thermal diffusivities of some polystyrene supported Schiff base complexes of cobalt (II), copper (II) with complexes of the type, $[ML_2X_2]$, (where M =Co (II) or Cu (II); L =NBPBI, 1-nitrobenzyl-2-nitrophenyl benzimidazole and X= Cl^{-1}, Br^{-1} or I^{-1}) have been determined by laser induced photoacoustic effect. The effect of the metal as well as halogen part on the thermal diffusivities of these complexes has been studied.

7.1. INTRODUCTION

There has been a growing emphasis on the studies involving polymer-bound ligands [1,2]. Substantial differences have been observed between the complexation behaviour of polymer-bound ligands and simple ligands, probably due to the macroenvironment created at the coordination center, which causes steric, electrostatic, hydrophobic, and conformational effects. It has been shown that in metalloenzymes such as oxides and haemoglobin, where the metal complex is the active site, the macromolecular protein part plays a significant role or even controls the reactivity of the metal complexes [3-5]. Further, in many catalytic reactions involving polymer bound metal complexes the activity of the catalyst not only depends on the metal complex, but also on the polymer backbone [6].

Complexes of benzimidazole have attracted great deal of attention in recent years due to its potential applications in various fields like bio-medical, bio-chemistry etc. because of its antibacterial, antifungal, antiviral, anticancer, anti-inflammatory, analgesic, antipyretic, antihelmentic, germicidal and immuno-chemical agent activities. Complex compounds of transition metal

ions with imidazole, benzimidazole and their substituted ligands have been studied extensively [7-11]. Some of the Co(II) and Cu(II) complexes reported have shown better catalytic activity, particularly towards synthetically important reactions of oxidation of substituted phenols, in which Co(II) and Cu(II) play a major role in catalysing these types of reactions. Polymer-bound complexes also gained considerable attention recently due to its pronounced catalytic efficiency [1,12] particularly in the oxidation reactions. The studies on magnetic and optical properties reveal that the polymer support brings about modifications in the structure of the complex. Other physical parameters like melting point and molar conductance are also found to change on polymer support [13].

Apart from magnetic, optical and catalytic activity studies, evaluation of thermal parameters, like thermal diffusivity, are important means if thermal characterisation. It has been well recognised that photoacoustic effect is an effective technique for evaluating thermal diffusivity of samples. In this chapter, the study of the thermal diffusivities of the newly synthesised polymer supported halogeno benzimidazole complexes of Co(II) and Cu(II) by laser induced

photoacoustic technique is described. A search through the literature reveals that very few PA studies have been carried out on metal complexes and that no work has been reported on polymer supported benzimidazole complexes.

7.2. EXPERIMENTAL

7.2.1. PREPARATION OF POLYMER SUPPORTED SCHIFF BASE LIGAND

The materials required: Aminomethyl polystyrene, quinoxaline-2-carboxaldehyde, halogeno complexes of Co(II) and Cu(II) with 1-nitrobenzyl-2-nitrophenyl benzimidazole, L-ascorbic acid and other chemicals used are of Analar grade purity. Solvents employed are distilled before use.

Aminomethyl polystyrene has been prepared according to the literature [14] using chloromethyl polystyrene beads (2% crosslinked with divinyl benzene, 3.7 meq. of chlorine/g). Polymer bound Schiff base ligand is prepared by condensing aminomethyl polystyrene with quinoxaline -2-carboxaldehyde as described below.

A solution of quinoxaline-2-carboxaldehyde (0.5g in minimum amount of DMF) was added to aminomethyl polystyrene (5.0 g) and the reaction mixture is refluxed for about 5 h. Brown coloured product thus formed is filtered, washed several times with DMF and acetone and dried in air and also under vacuum over anhydrous $CaCl_2$ with yield 70 -80 %. The schematic representation of the polymer bound Schiff base is shown in figure 7.1.

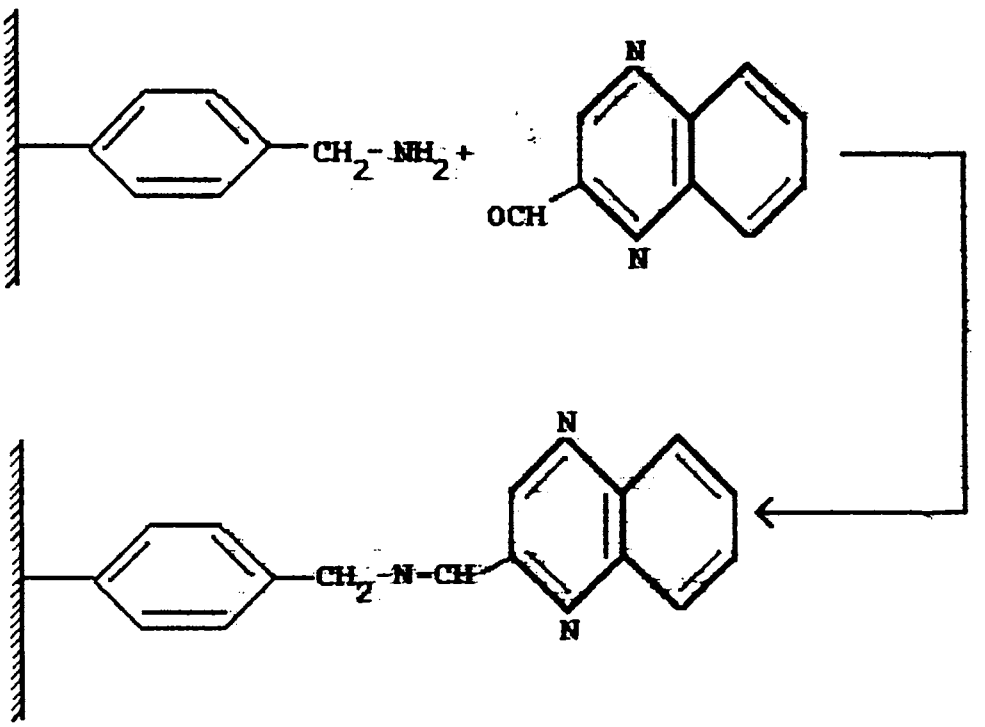

Fig. 7.1: Polymer bound Schiff base

7.2.2. PREPARATION OF POLYMER SUPPORTED COMPLEXES OF Co (II) AND Cu(II)

Polymer supported complexes are synthesised by reacting the polymer - bound Schiff base with already prepared Halogeno complexes of Co (II) and Cu (II) with NBPBI as given below. Halogeno complexes of Co (II) and Cu (II) with NBPBI are prepared in the same manner described in the previous chapter. Synthetic procedure followed was the same in all cases. The following is the synthetic route for the polymer bound Schiff base complex of Co (II).

Polymer-bound Schiff base ligand (2 g) was swollen in acetone for 1h and the solvent was decanted off. Fresh acetone (4 ml) was again added along with the chloro complex of Co(II) derived from 1-nitrobenzyl-2-nitrophenyl benzimidazole, $[Co(NBPBI)_2X_2]$ (100 - 200 mg). The reaction mixture was shacked well up to 1h and this was warmed over a water bath during shaking. The product formed was then filtered and washed several times with acetone and dried in air and also under vacuum over anhydrous $CaCl_2$. Yield = 70%

7.2.3. THERMOGRAVIMETRIC ANALYSIS

In order to get an information about the thermal stability of the material against decomposition, thermogravimetric study is essential. The study was carried out using Shimadzu TGA 50 thermogravimetric analyser at a heating rate of 20 °C/minute in air using platinum crucible in the temperature range between room temperature and 1000 °C. The amount of sample used for the study is about 5 - 12mg.

The thermogravimetric analysis shows that the sample does not decompose at temperatures lower than 250 °C. Hence, the exposure to the intensity modulated (chopped) laser beam of the power level used in the present experiment (~100 mW) does not decompose the samples. Therefore the sample is thermally stable throughout the study.

7.3. RESULTS AND DISCUSSION

To determine the thermal diffusivity, the sample is pelletised under high pressure. Keeping the sample in the PA cell, the frequency dependence of the acoustic signal is

studied [15]. The log-log plot of the variation of signal amplitude with frequency for polymer supported complexes are shown in figures 7.2- 7.8. Knowing the thickness (l_s) of the sample and the characteristic frequency (f_c) from the log-log plot, the thermal diffusivity (α) can be calculated. The thermal diffusivity values of the polymer supported complexes obtained from the present study are given in Table 1. In case of polymer supported $[Co(NBPBI)_2X_2]$, thermal diffusivity(α) increases where as the thermal diffusivity of polymer supported $[Cu(NBPBI)_2X_2]$ decreases in the order of X = Cl, Br and I. The metal as well halogen part of the complex is found to have profound effect on the thermal diffusivity values.

From the studies of magnetic and optical properties of the Co (II) complexes, similar to the present complexes, it has been found that the anchoring of the complexes to the polymer support bring about modifications in the structure of the complexes [16]. The studies reveal that the tetrahedral structure of $[M(NBPBI)_2X_2]$ (M = Co or Cu) changes into square pyramidal on polymer support. The physical parameters like melting point and molar conductance are also found to change when the complex is supported on the polymer [19]. Our studies show that

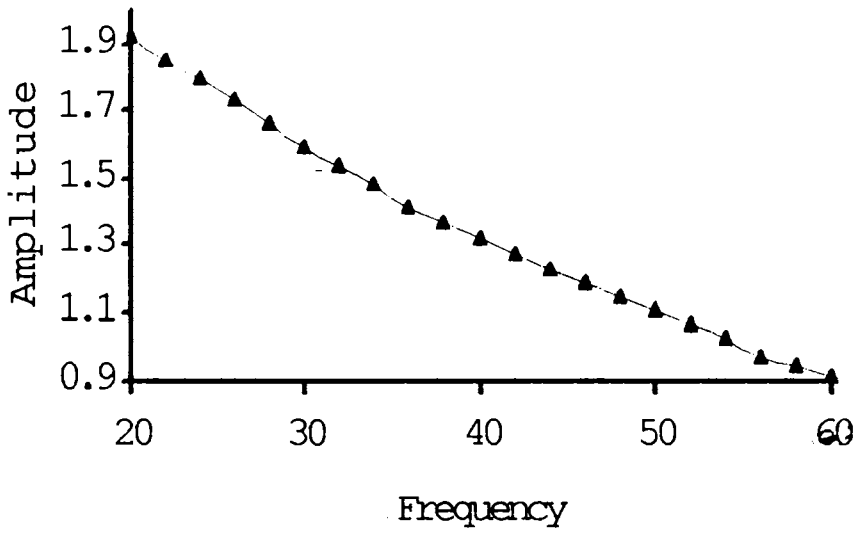

Fig. 7.2: Amplitude(mV) Vs Frequency (Hz) plot for P-CuL_2Cl_2

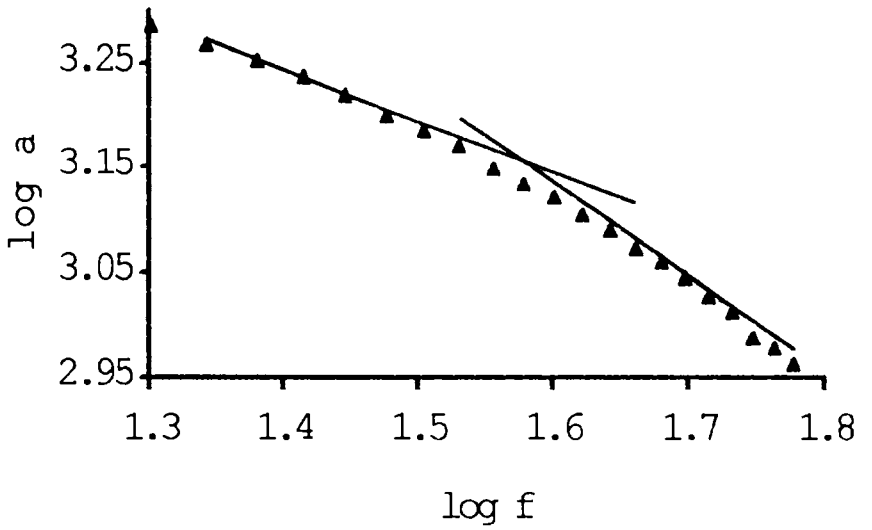

Fig. 7.3: log amplitude Vs log frequency plot for P-CuL_2Cl_2

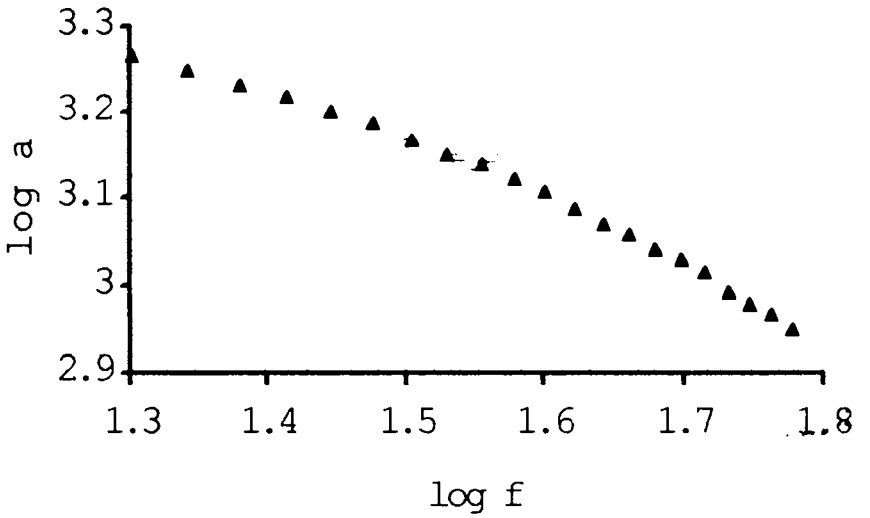

Fig.7.4: log amplitude Vs log frequency plot for P-CuL_2Br_2

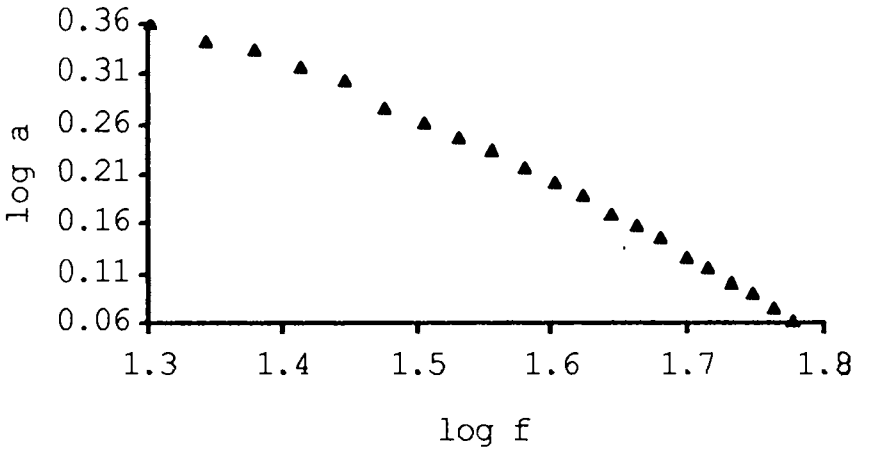

Fig.7.5: log amplitude Vs log frequency plot for P-CuL_2I_2

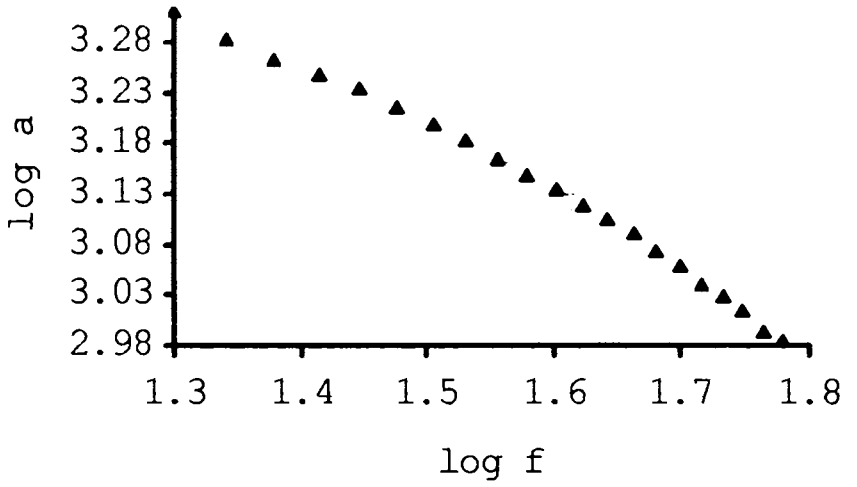

Fig.7.6: log amplitude Vs log frequency plot for P-CoL_2Cl_2

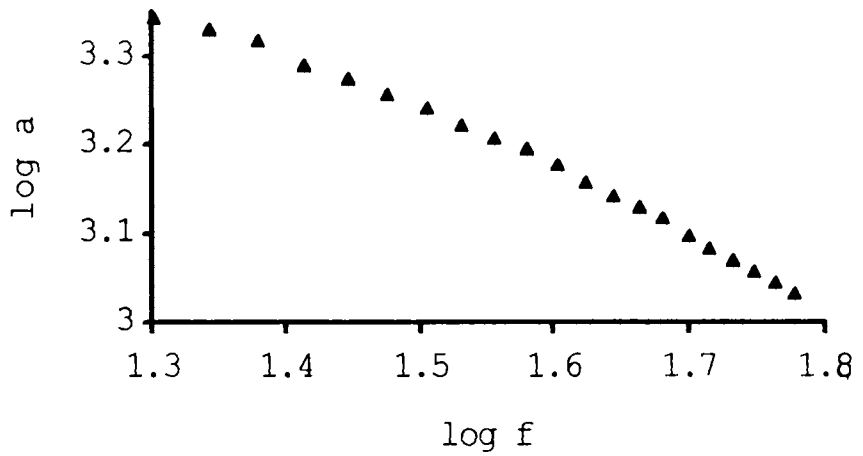

Fig.7.7: log amplitude Vs log frequency plot for P-CoL_2Br_2

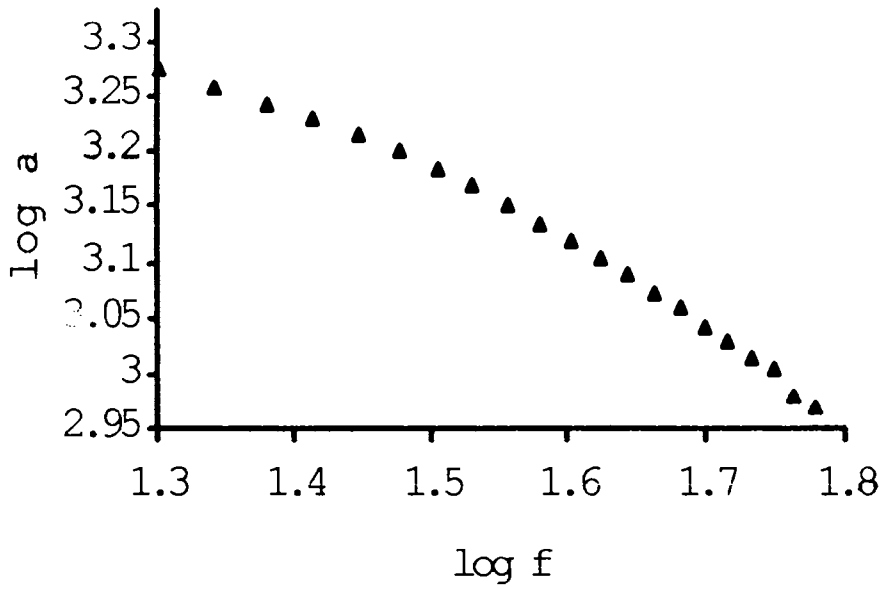

Fig.7.8: log amplitude Vs log frequency plot for P-CoL_2I_2

thermal diffusivity is another parameter that seems to change on polymer support.

The thermal diffusivities of the newly synthesised polymer supported complexes of Co(II) and Cu(II) have been determined by laser induced photoacoustic technique. The effect of metal as well as halogen part on thermal diffusivity of polymer supported complexes has been studied. Thermal diffusivity of Co complexes is found to increase while it decreases in Cu complexes with Cl, Br and I substitutions respectively.

Table 1. Thermal diffusivities of polymer supported halogeno benzimidazole complexes of cobalt(II).and copper(II)

Sample	Thermal diffusivity (cm^2/s)
[P-Cu(NBPBI)$_2$Cl$_2$]	0.305 ± 0.001
[P-Cu(NBPBI)$_2$Br$_2$]	0.242 ± 0.001
[P-Cu(NBPBI)$_2$I$_2$]	0.195 ± 0.001
[P-Co(NBPBI)$_2$Cl$_2$]	0.454 ± 0.001
[P-Co(NBPBI)$_2$Br$_2$]	0.544 ± 0.001
[P-Co(NBPBI)$_2$I$_2$]	0.640 ± 0.001

P - polymer

7.4 CONCLUSION

Thermal diffusivity of the newly synthesised polymer supported complexes of Co (II) and Cu (II) have been determined by laser induced photoacoustic technique. The effect of metal as well as halogen part on thermal diffusivity of polymer supported complexes has been studied. Thermal diffusivity of Co complexes is found to increase while it decreases

in Cu complexes with Cl, Br, and I substitutions respectively. The materials being newly synthesised and reported, a detailed characterisation in terms of structural, physical and chemical properties is required. Though the structure seems to be pyramidal, only through a detailed single crystal study one can exactly determine the structure and lattice properties. Since the thermal properties of insulators depend on lattice properties, now it is difficult to arrive at a conclusive reason why thermal diffusivity varies on metal or halogen part replacement.

REFERENCES

[1] E. Tsuchida and H. Mishide, Advances in Polymer Science, Vol. 24 (Springer-verlag Berlin Heidelberg, New York, 1977) p. 1.

[2] D. Wohrle, Advances in Polymer Science, Springer-Verlag, Berlin, 1983, Vol.50.

[3] M.N. Hughese, The Inorganic Chemistry of Biological Processes, 2nd ed., Wiley, Chichester, 1981.

[4] R.W. Hay, Bio-inorganic chemistry, Horwood, England, 1984.

[5] G.L. Eichhorn, Ed., Inorganic Biochemistry, Elsevier, Amsterdam, 1973.

[6] E.W. Neuse, Encyclopedia of Polymer Science and Technology, Interscience, New York, 1968, Vol.8.

[7] S.P. Gosh, J. Indian Chem. Soc. 28 (1951) 710.

[8] S.P. Gosh and H.M. Gosh, J. Indian Chem. Soc. 33 (1956) 894.

[9] G. Goodgame and F.A. Cotton, J. Am. Chem. Soc. 84 (1962) 1543.

[10] D.M.L. Goodgame and M. Goodgame, Inorg. Chem. 4 (1965) 139.

[11] J. Reedijik, J. Inorg. Nucl. Chem. 35 (1973) 239.

[12] N. Hugihara, K. Sonogashira and S. Takahashi, Advances in Polymer Science, Vol.41 (Springer-verlag Berlin Heidelberg, New York, 1981) p. 149.

[13] K.K. Mohammed Yusuff and R. Sreekala, J. Polymer Sci. 30 (1992) 2595.

[14] K.S. Devaki and V.N.R. Pillai, Eur. Polymer J., 24, 209 (1988).

[15] S. Sankara raman, V.P.N. Nampoori, C.P.G.Vallabhan, N. Saravanan, and K.K. Muhammed Yusuff, Mat. Sci. Lett. 15 (1996) 230.

* * * * *

APPENDIX 1

PHOTOACOUSTIC STUDY IN ARANMULA MIRROR

ABSTRACT

Aranmula mirror is a metallic mirror prepared by ethanometallurgical process by a group of families at Aranmula, a village in Kerala, south India. Recently there has been an interest in investigating the properties of Aranmula Mirror using modern scientific techniques. The present work describes the evaluation of thermal diffusivity and reflection coefficient using photoacoustic technique.

The art of making metal mirrors has been practiced in various parts of the world even before 1400 BC, for distortion free images. By 1400 BC people created a metal mirror of bronzes containing 30-weight percent tin. Although brittle, high-tin bronzes yielded a highly reflecting surface. The art of making metal mirrors from copper-tin bronzes was known in India. This ancient art of metal mirror making is still practiced by only a small number of families at Aranmula, a small village in Kerala, South India. The properties and method of casting of these mirrors have recently been studied by Pillai et al [1]. The mirror is found to be an alloy of Cu-70.4%, Sn-29.4%, Zn-0.06%, P-0.02%, & Fe-0.034% and Ni-0.052%. The present work deals with the determination of thermal diffusivity and reflection coefficient of Aranmula mirror using photoacoustic effect.

By studying the chopping frequency dependence of the acoustic signal generated in the coupling gas at a fixed optical wavelength, the thermal diffusivity of the sample can be evaluated [8,14,15]. By noting down the PA signal for the mirror and carbon black the reflection coefficient can be calculated.

To determine the reflection coefficient of the mirror by PA technique carbon black is used as the reference sample. If S_C and S_M are the PA signal amplitudes and A_C and A_M are the absorption coefficients for carbon black amd the mirror respectively, for the incident beam of intensity I_I we can write,

$$S_m/S_c = A_m I_I / A_c I_I = A_m \qquad (1)$$

(where A_C=1) and reflection coefficient

$$R = 1 - A_m \qquad (2)$$

To determine the reflection coefficient of the Aranmula mirror PA signal for the mirror and carbon black are noted for a given chopping frequency and laser power. The reflection coefficient is calculated from equations 1 and 2.

To determine the thermal diffusivity of the metal mirror a small piece of the sample is kept in the PA cell and the frequency dependence the acoustic signal is studied. Knowing the thickness (l_s) of the sample and characteristic frequency(f_c) from the log-log plot, the thermal diffusivity can be calculated using the relation

$\alpha = l_s^2 f_c$ [2-9]. The details of thermal diffusivity measurements are given in chapter 3.

The Aranmula mirror used for the present study has a thickness of 1.24 mm. From the log-log plot it is found that the characteristic frequency is at 68.79 Hz. The thermal diffusivity thus calculated gives the value 1.058 ± 0.001 cm^2/s, which differs much from the value of copper (1.18 cm^2/s) which is the major constituent (70.4%) of the sample [10].

The reflection coefficient of the Aranmula mirror used for the present study, calculated from equations 1 and 2 yielded the value to be 0.92.

REFERENCES

[1] S.G.K. Pillai, R.M. Pillai and A.D. Damodaran, J. Metals., (1992 March).

[2] A.C. Tam, C.K.N. Patel and R.J. Kerl, Opt. Lett., 4 (1979) 81.

[3] A.C. Tam, Rev.Modern Phys., 56 (1986) 2.

[4] C.L. Cesar, H.Vrgas, and L.C.M. Miranda, Appl. Phys. Lett., 32 (1978) 554.

[5] P. Charpentier, F. Lepoutre, and L. Bertrand, J. Appl. Phys., 53 (1982) 1.

[6] F.A. Mac Donald. G.C. Wetsel. Jr., J. Appl. Phys., 49 (1978) 4.

[7] A. Hordvik and H. Scholssberg Appl. Opt., 16 (1977) 101; 16 (1977) 2919.

[8] S. Sankara raman, V.P.N. Nampoori, C.P.G. Vallabhan, G. Ambadas, and S. Sugunan, appl. Phys. Lett., 67 (1995) 2939.

[9] S. Sankara raman, V.P.N. Nampoori, C.P.G. Vallabhan, N. Saravanan, and K.K. Mohammed Yusuff, J. Mat. Sci. Lett., 15 (1996) 230.

[10] S. Sankara raman, M.Phil Thesis,Cochin University, 1995.

APPENDIX II

THERMAL DIFFUSIVITY MEASUREMENTS ON SOME METAL PHTHALOCYANINES USING MIRAGE EFFECT

ABSTRACT

Mirage effect or photothermal deflection effect is another thermooptic effect that can be used to characterize thermal and optical properties of materials. The use of mirage technique in material studies is described by taking specific example of phthalocyanines, which have importance in photonic applications.

The "mirage" technique (optical beam deflection) first introduced by Boccara, Fournier and Badoz [1] in early 1980s, has recently been revived as an elegant method for measuring the optical and thermal properties of materials [2-4] because of its high sensitivity and non destructive nature[5]. The basic principle of the photothermal technique is that the specimen irradiated by an intensity modulated (chopped) laser beam (pump) undergoes optical absorption and is heated up by non-radiative transitions, The heat, which is periodically deposited in the sample, is transferred to the coupling medium by thermal conduction and this sets up a refractive index gradient (RIG) in the coupling medium. A second laser beam (probe) skimming the sample surface gets deflected due to the RIG produced by the beam. The deflection of the probe beam is detected by an optical fibre based position sensitive detector (PSD). The technique can be performed in two ways. (1) Transverse PTD - where we assume that the pump beam propagates through the medium in the z direction and the probe beam propagating perpendicular to the pump beam i.e. along y direction (2). Collinear PTD - where the probe beam propagates along the z direction itself or makes an angle with respect to the pump beam direction [6-11].

The technique finds profound applications in fields like spectroscopy, imaging, thermal studies, ablation studies, thermodynamic transport properties etc. In the present chapter we have employed PTD technique to determine the thermal diffusivity of some metal phthalocyanines, organic semiconductors.

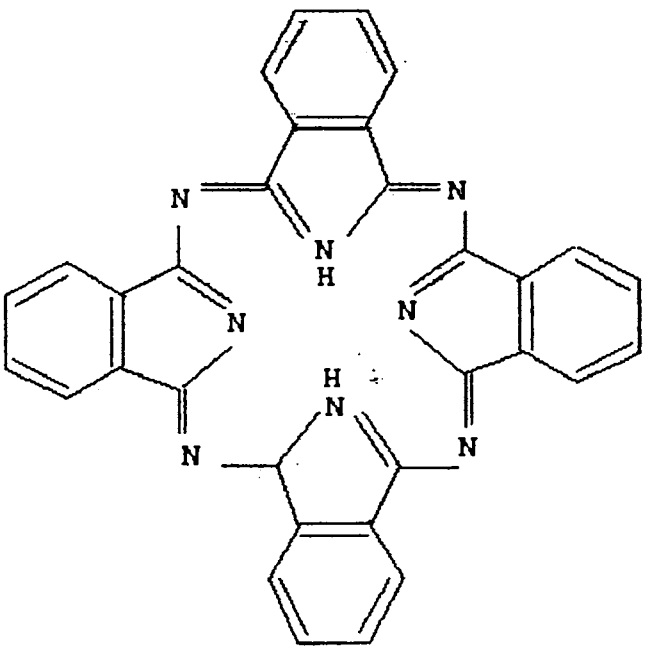

Fig.1: Structure of Phthalocyanines.

Phthalocyanines, the organic semiconductors, have attracted a great deal of attention in recent years due to their potential application in various fields like imaging, microelectronics, catalysis, photochemistry, sensors

photovoltaic devices, optoelectronics and information storage [12-19].

Phthalocyanines are macrocyclic compounds containing four pyrrole units, which are fused to an aromatic structure [Fig.1]. The compounds usually referred to under phthalocyanine class consist of metal derivatives of phthalocyanines. Two hydrogen atoms attached to the two-isoindole group can be replaced by atoms from every group in the periodic table to form the metal phthalocyanines. Also, each of the sixteen peripheral hydrogen atoms on the four benzene rings can be substituted by a variety of atoms and groups. In metal phthalocyanines, for example, the metal atom supplies one electron each to the nitrogen atoms of the isoindole groups and these isoindole nitrogen atoms in turn supplies an electron to the metal atom, forming a covalent bond. The unshared pairs of electrons in the remaining two isoindole nitrogen atoms presumably from coordinate covalent bonds with the metal atom.

PTD technique has been proved to be a useful, elegant and sensitive tool for the measurement of thermal diffusivity [2,20-24]. The schematic of the PTD process (transverse geometry) is shown in figure 2.

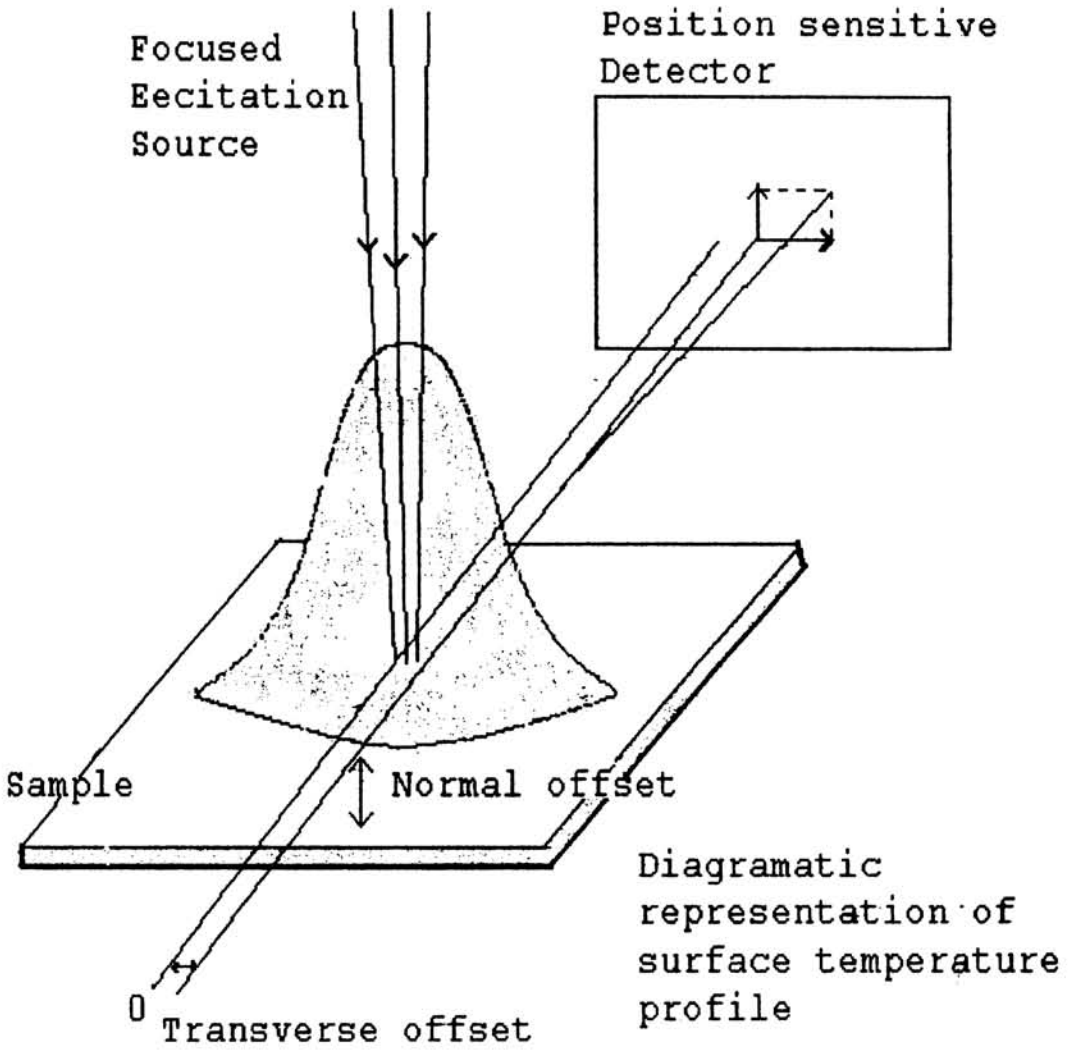

Fig. 2: Schematic of the PTD method showing the two deflection components (transverse configuration)

Let y and z be the transverse and vertical offset of the probe beam with respect to the pump beam axis [2, 20,

23]. Resolving the deflected beam, the transverse (ϕ_t) and normal (ϕ_n) components can be estimated as

$$\phi_t = (1/n)(\partial n/\partial t)\int(\partial T/\partial y)\, dx \qquad (1)$$

$$\phi_n = (1/n)(\partial n/\partial t)\int(\partial T/\partial z)\, dx \qquad (2)$$

where n is the refractive index of the medium and T is the temperature near the heated sample at time t. The total deflection is given by

$$M = |\phi_n|^2 + |\phi_t|^2 \qquad (3)$$

Since $(\partial n/\partial t)_{sample} >> (\partial n/\partial t)_{gas}, \nabla T_s > \nabla T_g$.

Hence $|\phi_s| >> |\phi_g|$, which is true for both normal and transverse components. 's' and 'g' stands for the sample and gas. The normal deflection $\nabla T = (\partial T/\partial z)$ includes the cosine term which makes the deflection symmetrical with respect to the pump source, whereas the transverse deflection $\nabla T = (\partial T/\partial y)$ includes the sine term making it antisymmetric about the source. Therefore ϕ_t goes to zero and changes the phase by 180 at the origin. The effect of

ϕ_t dominates over the normal component near the interface along the source, while ϕ_n dominates near the interface away from the source [25]

In order to determine the thermal diffusivity, the sample is illuminated by an intensity modulated laser beam (pump beam). The excitation and subsequent non-radiative de-excitation process occuring inside the sample result in the heating of the sample. The thermal waves generated from the sample sets a refractive index gradient with in the sample or in the adjacent coupling medium. If a second laser beam (probe beam) is allowed to graze the sample surface at a finite height h, the beam gets deflected. The in phase component of the deflected signal is measured at different positions (x) of the probe beam across the pump beam spot on the sample surface. From the plot of x Vs phase, the zero crossing points on either side of the central zero at which the signal are shifted in phase by ± 90 relative to the central position. The distance of separation between (x_o) these points can be used to determine the thermal wavelength as a function of frequency (Thermal wavelength is given by $\lambda_t = 2(\pi\alpha/f)^{1/2}$). The slope of thermal wavelength Vs the reciprocal of the square root of the frequency gives the thermal diffusivity of the solid.

Numerical analysis shows that [26] the distance x_o is given by

$$x_o = d + (\gamma\pi\alpha/f)^{1/2} \qquad (4)$$

where d is the intercept that is of the order of the pump beam diameter and f is the chopping frequency $(\gamma\pi\alpha)^{1/2}$ is the slope of x_o Vs $(1/f)^{1/2}$ plot. γ is a parameter, which depends on the bulk thermo-optical properties of the material [27]. It has been proved that $\gamma = 1.44$ for optically opaque and thermally thick samples [28] but $\gamma = 1$ for all other cases. As the thermal wavelength decreases with the increase of chopping frequency, the low frequency portion of the graph should be given greater importance in the determination of thermal diffusivity.

The schematic of the experimental set-up arranged for the present investigation is shown in figure 3. The 488 nm line of an Argon-ion laser [LiCoNiX 5302A] is used as the pump source whereas a He-Ne laser at 632 nm wavelength and power 5mW [Spectra Physics] is used as the probe beam. In order to reduce the probe beam diameter, it is passed through a fine aperture, without diffraction. An electromechanical chopper is used to modulate the pump beam. This modulated pump beam is focused into the sample

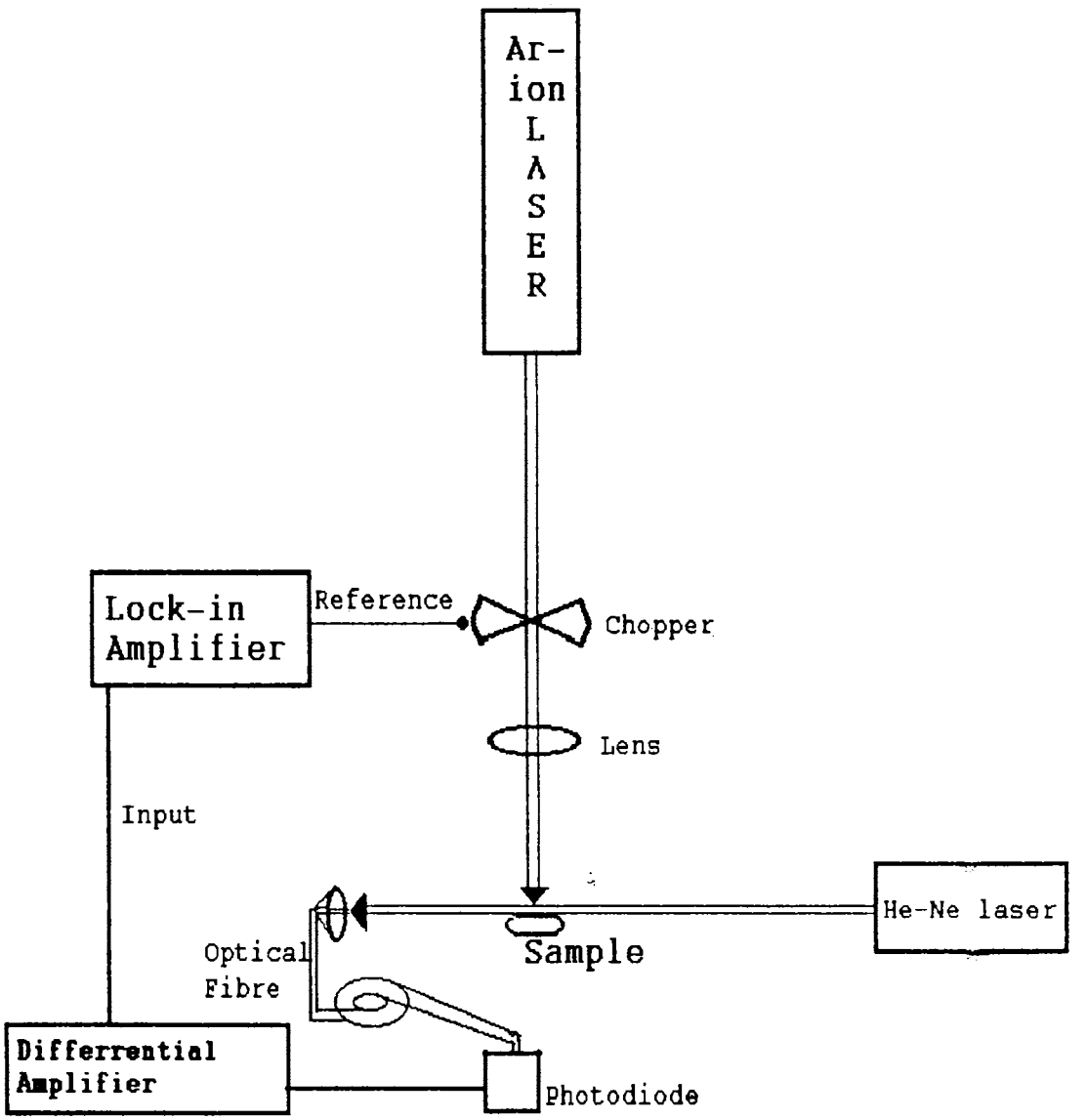

Fig.3: Schematic of the experimental set-up for PTD studies

surface. The deflection is measured using a position sensitive detector and its output is amplified by a differential pre-amplifier and analysed using a lock-in amplifier [EG & G 5208].

The sample is taken in the form of pellets and mounted on a xyz translator. The probe laser and the PSD are also arranged on a xyz translator. The inphase component of the deflected signal is measured for various values of x. Determining x_o, the distance between the zero crossing points separated by a phase 180^o, from the x Vs phase graph another graph x_o Vs $(f)^{-1/2}$ is drawn. From the slope of x_o Vs $(f)^{-1/2}$ graph, thermal diffusivity can be calculated.

The experimental set-up is standardised by determining the thermal diffusivity of copper (1.14 cm^2/s). Thermogravimetric analysis shows that the samples do not decompose at temperatures lower than 300 ^oC. Hence the exposure to the intensity modulated laser beam of power levels used in the present investigation (~100mW) does not decompose the samples.

Variation of the phase of the PTD signal with distance from the heating beam spot for FePc for three different chopping frequencies is shown in figure 4. From the slope of the $(1/f)^{1/2}$ Vs x_0 graph (Fig. 5) the thermal diffusivity (α) can be calculated using the relation

$$\text{Slope of } (1/f)^{1/2} \text{ Vs } x_0 \text{ graph} = (\pi\alpha)^{1/2}$$

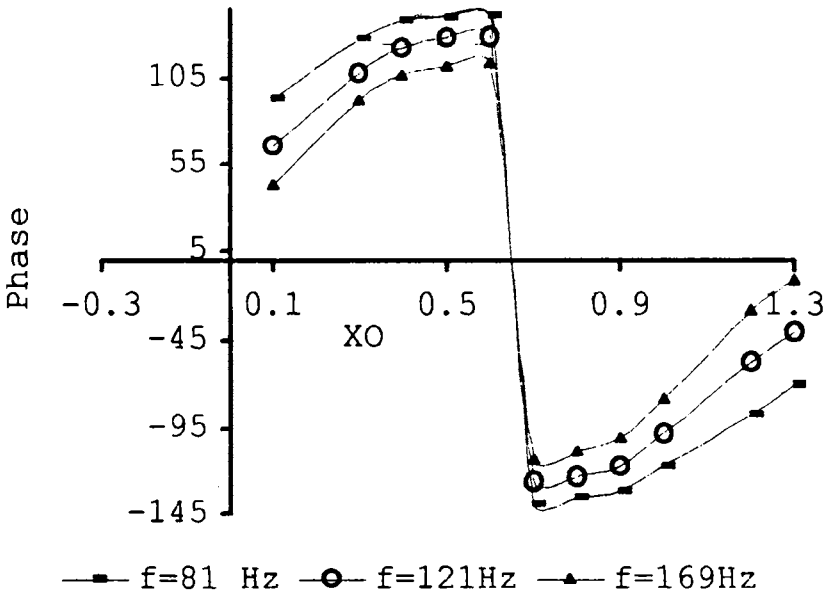

Fig.4: Variation of the phase of the PTD signal with distance (mm) from the heating beam spot for FePc for three different chopping frequencies.

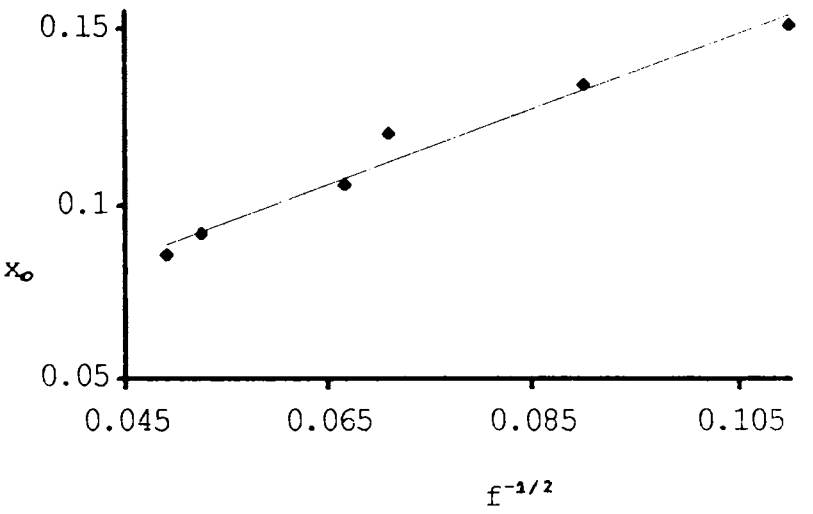

Fig. 5: x_0 (cm) vs. $f^{-1/2}$ plot for FePc.

The values of thermal diffusivities of FePc and EuPc and their iodinated samples are given in Table 1. It is found that the thermal diffusivity increases on iodination.

Table Thermal diffusivity of some metal Phthalocyanines by PTD technique

SAMPLE	Thermal diffusivity(cm^2/s)
FePc	0.380
FePc(I)	0.630
EuPc	0.717
EuPc(I)	0.820

Phthalocyanines are inorganic semiconductors with the carriers, conjugate π electrons. When the samples are iodinated, I^{-1} exists as I_3^- in the inter cavities of the quasi one-dimensional lattice of Phthalocyanines [29]. The presence of I_3^- in the cavities may alter the natural vibrational frequency of the lattice along with other factors which depends on lattice parameters. Thermal diffusivity is one such parameter, which depends on the lattice. The observed increase in the thermal diffusivity of these metal Phthalocyanines can thus be attributed to the incorporation of I_3^- in the cavities of Phthalocyanines.

The PTD technique is effectively employed in the determination of thermal diffusivities of some metal Phthalocyanines, organic semiconductors. The effect of iodination on the thermal diffusivity of FePc and EuPc are also studied.

REFERENCES

[1] A.C. Boccara, D. Fournier and J. Badoz, Appl. Phys. Lett., 36 (1980) 130.

[2] J.C. Murphy and L.C. Aamodt, J. Appl. Phys., 51 (1980) 4580.

[3] W.D. Jackson, N.M. Amer, A.C. Boccara and D. Fournier, Appl. Opt., 20 (1980) 1331.

[4] G. Rousset and F. Lepoutre, Rev. Phys. Appl., 17 (1982) 201.

[5] R.L. Thomas, L.J. Inglechart, M.J. Lin, L.D. Favro and P.K. Kuo in `Review of progress in Quantitative NDE', edited by D.O. Thomson and D. Chimenti (Plenum, New York, 1985) Vol. 4, p. 745.

[6] L.C. Aamodt, J.W. Maclachlan, Spicer and J.C. Murphy, J. Appl. Phys., 59 (1986) 348.

[7] P.E. Nordal and S.O. Kanstad in :Scanned Image Microscopy ed E. Ash (Academic Press, New York, 1980).

[8] G. Bausse, in :Scanned Image Microscopy ed E. Ash (Academic Press, New York, 1980).

[9] M.A. Olmstead, N.M. Amer, S. Kohn, Bull. Am. Phys. Soc., 27 (1982) 227.

[10] M.A. Olmstead, N.M. Amer, S. Kohn, D. Fournier, and A.C. Boccara, Appl. Phys. A, 32 (1983) 141,

[11] J. Stone, Appl. Opt., 12 (1972) 327.

[12] C.C. Leznoff, A.B.P. LEVER, `Phthalocyanines - Prospects and applications' (VCH Publications, New York, 1984).

[13] V. Gulbinas, M. Chachisvilis, A. Persson, S, Svasberg and V. Sundstorm, J. Phys. Chem., 98 (1994) 8118.

[14] P. Kivits, R. de Bont and VanderVeen, J. Appl. Phys., A 26 (1981) 101.

[15] D. Worhle, D. Meissner, Adv. Matter, 3 (1991) 129.

[16] T. Klofta, T.D. Sims, J.W. Pamkow, J. Danziger, K.W. Nebersny and N.R.Armstrong, J. Phys. Chem., 91 (1987) 5651.

[17] R. Brina, G.F. Collins, P.A. Lee, M.R.Armstrong, Anal. Chem. 62 (1990) 2367.

[18] J. Danziger, J.P. Dodelat and N.R.Armstrong, Chem. Mater. 3 (1991) 812.

[19] W.S. Williams, J.P. Sokoloff, Z.Z. Ho, C. Arbor, N, Peyghambarian, Chem. Phys. Lett., 193 (1992) 317.

[20] P.K. Kuo, M.J. Lin, C.B. Reyes, L.D. Favro and R.L. Thomas, A.C. Bccara and N. Yakobi, Can. J. Phys., 64 (1986) 1168.

[21] P.K. Kuo, E.D. Sendker, L.D. Favro and R.L. Thomas, Can. J. Phys., 64 (19986) 1168.

[22] W.B. Jackson, N.M. Amer, A.C. Bccara and D. Fournier, Appl. Opt., 20 (1981) 1333.

[23] A. Salasar, A Sanchew-Lavega and J. Fernandez. J. Appl. Phys., 69 (1991) 1216.

[24] K. Rajasree, Ph.D Thesis, 1995, Cochin University of Sci. And Tech.

[25] L.J. Inglehart and E Le Gal La Salle, Springer series in optical science, P. Hess and J. Pelzl (Ed) 58 (1988) 389.

[26] K. Kuo, L.D. Favro and R.L. Thomas, Ch.6, "Photothermal investigations of solids and fluids", J.A. Sell (Ed) (Academic, New York) 1988.

[27] A. Salasar, A Sanchew-Lavega and J. Fernandez, "Photoacoustic and phtothermal phenomena II, (Ed) J.C.Murphy, J.W. Maclachlan- Spicer, L. Aamodt and B.S.H. Royce (Springer, Berlin), p 331 (1990).

[28] C.B. Reyes, Ph D thesis, Wayne State University, (1988)..

[28] Jayan Thomas, Ph D thesis December 1995, Cochin University of Science and Technology.

* * * * *

CONCLUSION

The main objective of the thesis entitled *Investigation on thermal diffusivitty of some selected materials using laser induced photoacoustic technique* is to measure thermal diffusivity of materials using PA technique and to bring out some of the factors influencing / governing the thermal properties of materials. With this intention samples are selected from some representative groups of materials that find applications in various fields of science and technology. The samples selected include an important ceramic and substrate material (alumina), an important rare earth oxide (Nd_2O_3) that find applications in electronic component and device fabrication, and medically and industrially important metal complexes (halogeno benzimidazole complexes) and polymer bound metal complexes (polystyrene supported halogeno benzimidazole complexes).

Photothermal phenomena have gained considerable attention in recent years by virtue of its versatile applications in science and technology not only as a non-destructive technique but also as a spectroscopic technique where the conventional techniques collapse. The first chapter of the thesis describes various photothermal phenomena and their detection techniques with special reference to Photoacoustics (PA). Various possible causes

of PA generation in solids, liquids and gases with their detection techniques are briefly explained in it. Photoacoustic is clearly a form of optical spectroscopy as well as a form of calorimetry. Advantages of PA technique over classical calorimetry and spectroscopy are also given. Some fields of science and technology -viz. Photovoltaic de-excitation process, imaging, depth profile, microscopy, microwave and IR spectroscopy, chemical studies, surface studies, and Biology- are briefly described in it. A detailed reference that can throw light into various aspects of Photoacoustic spectroscopy also is included.

The theory for Photoacoustic spectroscopy (PAS) was given by Rosencwaig and Gersho. The theory is briefly presented together with some special cases in the second chapter. The theory for thermal diffusivity measurements is also given.

For thermal diffusivity measurements by PA technique a PA spectrometer is essential. The design and fabrication details of a PA spectrometer are described in the third chapter 'Instrumentation'. The experimental set up is standardised by determining the thermal diffusivities of materials of known values. The linearity

of the PA signal with power is studied. The results being in good agreement with the reported valued, the technique is extended for the measurement of other samples used in the present investigation.

Chapter 4 describes the influence of hydroxyl ion on the thermal diffusivity of γ-Alumina. Alumina (Al_2O_3) is an important material in microelectronics, low temperature physics, magnetic and optical devices and protective coatings. The high specific surface area and the monolayer of surface hydroxyl group play a significant role in chemical and physical properties. These hydroxyl groups at the surface can be minimised by doping it with rare earth oxides (Nd_2O_3). The thermal diffusivity of Al_2O_3 at different dopent levels and at different temperatures is determined and the effect of degassing temperature and doping is studied. The studies reveal the role of hydroxyl groups on thermal diffusivity as greater the amount of hydroxyl groups greater is the thermal diffusivity. Thus one can alter the thermal diffusivity of alumina by varying the amount of hydroxyl group.

Sample preparation route plays a significant role in the physical as well as chemical properties of a material. In chapter 5 an attempt has been made to understand the

influence of preparation route on thermal diffusivity of Nd_2O_3. Nd_2O_3 is prepared by two techniques viz. oxalate method and hydroxide method. The studies reveal that the change in preparation route changes the amount of surface hydroxyl groups, a characteristic of oxides. These differences in the surface properties seem to be the reason for the difference in thermal diffusivity of Nd_2O_3 prepared by the two methods.

Chapter 6 describes the thermal diffusivity studies on some halogeno benzimidazole complexes of cobalt and copper that finds applications in medicines, biotechnology, industrial chemistry etc. The effect of metal as well as halogen part on the thermal diffusivity of these complexes is studied. The effect of halogen part on the thermal diffusivity is found to be opposite in Co and Cu complexes. Replacement of Co by Cu seems to decrease the thermal diffusivity values. The structure of the complexes, as revealed by electronic spectra, magnetic susceptibility measurements and molar extinction coefficient measurements seem to be tetrahedral. But a detailed single crystal study is essential for the confirmation of the sample structure. The complexes being newly synthesised and reported other relevant physical as well as chemical data that are required for the analysis

of our results are not available. This inhibits from arriving at a conclusive reason for thermal diffusivity variations exhibited by these metal complexes.

The thermal diffusivity studies on some bio-medically and industrially important polystyrene supported schiff base compounds are described in chapter 7. Here also the effect of metal as well as halogen part on the thermal diffusivity of these complexes is studied. The effect of halogen part on thermal diffusivity is found to be opposite in cobalt and copper complexes. The materials being newly synthesised and reported, a detailed characterisation in terms of structural, physical and chemical properties is required. A rough estimation attributes square pyramidal structure to them. The physical and chemical data available are insufficient for the analysis and finding out the reason for the thermal diffusivity variations with halogen and metal part replacement in the complex. Only through a single crystal study one can exactly determine the structure and lattice properties and thereby arrive at a conclusive reason for thermal diffusivity variations. This is because thermal properties of insulators are associated with lattice vibrations.

The PA technique is also an excellent tool for the determination of optical properties of materials. The PA technique is also extended to determine the reflection coefficient of Aranmula mirror and is described in Appendix 1. Metal mirrors are well known for their distortion free images and long life.

An attempt has also been made to determine the thermal diffusivity of another class of materials, Phthalocyanines using another photothermal technique viz. Photothermal deflection or mirage effect. Phthalocyanines are organic semiconductors that find applications in fields like imaging, microelectronics, sensors, optoelectronics and optical data storage.

* * * * *